Hydraulic pressure and flow control of injection moulding

Guerrier, Paul Keith

Award date:
2001

Awarding institution:
University of Bath

Hydraulic Pressure & Flow Control of Injection Moulding

Submitted by Paul Keith Guerrier
For the degree of PhD
of the University of Bath
2001

Paul Keith Guerrier

ProQuest LLC
789 East Eisenhower Parkway
P.O. Box 1346
Ann Arbor, MI 48106-1346

Summary

This thesis documents an investigation into the improved control of injection moulding. Breaking the injection moulding process down into phases, the first phase in the injection moulding process is the *plastication* phase when solid polymeric material is melted. During the next phase, *filling*, molten polymeric material is forced out of the barrel by the screw, which is usually velocity controlled. Then once the mould is full, the *packing* phase begins when pressure control is required to counteract the effects of shrinkage during *cooling*. At a particular point in time, after *packing* has begun, the material in the orifice at entry to the mould (termed the gate) freezes. This is called *gate freeze* and once this has occurred the injection process is considered over. Good control of the *filling* and *packing* phases is crucial to ensure a good quality finished part is produced and it is the control of these 2 phases, with particular attention paid to the transfer from *filling* to *packing* and the start of the *packing* phase, that is detailed in this thesis. In hydraulic injection moulding machines velocity control is attained through flow control (often abbreviated to Q control) and pressure control (often abbreviated to P control) is attained through pressure control hence the term P-Q control. The work was sponsored and the commercial exploitation of any solution developed was a clear objective. This implied that a black box type control technique would be of questionable value. Also limits were put on the transducer signals available, only hydraulic pressure and actuator displacement were made available. The first stage in the work was to model the filling and packing phases of injection moulding and compare simulation with experimental results from a real injection moulding machine. Hence an injection moulding load model was implemented in the Bath*fp* simulation package. For the case of a pseudoplastic material (polypropylene) good agreement was achieved between simulated and experimental results of a 20ml mould. The effects of cooling at the onset of packing even with unreasonably fast cooling were found to be small. A real injection moulding machine was not available for new controller development and so a hardware-in-the-loop type emulation of the *filling* and *packing* stages of injection moulding process was developed. The test rig centred around metering flow out of an actuator. Armed with a good understanding of the injection moulding process a number of different strategies

for the filling and packing stage control of injection moulding were considered. Of the solutions considered separate control of *filling* and *packing* was found to be the most promising using model reference adaptive control (MRAC) for both phases with a bumpless transfer strategy connecting the pair. Of the adaptive solutions available the (MRAC) minimal control synthesis controller (MCS) was chosen. A 1st order implementation was found to be sufficient for packing pressure control. Such a controller was implemented in discrete time at a sampling frequency of 1kHz on the rig and compared with the existing industry standard fixed gain PI *packing* controller. Through careful design of the control scheme it was shown that for the specific mould and duty cycle investigated MCS packing pressure control could outperform PI pressure control of an emulated injection moulding load. MCS control was also shown to be robust to changes in operating conditions. However because of stability problems associated with load emulation the precise level of robustness was not ascertained. By correctly selecting the MCS integrator values that were maintained until switchover an element of bumpless transfer has also been incorporated. In this respect an improved control strategy for injection moulding has been identified and shown in an emulated environment to be an improvement on the current industry standard. Presently commercialisation of this solution would be premature as work remains to be done. However, through the use of a small 20ml mould and a high injection velocity of 0.1m/s the test conditions were demanding and sufficient promise has been demonstrated to warrant full scale testing of MCS packing pressure control as the next stage.

Acknowledgements

I would like to thank my supervisors Kevin Edge and Ken Cleasby for their support and input along with the technicians in the department for their unending willingness to help.

This PhD was undertaken with support from an Engineering and Physical Sciences Research Council grant in conjunction with a CASE award from Vickers Systems (now part of Eaton Corp.).

May the Department of Mechanical Engineering continue to be successful.

I would like to dedicate this thesis to my Mother.

Contents

Nomenclature

		Chapter Usage
A	Plant parameter matrix	4
A	Area	2, 3
A_m	Reference model parameter matrix	4
a_1	Transfer function coefficient	4
b_2	Transfer function coefficient	4
A_1	Actuator annulus area	3
b_1	Transfer function coefficient	4
B	Input parameter matrix	4
B_m	Reference model input parameter matrix	4
C	Coefficient of viscous friction	3
C_e	Output error output matrix	4
C_q	Valve flow coefficient	3, 4
d	Disturbance vector	4
F	Force	2,3
$G_c(s)$	Controller transfer function	3
$G_v(s)$	Valve actuator transfer function	3
h	Height of flowpath	3
k	Flow coefficient	4
k	Power law index viscosity	2
k_{cd}	Converging/diverging radius coefficient	2
K_{x1}	Valve position constant 1	4
K_{x2}	Valve position constant 2	4
K_{p1}	Valve pressure constant 1	4
K_{p2}	Valve pressure constant 2	4
K	MCS state feedback gain	4
K_r	MCS forward loop gain	4
l	Length	2
m	Mass	3

n	Power law index	2
P_E	Pressure to overcome extensional viscosity	2
P	Pressure drop	2
P	Pressure	4
P_1	Actuator pressure	3
p_1	Small perturbation in actuator pressure	3
P_1	Pressure at port 1	4
p_1	Small perturbation in pressure at port 1	4
P_s	Supply pressure	4
Q	Flow rate	3, 4
q	Small perturbation of flowrate	3
Q_S	Supply flowrate	4
q_S	Small perturbation of supply flowrate	4
Q_R	Return flowrate	4
q_R	Small perturbation of return flowrate	4
Q_1	Port 1 flowrate	4
q_1	Small perturbation of port 1 flowrate	4
r	Reference vector	4
R	Radius	2
r_1	Radius at the beginning of a section	2
r_2	Radius at the end of a section	2
S	Laplace operator	3
u	Control vector	4
V_1	Trapped volume of oil between load valve and actuator piston	3
V_{poly}	Trapped volume of polymer in the mould	2, 3
w	Width of flowpath	3
x	State vector	4
x_e	State error vector	4
x_m	Reference model state vector	4
X	Spool displacement	3, 4
x	Small perturbation in spool displacement	3

X_1	Valve annular flow area circumference	3
X_u	Valve spool underlap	4
y	Melt front position	2
Y	Actuator displacement	2, 3
y	Small perturbation in actuator displacement	3
y	Plant output vector	4
y_e	Output error vector	4
z	z-transform	3

Greek Symbols

		Chapter Usage
α	MCS integral adaptive gain weight (scalar)	4, 5
β	MCS proportional adaptive gain weight (scalar)	4, 5
β_{oil}	Oil Bulk modulus	3, 4
β_{poly}	Polymer Bulk modulus	2, 3
Δ	A small change in	4
$\dot{\gamma}$	Shear rate	2
η	Bingham viscosity	2
η_N	Zero shear Newtonian viscosity	2
λ_T	Extensional viscosity constant	2
μ	Viscosity	2
θ	Convergence angle	2
ρ	Oil density	3
σ_E	Extensional stress	2
τ	Shear stress	2
τ_y	Yield shear stress	2
ω_n	Natural frequency	3
ζ	Damping ratio	3

1.0 Introduction

1.1 Background

Hydraulics is essentially a very compact method of power transmission and since power is transmitted by oil or water at high pressure it is possible to remotely locate the prime mover from the powered actuator. As such it is much easier to power actuators in inaccessible locations compared to using mechanical power transmission methods. Electrical solutions offer the same flexibility but for producing large forces and torques electrical solutions are far heavier. Using high pressure hydraulics can also have a high power density with very large forces available from small actuators. For these two reasons hydraulics is widely used for the movement of flight control surfaces on aircraft. This method of power transmission also allows the direct conversion of rotary motion into linear motion and because of this hydraulic solutions are widely used in other engineering applications including earth moving equipment, materials testing machines and injection moulding. Hydraulics systems generally run with a maximum system pressure of between 100bar and 350bar and consequently actuators produce medium to large forces. This is why workpiece manipulation on a production line, which requires small forces, is often done using pneumatic systems which typically have a maximum system pressure of around 10bar.

At present hydraulics and to a greater extent pneumatics share of the power transmission market is being eroded by electro-mechanical solutions. Of the fluid based solutions pneumatics is at most risk of being replaced as the forces are lower. The driving force behind this is that electrical solutions can offer higher energy efficiency, lower cost and components from different manufacturers are easier to interchange. This is the same as the concept of *Plug and Play* used in personal computers. While hydraulics will always have a place in the market in the future it is likely that it will be forced into the high force and power end of the market. This is partly because hydraulic components from different manufacturers are far harder to interchange and doing so can lead to problems. A good introduction to hydraulic system design and analysis is given by **Watton (1989)**. The other advantages that electrical solutions have over hydraulic ones are lower maintenance and cleanliness. A typical example where an electrical

power transmission solution is replacing a hydraulic solution is in automobile power assisted steering. However, while some small cars (notably the Fiat Punto and Renault Clio) have electrically assisted steering as yet all 4 wheel drive or off road passenger vehicles still have hydraulically assisted steering. Even so, hydraulics is still by no means a declining industry and is an active research area.

Two of the main problems associated with hydraulic power transmission are that systems are often difficult to control and have a low energy efficiency compared to an equivalent electrical power transmission system. More and more is being done to improve hydraulic performance and efficiency by redesigning components and using more advanced control strategies. A good overview of the current state of research in hydraulic control is given in **Edge (1997)**. The work in this thesis is centred on improving dynamic performance by using advanced control.

1.2 Description of Injection Moulding

Injection moulding is the most important plastic part manufacturing process in terms of the number of parts produced. The overall idea behind the process is to melt a material and then force it into a mould where it cools and takes the shape of the mould. Injection moulding is a high volume low cost finished part process where tooling costs are high. The process is cyclical and repetitive and provided process disturbances are low then once set-up is complete little machine supervision is required. A detailed introduction to injection moulding is given by **Rosato & Rosato (1995)**. A diagram of a simplified injection moulding machine is shown in Figure 1.1. The actuator that translates the screw and the motor that turns it have been omitted for clarity.

Breaking the process down into phases, the first phase in the process is the *plastication* phase when solid polymeric material in pellet form is screw fed from a hopper into the heated barrel where it melts. The nozzle at the end of the barrel is then moved up to the entry point (gate) to the mould. Molten polymeric material is forced out of the barrel by the screw, which is forced forwards either electrically or hydraulically. Injection is velocity controlled to avoid excess shear

heating which can lead to scorching of the molten polymeric material. Then once the mould is full, pressure control is required to counteract the effects of shrinkage during cooling. The velocity controlled phase of injection is called *filling* and the pressure controlled phase is called *packing* whilst more material is forced into the mould and then called *holding* once the packing pressure has been reached. Although it is not shown in Figure 1.1, the mould dies themselves are usually oil or water cooled to speed up the heat transfer from the polymeric material to the mould. At a particular point in time, after *packing* has begun, the material in the orifice at entry to the mould (termed the gate) solidifies. This is called *gate freeze* and once this has occurred the injection process is considered over as no material can pass in or out of the mould. Polymeric material begins to cool the moment that it is injected into the mould but it is not until after *gate freeze* that the *cooling* phase proper begins. Once the moulded part has solidified sufficiently to retain its shape after *ejection* from the mould the mould dies are opened and the part is ejected. In most cases *ejection* is automatic but in smaller batches the machine operator may be required to manually pull the moulded part out of the mould.

A labelled drawing of a moulded part is shown in Figure 1.2. Clearly only the moulded part is required as the final product however there is always an amount of scrap produced because of the need to get the polymeric material from the inlet to the mould to the moulded part. Scrap material is often ground up, mixed back in with virgin material and fed back into the injection moulding process. While this does not cause significant problems with small amounts of regrind a better solution is to use a hot runner system which minimises the production of scrap material. Such a solution is already commercially available. A further advance recently proposed by **Kazmer & Barkan (1997)** is to use variable restrictors at the end of the hot runners to control in-mould pressure more accurately. This is currently being productionised.

As with other mass production processes the reduction of cycle times is an important consideration. However, in contrast to other processes, once the tooling design (mould design) is complete there is a significant amount of machine set-up to be carried out before the moulded parts produced will be

acceptable. To aid mould designers there are a number of commercially available, finite element based, mould filling simulation packages. The longer the set-up period lasts the more scrap parts are produced. Consequently there has been a large amount of research into improving machine set-up time by using this mould filling software to predict the best velocity and pressure demand profiles to use. However if the machine controllers are not capable of achieving the demanded profiles then complicated demand profiles will be wasted. In a small 20ml mould the *filling* phase of a typical injection moulding cycle will take fractions of a second, as will *packing*, while both *holding* and *cooling* will take a time of the order of seconds. Large mould volumes up to about 25 litres are also possible with much larger machines in which case although all phases will take minutes to complete, *filling* and *packing* will still be the quickest phases.

Injection moulding control is traditionally split, according to machine area, into barrel temperature control, injection (*filling, packing and holding*) control and mould temperature control. While attempts have been made to have a single machine controller which co-ordinates all 3 control systems, most machines are still controlled in a decentralised manner. This means that the machine is only as capable as the worst control system i.e. if barrel temperature control is poor this will hamper repeatability no matter how good the other control systems are.

Since injection moulding is a repetitive mass production process the results are generally judged over a production run rather than just one finished part as is the case in lower volume processes. It is also generally accepted in injection moulding that there will be a certain amount of scrap produced at the start of a production run. Of course the less scrap produced the better but generally 4 cycles worth of scrap before acceptable settings are achieved is considered good. Since production runs can last for many hours it is also not surprising to find that part quality needs constant monitoring and often original machine set-up will need to be re-visited. This is mainly due to differences in polymeric material batches.

1.3 Current Problems in Injection Moulding Control

Injection moulding is a time-varying non-linear process whose dynamic characteristics are, for the most part, determined by the mould and the material being injected. One of the major strengths of injection moulding is that one machine is capable of making an infinite number of different parts, within a limited volume range, by changing the mould. It is hardly surprising to find that moulds are changed frequently and that any injection moulding controller must be robust to a change in mould. However the wish list for injection moulding machine technological advances does not stop here.

With reference to **Kazmer & Speight (1997)** major advances in injection moulding are required in the following areas: reduced material usage, decreased cycle time, increased energy efficiency and improved quality. Reduced material usage, (an average of 20% possible reduction is calculated by **Kazmer & Speight (1997)**) will be achieved by 2 methods. Firstly hot runners can be employed instead of cold ones which will mean that only the required part will be cooled and ejected from the mould. Secondly improved mould temperature control could allow the use of thinner walls which will bring finished parts closer to their minimum designed mechanical strength. With reference to **Kazmer & Hatch (1999)**, a reduction in cycle time is usually brought about by decreasing the mould temperature. However injected material begins to cool as soon as it enters a cooled mould, forming a skin on the cold mould wall and restricting further material flow into the mould. Skin formation also results in non-homogeneous polymer orientation and different locked-in stress levels. This then leads to a requirement for higher injection pressures. Ideally the mould should be maintained at a high temperature close to the barrel temperature which will inhibit skin formation and lead to lower injection pressure as well as more homogeneous polymer orientation and stress levels. Once the mould is full, faster cooling will then be required to attain the same cycle time as with a cold mould. Of course using this method the mould will also have to be heated up at the beginning of the next cycle. While this approach is still some way from being implemented the first steps have been taken by using insulating inserts and thermo-electric inserts in moulds to better control heat transfer.

The third area where improvements are required is increased energy efficiency. Firstly this can be made possible by reducing injection pressure which could be achieved by better mould temperature control as explained above. In hydraulic moulding machines improved hydraulic component designs with lower pressure losses have a part to play alongside the more widespread use of variable displacement pumps and speed-controlled fixed displacement pumps. In addition work recently reported by **Helduser (1999)** has shown that under part-load conditions variable speed control of a fixed displacement pump can be more efficient than control of a variable displacement pump driven by a fixed speed electric motor. However fixed displacement pumps are not yet designed to be run in such a manner and have a minimum speed which limits the efficiency gains possible. The advent of all-electric injection moulding machines also promises improved energy efficiency with one manufacturer claiming a decrease in power consumption of 50-90% compared to equivalent hydraulic machines. However all-electric machines have yet to gain widespread market acceptance and are also more expensive compared to equivalent hydraulic ones.

Finally, possibly the most important area where improvement is required is moulded part quality. In this instance quality covers: dimensional accuracy, mechanical properties, optical properties and surface finish. Currently quality control is done after moulding is complete but in the future it should be possible with more sophisticated instrumentation to have information of what is happening in the mould and predict the quality of the moulded part before ejection. Quality control is also typically a labour-intensive task but hopefully in the future the human element can be removed by using such techniques as machine vision.

The control of injection moulding is also an area where further work is required with 3 different broad strategic approaches pointed out by **Agrawal et al. (1987)**. These are: all-phase control, phase-dependent control and cycle-to-cycle control. Of these 3 different approaches phase-dependent control is the most common with each phase of injection moulding controlled separately with interactions between phases treated as disturbances. All-phase control may ultimately be the

best as it implies a thorough understanding of the entire process and how varying process inputs affect the moulded part produced. The most pragmatic approach is cycle-to-cycle control which takes advantage of the repetitive nature of the injection moulding process and tries to improve the next cycle using information from the previous one. Although a thorough understanding of the process would undoubtedly help, for effective implementation only cause and effect type relationships along with iteration would be required. While single-phase control is common and cycle-to-cycle control of particular phases is gaining popularity, as yet all-phase control has not been realised. However partial all-phase control has been investigated. **Michael & Lauterbach (1989)** proposed a pressure mass and temperature (pmT) control scheme which took account of the material properties of the cooling part. The material properties of polypropylene are shown in Figure 1.3. The basic idea was to ensure that the moulded part properties on ejection from the mould were always the same by taking account of the pressure volume temperature (PVT) relationship of the moulded material. Only pressure and volume were controlled with temperature treated as a disturbance. From the results presented the strategy worked quite well but required at least 8 cycles of learning for tuning.

Another less obvious variable in injection moulding is moulded material properties. It is not uncommon for injection moulding machine settings to need modifications after a change in raw material batch. This is because of slight, but significant, changes in material properties between manufactured batches. Consequently on-line test equipment is commercially available to monitor and feedback material property information such as viscosity and melt flow index to the process controller. However the equipment is costly and not widely used.

1.3.1 Instrumentation

As with the control of any system, good control is determined by the information supplied by instrumentation. If the information cannot be supplied then it has to be inferred using an observer. As a general rule, good instrumentation makes higher performance control possible. In the case of injection moulding the basic variables to be controlled are: velocity, pressure and temperature. Since injection moulding is judged by the moulded part, the in-mould values of these variables

are potentially the most useful. However because of mould construction they are not all easily measured.

In-mould pressure is commonly referred to as cavity pressure. Cavity pressure transducers are commercially available and frequently used for closed loop pressure control during packing. However incorporating a transducer in the mould can require a more complicated mould design and also leave an undesirable mark on the moulded part. Consequently they are not used in all moulds. Nozzle pressure transducers are also available which as the name suggests measure nozzle pressure during moulding. Again the transducers are expensive and not widely used. However work reported by **Coates & Speight (1995)** has shown that hydraulic pressure measurement (clearly this is only relevant to hydraulic injection moulding machines and not to all-electric ones) gives a good indication of changes in the process. The implication of this is that hydraulic pressure measurement is in most cases sufficient for control.

In-mould melt front velocity is much more difficult to measure and it is currently calculated from injection velocity. Eventually ultrasonic methods may allow direct measurement.

In-mould temperature is currently measured either by thermocouples or resistance thermometers. As with mould pressure it is undesirable to mount transducers in the mould as this adds complexity. However the real problem with mould temperature is the thermal inertia of the mould. Work by **Gao et al. (1996b)** on controlling mould temperature in order to control cavity pressure during cooling (after gate freeze) showed that 3 or 4 cycles were required for mould temperature to be controlled around a new value.

It was decided early on in this research into P-Q control that any proposed control strategy should use the minimum number of transducers necessary. Ideally on a hydraulic injection moulding machine this would be actuator displacement and hydraulic injection pressure, since these transducers are already necessary for any basic process control.

1.4 Injection Moulding Inject-Phase Control

A more detailed review of possible injection moulding control strategies and their strengths and weaknesses is given in Chapter 4. This section is intended to give an introduction to the work that has been published in this field and the current industry practice.

Inject-phase control covers the filling, packing and holding phases of the injection moulding cycle. Two different approaches can be taken depending on whether a suitable cavity pressure transducer is fitted. If one is fitted, then injection control can be based on cavity pressure alone and a learning, neural network based controller is commercially available from Kistler. While only brief details are given in the brochure convergence to the desired cavity pressure profile is claimed after 10 moulding cycles. Clearly the success of a such a method is dependent on the design of the mould and more importantly the positioning of the cavity pressure transducer. Promising results for an adaptive model-following scheme have been presented by **Chiu et al. (1991)**. The scheme was implemented to control cavity pressure during filling and then to switch to packing pressure control once a certain pressure was reached. The scheme was compared to a proportional plus integral (PI) cavity pressure filling controller and shown to have a smaller pressure tracking error. Another similar paper on the cavity pressure control of the filling phase is that by **Gao et al. (1994)**. In this instance a self-tuning regulator was implemented and shown to be robust to a change in mould. Again packing-phase control was not addressed.

If no cavity pressure transducer is fitted then filling control is typically velocity controlled and packing is pressure controlled (nozzle or hydraulic). Adaptive velocity control of the filling phase has been reported by **Zhang et al. (1996)** but again this was considered in isolation from packing control. More recently fuzzy logic control of filling velocity has been reported by **Tsoi & Gao (1999)**. The controller was shown to outperform a fixed gain PI velocity controller and was shown to be robust to changes in barrel temperature, material and mould. Fuzzy logic control of filling and packing has also been reported by **Huang & Lee (2000)**. Although the controller regulated filling velocity and packing pressure

the switch between the 2 control objectives was on actuator position which was set manually.

1.5 Scope of Research Undertaken

In the course of a 3 year PhD research program it would be impossible to try to tackle, with sufficient detail, the control of an entire injection moulding machine using the all-phase approach. Also while the cost of microprocessors continues to fall it is still unlikely that a sufficiently fast processor is available at a low enough price for such a solution to be commercially viable for some time. At the outset the *filling* and *packing* phases of injection moulding were therefore chosen for analysis and improved control. However as the work progressed and knowledge was gained the control of *packing* and the *filling* to *packing* transition was identified as an important and often overlooked area to be focused on. The *filling* and *packing* phases were also chosen because of the hydraulic control bias of this work and the involvement of Aeroquip Vickers (now part of Eaton Corp.), who sponsored the work via an EPSRC CASE studentship. Aeroquip Vickers supply hydraulic components to injection moulding machine original equipment manufacturers and the phases in injection moulding that their components have most impact on are *filling*, *packing* and *holding* as well as die movement and clamping force control. However it is important to stress that the plant models identified in this work could be relevant to an all-electric injection moulding machine. If the results were to be applied to such machines account would have to be taken of the different machine dynamics.

Two of the most important phases of injection moulding are *filling* and *packing* and it is the control of these two phases that is considered in this thesis. The broad requirements for the control of these two phases are velocity controlled filling to give a nominally constant melt front advancement velocity through the mould and smooth pressure controlled packing without overshoot. This is often done on a hydraulic machine using a pressure and flow controller (P-Q controller); currently an engineer is required to tune P-Q controllers during commissioning. P-Q control can either be performed in conjunction with a proportional flow control valve and a proportional pressure relief valve, as in the

work by **Alleyne & Zheng (2000)** or using a single P-Q valve. It is perhaps convenient to separate pressure and flow control into the control of 2 valves; however the hardware costs are always likely to be more than for the single valve solution. For this reason the single valve approach was chosen for this work.

It was also the aim of this work to produce a "self -commissioning" controller working in conjunction with a single P-Q valve for hydraulic injection moulding machines. Clearly the control of flow and pressure in hydraulics is a fairly common task and it was envisaged the results of this work could be applied to other systems. It was also noted early on that concepts used in other force and velocity control applications, hydraulic or otherwise, could be used in injection moulding. It was also noted early on that for commercial exploitation by Aeroquip Vickers any solution would have to be potentially saleable and based on a sound understanding of the injection moulding process. This implied that a black box type control technique would be of questionable value. Moreover any solution developed should not be reliant upon expensive transducers that will require retrofittment. This means that only hydraulic pressure and actuator displacement were made available.

The methodology used to evaluate potential controllers was to:

1. Model the filling and packing phases of injection moulding and compare simulation with experimental results from a real injection moulding machine (Chapter 2).
2. Construct a hardware-in-the-loop type emulation of the injection moulding process so that control solutions can be tested in a more realistic environment as compared to simulation (Chapter 3)
3. Carry out analysis of the now-understood injection moulding phases and armed with this knowledge make an informed choice of the most suitable control strategies (Chapter 4).
4. Test the most suitable control strategy and compare its performance against the current industry standard one (Chapter 5).
5. Draw conclusions from the work undertaken (Chapter 6).

Literature reviews relevant to each separate topic are included in each chapter.

Figure 1.1 A Simplified Injection Moulding Machine

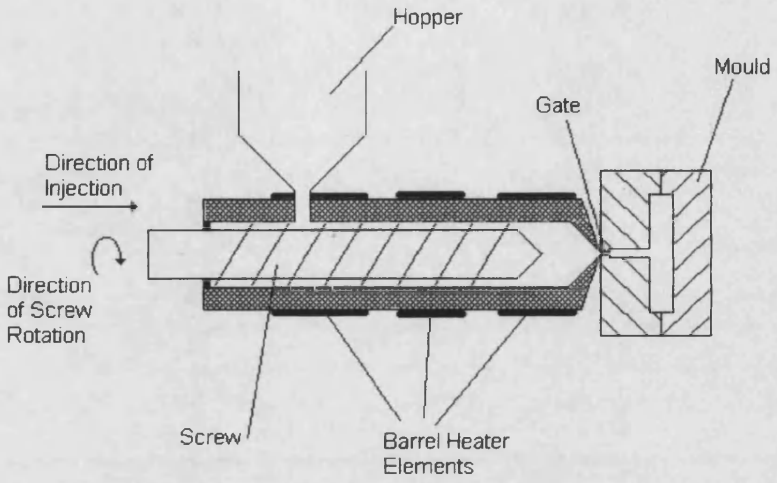

Figure 1.2 Moulded Part & Runners

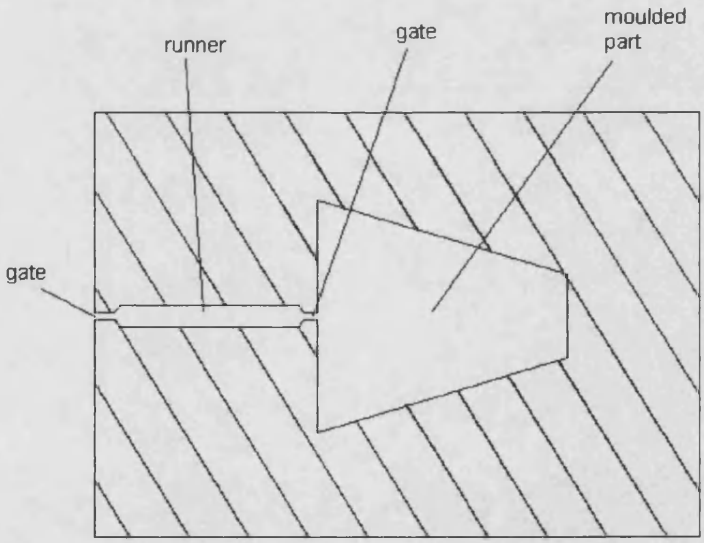

Figure 1.3 Polypropylene Pressure Volume Temperature Diagram

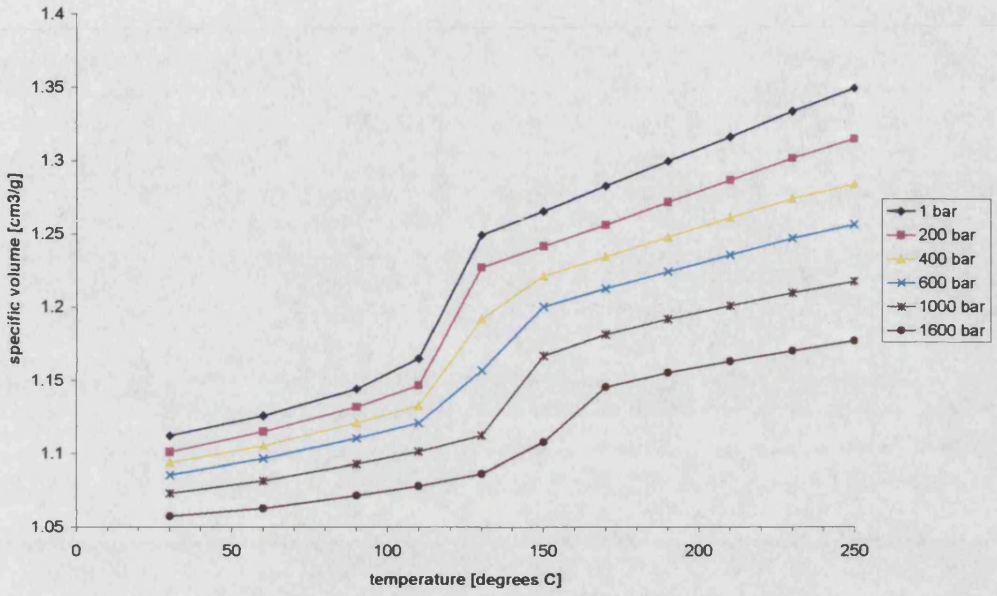

2.0 Modelling & Simulation of Injection Moulding

2.1 Introduction

Whilst it would be advantageous in many ways to test a new P-Q control strategy on a full size injection moulding machine, this would be very costly. Simulation offers a cheap and effective way of filtering out unsuitable strategies, with only the most promising being evaluated using full scale testing. However, as a result of simplifications and assumptions effects such as pump pressure ripple and electrical noise are not adequately modelled. For this reason a more detailed evaluation following on from simulation is required. Ideally this should be cheaper and more flexible than through full scale testing. Such a requirement can be met using a 'hardware-in-the-loop' approach (**Ramden et al. (1997)**). Such an investigation is detailed in the next chapter. This chapter describes the mathematical modelling and simulation of the inject phase of injection moulding. The mould used had a capacity of 20ml and was filled with polypropylene. The work detailed in this chapter resulted in a paper presented at the 1999 American Society of Mechanical Engineers (ASME) Winter Annual Conference, a copy of this work is included in Appendix A.

2.1.1 Bath*fp* *Simulation Software*

The Bath*fp* simulation package (**Tilley & Richards (1991)**) was employed for the simulation study. This package is based on a type-insensitive integrator incorporating 2 radically different variable step variable order integration algorithms with an automatic switching mechanism. See **Richards et al. (1990)** for a more detailed explanation of type-insensitive integrators and automatic switching. There are 2 different type-insensitive algorithms available to use in Bath*fp*; a modified LSODA integrator (originally developed by **Petzold (1983)**) and the RADAU5 integrator described by **Hairer & Wanner (1991)**. A study was carried out and reported on by **Lo (1995)** which determined that compared to LSODA the RADAU5 integrator was better suited to the solution of certain types of numerically stiff problems. Hence the RADAU5 integrator was used in this work. This is not to say that the LSODA algorithm is ineffective; it is in fact used extensively in commercially available dynamic system simulation software (Amesim) produced by Imagine S.A. of France

The mathematical model of the injection moulding process is represented in Bath*fp* as a 'load'. This can be linked to an actuator and will from this point on be referred to as the load model.

2.2 Polymer Structure & Flow Characteristics

To model the injection moulding process it is essential to have an appreciation of the non-Newtonian properties of polymeric liquids.

Polymeric fluids are often called viscoelastic fluids. Such materials have elasticity and after deformation will attempt to return to the original shape but will not usually reach it because of the viscous properties. Full mathematical modelling of viscoelastic behaviour is complicated, usually containing temperature-dependent relaxation constants which describe how the fluid body reacts to forces acting on it (**Bird et al. (1987)**). This level of detail is unnecessary for the study reported here.

Newtonian viscosity is of little or no use for describing polymer flow. There are 5 recognised relationships for predicting shear rate of non-Newtonian fluids. These are as follows:

- Pseudoplastic (shear thinning), where

  $$\tau = \eta_N \dot{\gamma}^n \qquad (2.1)$$

  with n<1
- Dilatant (shear thickening), which again follows equation (2.1) but with n>1
- Bingham, where

  $$\tau - \tau_y = \eta\dot{\gamma} \qquad (2.2)$$
- Plastic, which is a combination of the Bingham and Pseudoplastic relationships.
- Ostwald (Which according to (**Lenk (1978)**) is yet to be fully proven as existing.)

Graphical illustrations of the relationships between shear stress and shear rate for these 5 flow phenotypes together with Newtonian Behaviour are shown in Figure 2.1. Of these the Ostwald and Bingham types are not relevant here as they do not

describe polymer flow. Pseudoplastic (shear thinning) and dilatant (shear thickening) are of greatest interest with good examples being polypropylene (used in this study) and a blend of polycarbonate and ABS respectively. The plastic relationship is also relevant to polymer although, in practice the yield stress needed for polymer flow to start is so low that there is no need for the inclusion of the Bingham relationship in practice.

For both the pseudoplastic and dilatant relationships described by equation (2.1) η_N is the zero shear (Newtonian) viscosity. If n=1 then the equation (2.1) describes the Newtonian relationship.

2.2.1 Polymer Flow Governing Equations

For simulation purposes a relationship between polymer flow and injection actuator pressure is required. Incorporating the power law for viscosity into the Hagen-Poiseuille equation for flow through pipes gives equation (2.3) which describes the pressure drop over a pipe of radius R and length l, where k is both material and temperature dependent. Equation (2.4) is the equivalent for rectangular channels with height h and width w.

$$P = \frac{2\left(\frac{4}{\pi}\right)^n klQ^n}{R^{3n+1}} \qquad (2.3)$$

$$P = \frac{2(6)^n klQ^n}{w^n h^{2n+1}} \qquad (2.4)$$

(if $n=1$ then the power law index equation becomes the Hagen-Poiseuille equation)

With some manipulation, equations based on equation (2.3) can be derived to describe pressure requirements for diverging and converging sections. However, in such sections, a further flow elongation effect occurs that needs to be taken into account. Figure 2.2 shows an example of the behaviour in a converging section. The corresponding differential pressure over the converging section is described by equations (2.5) and (2.6) where λ_T is both material and temperature dependent.

$$\sigma_E = \lambda_T \frac{\dot{\gamma}}{2} \tan\theta \qquad (2.5)$$

$$P_g = \frac{2}{3}\sigma_g \left[1 - \left(\frac{r_2}{r_1}\right)^3\right] \qquad (2.6)$$

2.2.2 Bulk Modulus and Shrinkage During Cooling

During the cooling phase of injection moulding the polymeric material in the mould shrinks. To counteract this the material in the mould is pressurised during the *packing* and *holding* phases. The higher the *packing* and *holding* pressures the less shrinkage that will occur. Care must be taken when setting these pressures as if they are too high negative shrinkage (expansion) can occur which leads to *sticking* with the finished part stuck in the mould. Molten polymeric material is more compressible than solid material and as it cools in the mould the bulk modulus increases.

The equations describing polymeric material solidification during cooling are complex and many papers have been published on of the process. The aim of most of this work is to better understand the mechanisms that lead to shrinkage and residual stresses in moulded parts. Notable works are those by **Bushko & Stokes (1995a, 1995b, 1996a, 1996b)** and **Kambour et al. (1996)**. The principal sources of complexity arise from the change in polymeric material properties during the transition from liquid to solid and the effects of temperature and pressure histories on the moulded part. It is the intention of this work to model mean values of bulk modulus change and shrinkage during cooling rather than trying to predict final part warpage or stress levels.

Since the mould walls are much colder than the polymeric glass transition (softening) temperature the process of polymeric material cooling begins with rapid skin formation in any part of the mould reached by the melt front. This means that effective flow area through any part of the mould will decrease due to skin formation. In this work, as in others before it, this effect has been ignored and shear heating is assumed to be sufficient to minimise significant skin formation.

Pressure volume temperature data for polypropylene from **Kenndaten für die Verarbeitung** (previously presented in Figure 1.3) is reproduced in Figure 2.3. The graph shows that in the range 1 to 1600 bar as the material cools from 250°C to 30°C the specific volume decreases i.e. it shrinks. 1600 bar may at first sight seem to be too high a pressure to consider. However in injection moulding there is typically a 10:1 pressure increase between hydraulic injection pressure and nozzle injection pressure. 1600 bar nozzle pressure is therefore the same as 160 bar hydraulic injection pressure. The graph also shows that if the pressure increases the specific volume drops. i.e. the polymer is compressed. More generally the lines on the graph all appear to be made up of a high temperature region between 250°C and 150°C where specific volume changes linearly with temperature and a low temperature one between 110°C and 30°C. These 2 regions are then linked by a transition region. These 3 regions all relate to the physical state of the polymer. The low temperature region is the solid phase, the high temperature phase is the liquid phase with the transition region between the two.

The data in Figure 2.3 was manipulated to give the more useful graphs of bulk modulus and shrinkage, shown in Figure 2.4 and Figure 2.5 respectively. The bulk modulus calculated from the original data is the secant bulk modulus using the 1 bar data set as the starting point in all cases. The shrinkage calculated was the cumulative shrinkage, which considered the polymer start point to be at 250°C.

From Figure 2.4 it is clear that bulk modulus increases with pressure. Bulk modulus also increases as the polymer cools during the liquid phase, dips slightly during transition from liquid to solid and then increases as it cools during the solid phase. This is all except the data for 200 bar, where bulk modulus does not dip during transition and decreases slightly between 60°C and 30°C in the solid phase. During the liquid phase (250°C – 150°C) the bulk modulus is between 15000 bar and 8000 bar depending on temperature and pressure. Overall during the solid phase (110°C - 30°C) the bulk modulus is between 13000 bar and

33000 bar. For the purposes of this research it is only the bulk modulus during the liquid phase that is of interest.

Volumetric shrinkage also occurs during *cooling*, percentage shrinkage is plotted against temperature for a range of pressures in Figure 2.5. Again the liquid and solid phases are clearly defined and as one would expect the higher the pressure the lower the shrinkage. What is slightly surprising is the level of shrinkage occurring between 250°C and 30°C, which varies between 10% @ 1600bar and 18% @ 1bar. This alone illustrates the need for a *packing* phase. From the point of view of *cooling* phase modelling, if the liquid phase is defined as between 250°C and 150°C then volumetric shrinkage at the end of the liquid phase will vary between 4.5% and 6.5% depending on packing pressure.

It is also important to remember that compared to the *filling* phase *cooling* takes a long time. A typical *cooling* phase will take several seconds and can last up to tens of seconds for larger moulds. Clearly cooling time is governed by the mould temperature, the heat transfer rate in the polymeric material, the heat transfer rate in the mould itself and the volume of polymeric material in the mould. Generally the larger the mould the longer the cooling time.

2.3 Injection Moulding Process Modelling & Simulation

At the onset of *packing* the polymeric material being injected is still molten but since the mould temperature is well below the melting temperature of the polymer it soon cools and freezes. According to **Gao et al. (1996b)** the only feasible way to effect the mould cavity pressure after gate freeze is by changing the temperature of the mould itself. This can be achieved by passing a cooling fluid (typically water or oil) through channels in the dies. Since the work in this thesis is intended to aid the study of the control of the *filling* and *packing* phases, the *cooling* phase after gate freeze is not addressed here. Even so, the effects of cooling before *gate freeze* may have an effect on *packing* pressure control. As such *cooling* is simulated but no attempt is made to model gate freeze.

As previously mentioned, the injection moulding load model was developed in the package Bath*fp*. A screenshot of the environment with the icon used for the load model is shown in Figure 2.6. The package allows models to be written in the C or Fortran programming languages and associated with an icon constructed using the Bathicon utility. Standard model file structures help simplify the inclusion of new models within the package using the Bathmat utility. The icon can then be connected up with other models via ports to allow variable values to be exchanged. While the package runs in a Unix environment it is controlled via a graphical user interface. Clicking on most of the buttons in Figure 2.6 reveals other sub menus with further choices including setting component and simulation parameters. Many hydraulic components exist within the package as standard models and were used as part of this work.

To model *cooling* effectively, both shrinkage and bulk modulus increase have to be incorporated. In a real mould the finished part will not cool uniformly and so bulk modulus change and shrinkage will occur locally and in a non-linear time-varying fashion. The development of a Bath*fp* model of injection moulding has only ever been intended to give an approximation of injection moulding for controller design and evaluation. With this in mind, shrinkage and bulk modulus change need to be taken into account but only global changes will be considered. In any case if local changes in bulk modulus and shrinkage were to be simulated a finite element method would have to be employed which would require a completely different approach to simulation compared to the one taken here.

The increase in bulk modulus was therefore included in the Bath*fp* load model by defining the cooling time, together with the bulk modulus at the start and end of cooling. Using equation (2.7) the bulk modulus was then increased linearly between the 2 values over the cooling period. This is shown in Figure 2.7. The values chosen from the data in Figure 2.4 were: start bulk modulus 8000bar, end bulk modulus 15000bar.

$$\frac{F}{Y} = \frac{A^2 \beta_{poly}}{V_{poly}} \qquad (2.7)$$

The reality of shrinkage during *cooling* is that more material is forced into the mould until gate freeze occurs. Hence during *cooling*, because of shrinkage there will be a small flow of material into the mould. It was decided that the simplest way to incorporate this in the Bath*fp* model was to introduce an artificial flow path at the onset of packing. This user-defined cylindrical flow path was positioned to bleed off flow to atmosphere directly out of the injection barrel. The diameter and length of the flow path determines the flowrate of polymeric material out of this flow path. Flow elongation effects were not taken into account but the flow was treated as non-Newtonian and the modified Hagen-Poiseuille equation (3), incorporating the power law index, was used. In light of the data in Figure 2.5 the shrinkage flow path was set up to bleed off 10% of the total mould volume during *cooling*.

2.3.1 Load Model Description

The load model was developed for the case of a real mould (comprised of two "materials testing machine specimens"). An image of the part produced by this mould can be seen in Figure 2.8. In order to model the mould the following assumptions were made:

- Flow is one-dimensional and laminar.
- Flow is incompressible during the filling stage. This assumption is adopted in the majority of simulations detailed in previously-published work. If the flow were to be modelled as compressible during the filling phase this would complicate the model considerably and a finite element method would have to be used.
- Flow is compressible as soon as the mould is full.
- Once the mould is full bulk modulus increases linearly with until the end of cooling time.
- Shrinkage due to cooling begins once the mould is full.
- Cooling takes place over a period of 1 second after the mould is full.
- Polymer flow is perfectly balanced between the 2 flow paths.
- Viscous filling forces include both the power law index and extensional viscosity.

- The process is isothermal. This is another simplification that has been used in the majority of simulations detailed in previously-published works. To include the effect of different temperatures throughout the part would add complexity and again require a finite element approach. The current model can however be run at different polymer temperatures.
- The mass of the polymer being injected, about 20g for the materials testing specimen mould, is considered negligibly small in comparison to the mass of the moving parts of the machine, 60kg. The mass of the polymer is not included in any calculation.
- Leakage past the screw in the injection barrel was ignored.

These assumptions are generally in agreement with those adopted by previous researchers, in particular **Shankar & Paul, (1982), Chiu et al. (1991), Wei et al. (1994), Rafizadeh et al. (1996)**, and 2 companion papers **Chiang et al. (1991a)** and **Chiang et al. (1991b)**. If anything the *cooling* phase time used in this work is too short. However more rapid cooling will have a greater effect on *packing* control.

The Bath*fp* load model has been developed such that a force is the output and injection actuator position and velocity are required as inputs. To determine the equations required to calculate the load force, the mould melt front is tracked during mould *filling*. The mould melt front position is calculated from the volume of material that has entered the mould, which is then compared with the total volume of the mould. This calculation is generally straightforward except in the case of converging and diverging sections when there are cubic equations to be solved an example is included below.

$$volume = \pi\left(\frac{1}{3}k_{cd}{}^{2}x^{2} + k_{cd}r_{2}x^{2} + xr_{2}^{2}\right) \tag{2.8}$$

where $k_{cd} = \frac{r_2 - r_1}{x}$ (2.9)

A Newton-Raphson approximation was included in the code to deal with this requirement. While this method of solution usually takes 7 iterations to converge this did not slow down computation significantly.

The Bath*fp* model treats the part shown in Figure 2.8 as being comprised of the following series of shapes in series (a diagram showing this representation is presented in Figure 2.9):

At the extreme left of the figure is a converging section, equivalent to the injection moulding machine nozzle (this has no region number as it is permanently full). This is followed by a short, constant radius, section, corresponding to the mould entry gate (region 1) and then a diverging section, corresponding to the section joining the larger diameter runner to the small cross section gate (region 2). Region 3 corresponds to a constant radius section, equivalent to the runner and region 4 compromises two constant radius sections in parallel, equivalent to the runners serving each "materials testing" part. The two short converging sections at the end of each runner (region 5) join the larger radius runners with the small second gates at entry to the moulded parts. This is followed by two short constant radius sections, equivalent to the gates before the moulded parts (region 6) and finally two constant area rectangular sections, equivalent to the parts to be moulded (region 7).

The different regions were modelled using equations (2.3), (2.4), (2.5), (2.6) and (2.7). As the melt front advanced further instances of each equation were introduced and added to the existing set of equations.

The end of each region was dealt with as a discontinuity, as after a discontinuity the information held by the integrator no longer applied and needed to be changed. Once the integrator stepped over a discontinuity the event was flagged within the model code and the current value of time used by the integrator was successfully reduced until it was within 1×10^{-10}s of the occurrence of the discontinuity. The integrator was then restarted and allowed to continue until either the next discontinuity or the end of the simulation run. While this undoubtedly increased simulation time the time taken was still typically less than 10 minutes which was considered acceptable.

This model readily allows the simulation of other moulds of similar geometry since the dimensions of each section can be changed.

2.4 Simulation Study

The first simulation runs were done using the load model connected directly to a hydraulic actuator. The electrohydraulic circuit diagram of this is shown in Figure 2.10. Except for the actuator all the hydraulic components and the signal input are standard library models within Bath*fp*. Full details of these models are given in **Tilley & Richards (1997)**.

The actuator model included stiction, Coulomb and viscous friction terms. The default values of 100N of stiction, 50N Coulomb friction and 300N/m/s viscous friction were used. Load forces were supplied to the actuator model from a separate load model. The model required extend-port flow rate (l/min), retract-port flow rate (l/min) and load force (N) from adjoining models. The model supplied retract-port pressure (bar), extend-port pressure (bar), displacement (m) and velocity (m/s) to adjoining models. The model (named HA01 in **Tilley & Richards (1997)**) was modified to have different annular areas as in the real injection moulding machine.

The standard programme library pipe model (named HP01 in **Tilley & Richards (1997)**) used was a constant volume hydraulic pipe or hose model which included pipe friction. Compressibility and air release/cavitation effects were taken into account but inertia was not included. Friction was taken into account using Darcy's equation with the turbulent friction factor obtained from the Colebrook formula. The pipe had a single outlet port and from one to three inlet ports. To simplify the model by lumping pressure losses due to end fitting together a single friction orifice was positioned at the outlet connection.

The relief valve model, referred to as RV01 in **Tilley & Richards (1997)**, from the standard programme library was used. This model was able to represent single stage or 2 stage type relief valves. This is because the model calculation relied solely upon pressure/flow characteristics. Fluid compressibility effects were not taken into account nor were the dynamics of the valve (the model reacted instantaneously to an increase in pressure) nor were hysteresis effects. The model also assumed that pressure rise, once cracking pressure had been

exceeded, is positive and linear with respect to flow. This pressure rise was set to 600L/min/bar. The inputs to the model were the inlet and output pressures (bar) and the outputs were the inlet and outlet flows (l/min).

Pump modelling was done using the simplest model from the standard programme library. Details of this model named PU00 can again be found in **Tilley & Richards (1997)**. The model considered only the steady state behaviour of the pump and did not take into account slip or case leakages, compressibility losses, viscous or pressure dependent losses. To take some account of these effects the pump displacement used in simulation was reduced by 20% compared to the pump fitted to the Arburg injection moulding machine. The model required inlet pressure (bar), outlet pressure (bar) and angular velocity (rpm) as inputs from adjoining models. From these inputs the model supplied inlet flowrate (l/min), outlet flowrate (l/min) and net torque (Nm) to adjoining models.

The standard programme library prime mover model named PM01 in **Tilley & Richards (1997)** was used to drive the pump and supplied a constant angular velocity in rev/min to the pump. This model required no inputs.

The tank model used was again from the standard programme library and considered the tank to be a fixed pressure source, either the pressure in a tank or from any other sources. There model required no inputs and the single output was pressure (bar).

The 3 position, 4 port directional control valve model from the standard programme library called VB02 in **Tilley & Richards (1997)** was used. This valve had the following central configuration; supply and return ports connected, A and B ports isolated. The valve could be actuated in a number of different ways including electrical solenoid, mechanical lever and pressure pilot line. Actuation signals were received by the valve from end-cap models attached to either end of the valve body. Dynamics of the valve spool were not included and the valve flow rate was calculated using steady state pressure/flow characteristics. The valve was in the central position when the net actuation signal was zero and fully open when +1 or –1. The model received inlet pressure

(bar) on the supply, return, A and B ports from adjoining models and supplied associated flows (l/min) for these 4 ports to adjoining models. In addition, the model received dimensionless spool position signals from adjoining end-cap models.

Two identical instances of a simple electrical solenoid valve actuator model (referred to as VA00 in **Tilley & Richards (1997)**) were used as end cap models. This model received an electrical signal and gave a dimensionless signal as an output to the valve. The output could be scaled using a user-defined maximum rated current.

Inputs to the valve actuator models were given by the standard programme library models for: a second order lag model (referred to as SOL0 in **Tilley & Richards (1997)**) and a duty cycle input (referred to as SIG0 in **Tilley & Richards (1997)**).

Values of n (in equations (2.3) and (2.4)) between 0.1 and 0.7 were tested in simulation and it was found that higher values of n lead to higher pressures throughout injection and that lower values of n lead to lower pressures. The final value chosen was n=0.5 which was in line with values reported by others including **Lenk (1978)** for similar materials.

Results from the simulation without the effects of cooling (constant bulk modulus during packing and no shrinkage) are shown in Figure 2.11. During the initial increase in pressure up to 0.18s mould regions 1-5 are filled. The subsequent short sharp rise in pressure at 0.2s occurs as regions 5 and 6 are filled. This is because flow elongation effects are significant in these regions and because region 6 is a small constriction.

Injection pressure results with the effects of cooling included (bulk modulus increasing from 8000bar to 15000bar and 10% shrinkage during the 1st second after the mould was filled) are shown in Figure 2.12. No difference can be seen between results with and without cooling included. In fact if the 2 injection pressure results are put on the same graph the resulting lines overlap perfectly.

The only difference between the 2 sets of results is in actuator displacement. This is shown in Figure 2.13 but the difference between displacements only becomes significant after 1.0 seconds 0.55 seconds after the onset of packing.

2.5 Experimental Work

To achieve confidence in simulation results experimental tests were undertaken on an Arburg 25 tonne clamping force injection moulding machine using the same mould that was used in simulation. Two injection actuators, connected in parallel and of equivalent area to the single actuator used in simulation, were instrumented with pressure transducers and a displacement transducer. The injection moulding machine was set up with just enough material in the barrel to fill the mould and the injection controller was set up to give the maximum injection velocity with no switch to pressure control. The results obtained experimentally are presented in Figure 2.14. The rise in pressure up to 0.2s corresponds to the mould fill up to the moulded part section. The injection pressure peak at the end of injection (0.55s) is at the point where filling is complete the material is being compressed. However, this compression only accounts for the first 5 bar of the pressure transient with the rest of all the transient is due to the injection actuators hitting their endstops.

2.6 Comparison of Experimental & Simulation Results

Experimental and load model injection pressures without cooling are compared in Figure 2.15. Mould fill can be seen to occur in both sets of results with the pressure increasing sharply at 0.45s in simulation and at 0.55s in the experimental results. The reason for this discrepancy is that polymer was able to leak internally in the injection barrel of the moulding machine used. This leakage was not modelled in simulation.

Simulation and experimental displacement results are compared in Figure 2.16. Clearly actuator velocity during filling is very similar. This was ensured by choosing the correct pump size in simulation. However actuator displacements after 0.45s cannot reasonably be compared. This is because in the experimental work the actuators hit their endstops rather than being decelerated by compressing the polymeric material in the mould as in the simulation results.

2.7 Further Simulation Validation

Further simulation validation work was carried out using commercially available injection moulding software. The pressure time results obtained contained the same features at similar times and pressures and compared well with the Bath*fp* load model results and the results obtained experimentally. However the work was done during a 1 month free evaluation period for the software and it was therefore not considered appropriate to include results from this investigation in this thesis.

2.8 Concluding Remarks

An injection moulding load model has been implemented in the Bath*fp* simulation package. For the case of a pseudoplastic material (polypropylene) good agreement has been achieved between simulated and experimental results. The effects of cooling at the onset of packing even with unreasonably fast cooling are small.

Figure 2.1 Flow Phenotypes

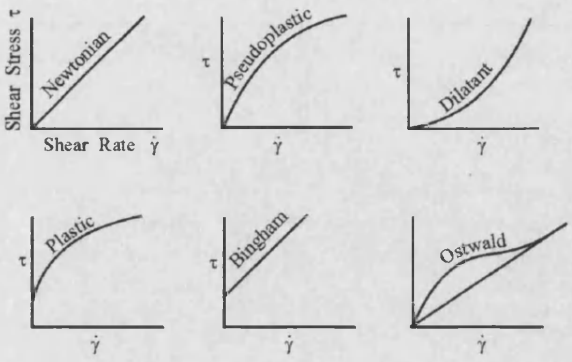

Figure 2.2 Flow Extension

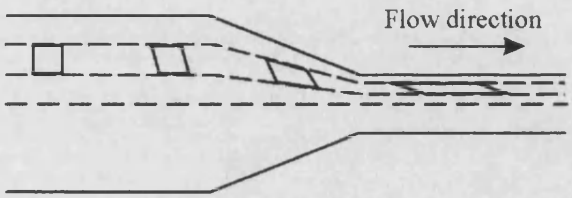

Figure 2.3 Polypropylene Specific Volume

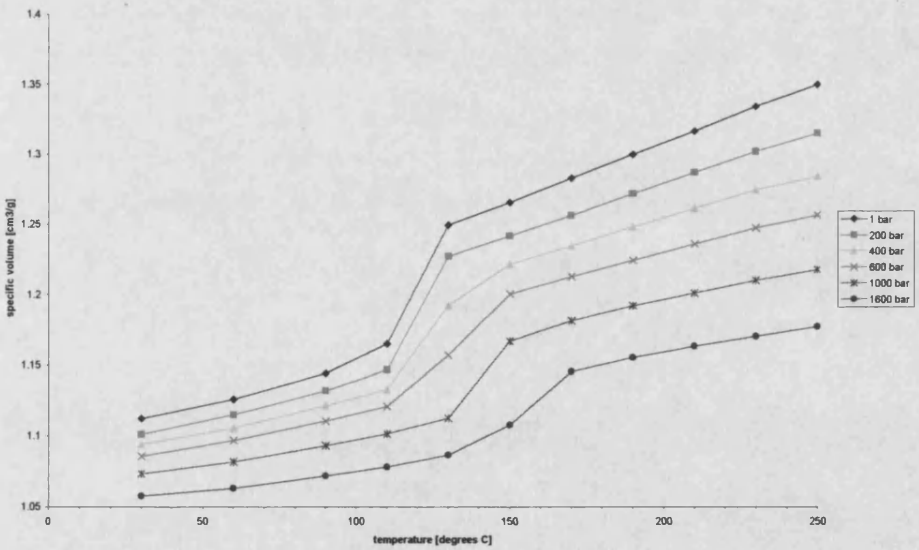

Figure 2.4 Polypropylene Secant Bulk Modulus

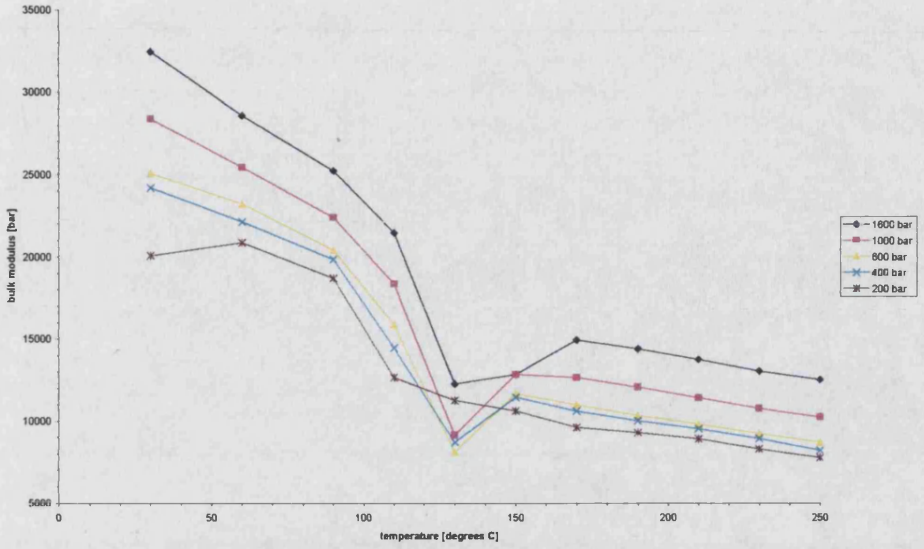

Figure 2.5 Polypropylene Shrinkage

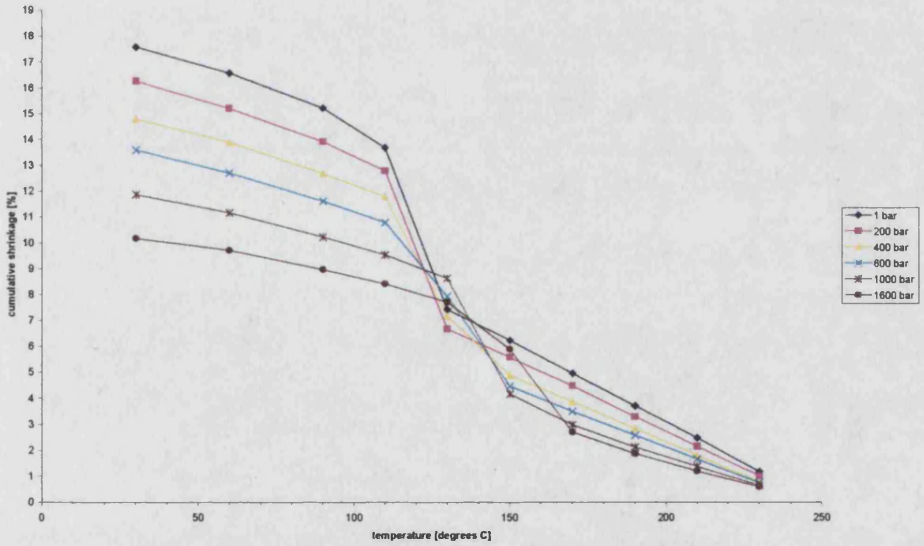

Figure 2.6 Bath*fp* Environment

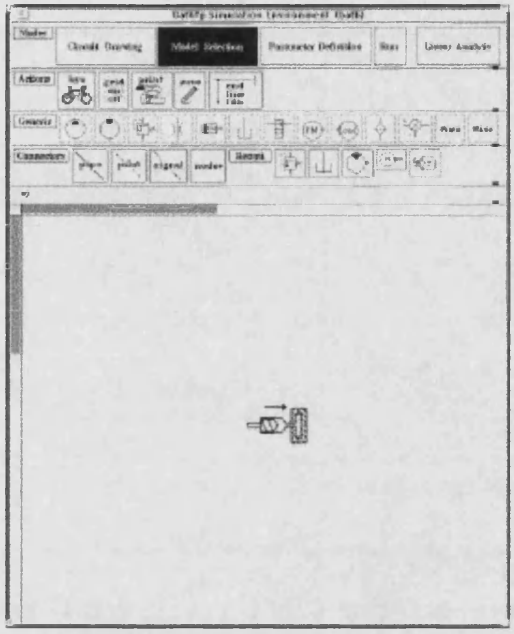

Figure 2.7 Simulated Bulk Modulus Change

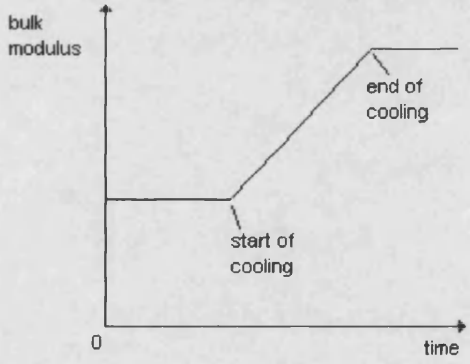

Figure 2.8 Image of Materials Testing Specimen Moulding

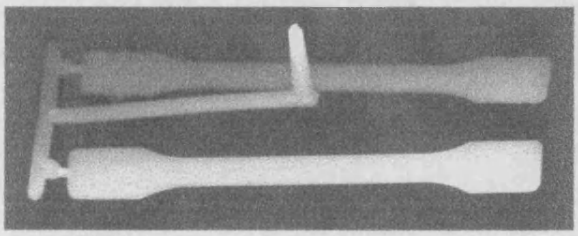

approximate scale 1:2

Figure 2.9 Simulated Mould Region Diagram

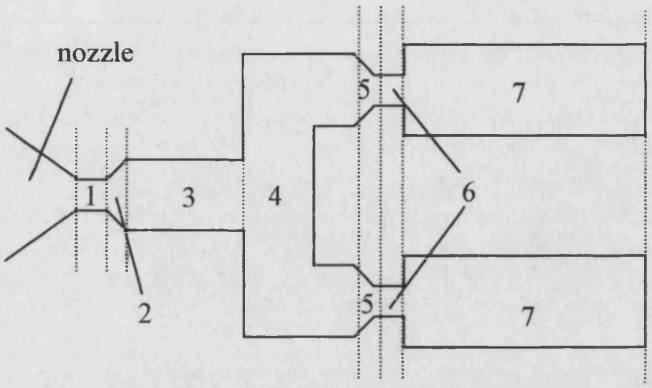

Figure 2.10 Hydraulic Load Simulation Circuit Diagram

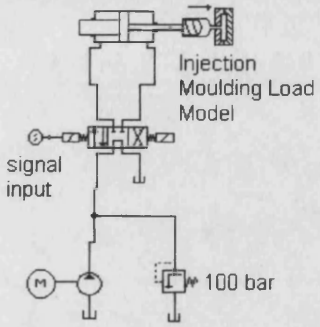

Figure 2.11 Load Model Simulation Results Without Cooling Effects

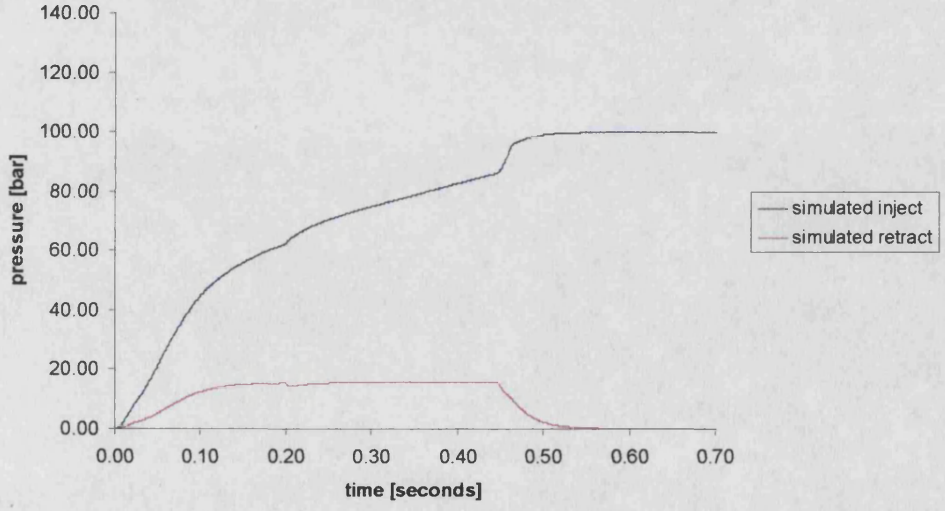

Figure 2.12 Load Model Simulation Results With Cooling Effects

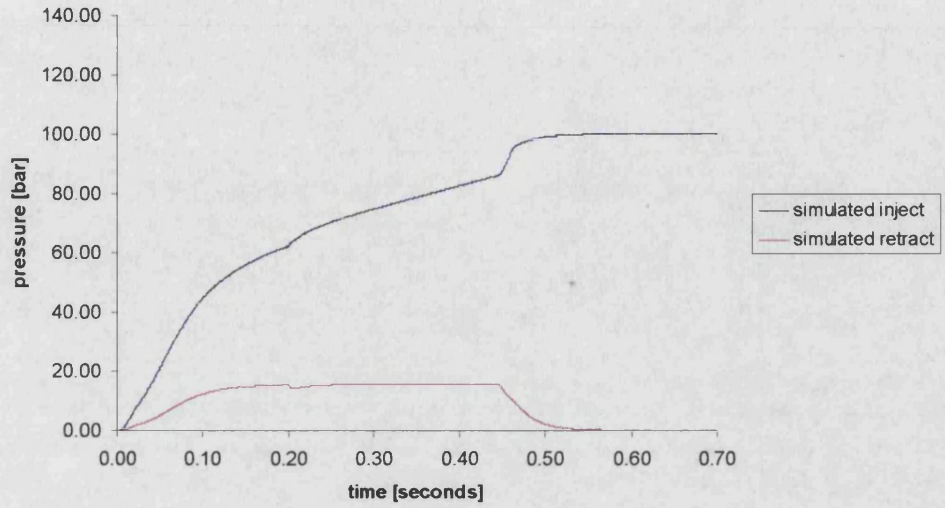

Figure 2.13 Simulated Actuator Displacement

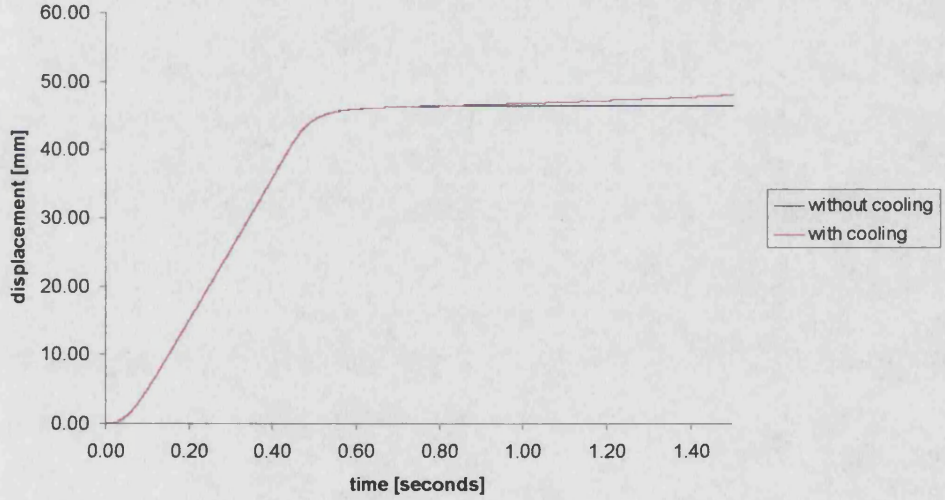

Figure 2.14 Experimental Results

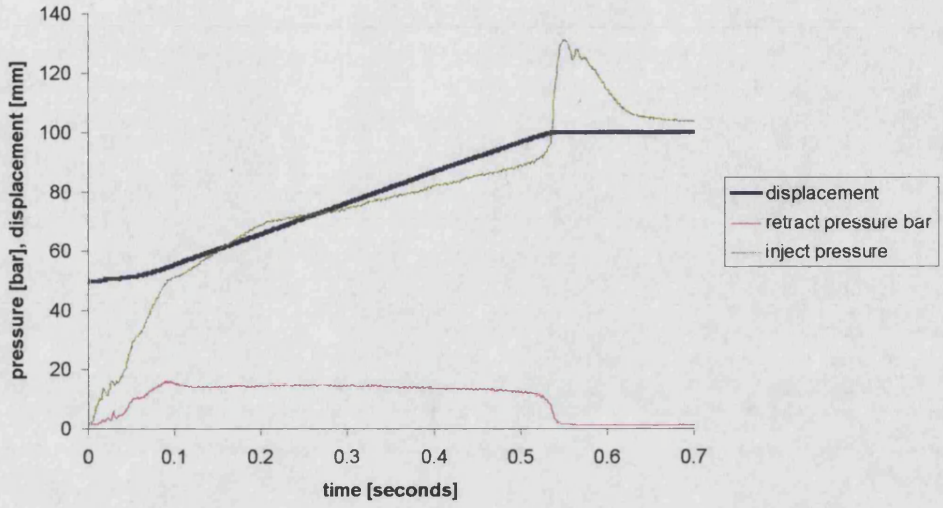

Figure 2.15 Experimental & Load Model Pressure

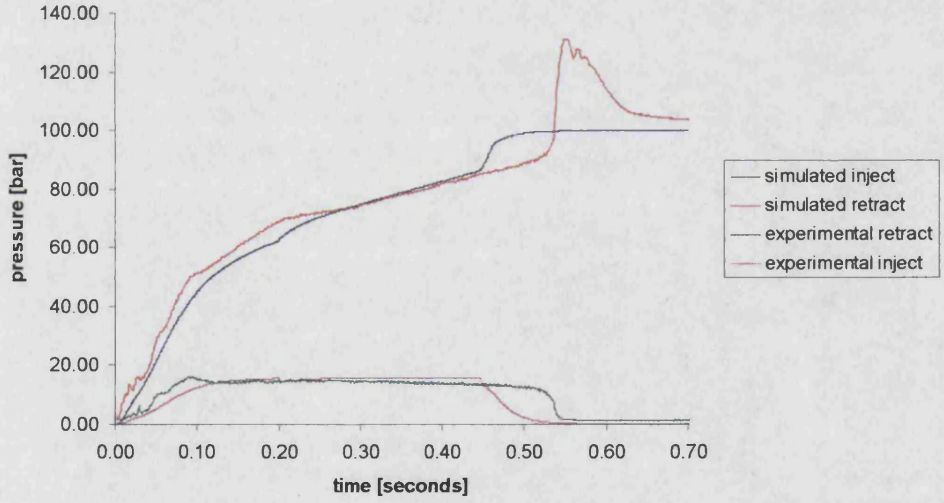

Figure 2.16 Experimental & Load Model Displacement

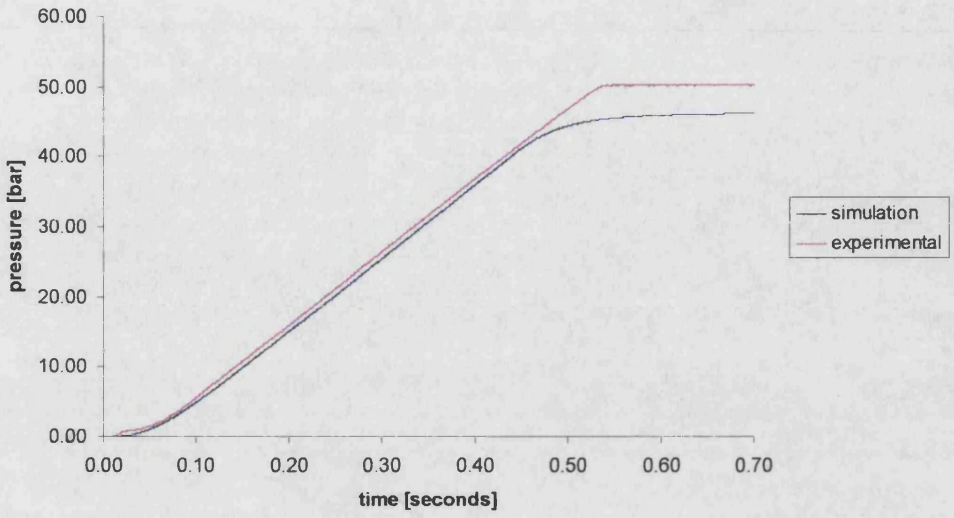

3.0 Load Emulation

3.1 Introduction

Currently many real life effects present in hydraulic systems, such as cavitation, are not fully understood and it is often the case that random (or non random) transducer noise is not included in simulation studies. As a result, system modelling and simulation results are simplifications and not all of a system's behaviour is predicted. These simplifications to some degree render simulation results idealistic. Because a load model, presented in the previous chapter, has been successfully constructed and injection moulding is better understood it may be considered appropriate to start new P-Q controller design and evaluation full scale testing. However although an injection moulding machine was available for pressure and displacement measurement during injection, the same machine was not available for controller testing. Instead an hydraulic representation of an injection moulding load (a load emulation) was designed, proven in a simulation study and built. The aim of this undertaking was to create a flexible platform to test existing and new control strategies in discrete time. Load emulations of other systems have been reported in the literature. This chapter commences with an evaluation of advantages and disadvantages of load emulation over full scale testing; a literature review is included. This is followed by rig design, load emulation control analysis and controller design.

3.1.1 Advantages and Disadvantages of Full Scale Testing or Load Emulation

First of all a load emulator can be defined as a system which statically and dynamically approximates the load from a real system. The reason for using a load emulation is often that the real system is too expensive or unsafe to run during prototype testing. Also, in full scale testing it is often only possible to test on one machine while there can be significant variations encountered between identical machines due to manufacturing tolerances. Emulating such differences is generally simple once the load emulation system is set up. The major disadvantage of load emulation is that the load is only an approximation and false dynamics may be present under certain operating conditions. This is especially true of a load emulation which is driven by another controlled system.

This is partly due to problems of causality. However this does not occur if the load emulation is acting on a purely passive system.

An advantage of full scale testing over load emulation is that the load supplied is true and without spurious dynamics. In any product design cycle a degree of full scale testing is required before the new product can be released to market. It is apparent from recent publications that with the current level of expertise in load emulation in new component or controller design, load emulation testing should be seen as an intermediate step in-between simulation and full scale testing. However one day it should be possible to omit full scale testing.

3.2 Literature Review

Load emulations can first of all be split up into 2 different types, forced and unforced. A forced load emulation is one where both the loading system and loaded system are powered. An unforced load emulation is one where only the loading system is powered. A good example of an unforced load emulation is detailed by **Saikko et al. (1992)**. In this example 5 artificial hip joints were subjected to an emulated load over an extended period of time as part of a wear study. The hip joints were not powered in any way and simply reacted to the independent load. The emulation detailed by **Ooi et al. (1991)** was of a video cassette recorder (VCR) mechanical deck. The emulation differed from the real system in that it was entirely electrical and was built to help evaluate new servo controllers. As such the emulation was of the forced type as it reacted to outputs from a controlled system (the servo controller). It seems from the paper that the emulator was in part intended for post production checking of VCR servo controllers. This is sensible since, as the authors pointed out, such a consumer device was intended for a light duty cycle. Prolonged and continuous use of a real mechanical deck would undoubtedly lead to mechanical deck breakdown. Whilst the emulation appears thorough, the mechanical deck must surely have suffered from some non-linearities and discontinuities such as stiction and backlash. By modelling mechanical components as equivalent electrical ones with the same time constants these effects seem to have been ignored or possibly even replaced with different ones. However it may be the case that in such a mechanism these are secondary effects. Even so there is some doubt as to the

applicability of a purely electrical emulator of a mechanical system for the testing of new control strategies.

Work on electrical motor load emulation using an electrical dynamometer (in the form of a vector controlled induction motor) is presented in **Akpolat et al. (1999)**. The experimental set-up used involved 2 vector controlled induction motors connected via a common shaft. As such the load emulation was forced. One of the motors was designated as the drive machine and the other one was designated as the loading machine. The load machine drive signal was determined from load torque and a reference model of the load being emulated. It is claimed that this preserved the physical causality of the real mechanical system, although this is not in agreement with other works reviewed later in this section. According to the authors most dynamometers of this type use the principle of 'inverse mechanical dynamics' to cancel out the inherent characteristics of the load machine before implementing the load model. It is shown that while the principle of 'inverse mechanical dynamics' may work well in simulation, when converted into discrete time this leads to instability. A speed tracking method is instead presented which gives accurate load emulation within the bandwidth of the load machine (in this case up to 50-100Hz).

More relevant work on hydraulic forced load emulation is detailed in **Ramdén et al. (1997)**. Importantly this also explains the 'hardware-in-the-loop' concept. This describes a system in which components are recreated in software with a suitable hardware interface to appear identical to the system as the component replaced. (Although it was not mentioned by the authors, the works by **Ooi et al. (1991)** and **Akpolat et al. (1999)** used this technique.) In order to emulate virtually any load for a 4 way 3 position hydraulic test valve it is necessary to vary the pressure and flow at both the service ports of the test valve. This was done using a load simulator which consisted of 2 servovalves, one for each service port. A circuit diagram is shown in Figure 3.1. For the results presented in the paper the 2 servovalves were controlled by a model of a linear actuator with an inertial load. However, as pointed out by the authors, the same arrangement could be used to emulate a hydraulic motor. Simulation and experimental load emulation results were compared and good agreement was

demonstrated using either pressure or estimated flow to control the load emulation. While this was encouraging, the emulation results were not compared with results from the real system.

One particular instance where full scale testing is expensive or inconvenient is in heavy vehicle suspension testing. A good paper on the modelling and tuning of a 4 axis road simulator (4 servo-controlled actuators, one under each wheel) is that by **Gardner et al. (1995)**. In this work each actuator was position controlled to follow a road profile supplied by a reference model. To ensure accurate reference model following it was shown by simulation that the proportional gain and pressure feedback gain of the servo-controlled actuators should be varied depending on the road surface being reproduced.

A much earlier work on load emulation is that by **Ohuchi & Ikai (1989)**. The focus of the work was to replace a linear viscous load and mass with a servovalve-controlled hydraulic actuator load emulation. The drive system was also a servovalve controlled actuator and as such this was a forced load emulation. The only description supplied of how the actuators were connected was with 'floating couplings'. It is important to note that while a coupling is undoubtedly required to take account of misalignments this may also add significant and spurious dynamics to the loading system. If instead the drive and load actuators were to be rigidly connected it would be very likely that misalignments would lead to non-linear friction levels in either the load or the drive actuator. To close the load emulation loop for mass and viscous friction, acceleration and velocity were used as feedback signals. This allowed the force being applied by the load emulation actuator to be calculated. Problems were encountered using acceleration signals and pressure feedback had to be included. While the results presented are useful in adding weight to the idea that hydraulic load emulation is possible, no details were given of the control system sampling rate or load dynamic response.

Possibly the most relevant work on hydraulic load emulation of linear motion is that by **Nimegeers et al. (1996)**. In this work the authors set out to emulate a non-linear load with one actuator (the load actuator) and drive the system with

the other (the drive actuator). The 2 hydraulic actuators were connected with a coupling. In this respect this is identical to the work by **Ohuchi & Ikai (1989)**. Controlling the load actuator under force control to emulate viscous friction and mass was found to lead to a dynamic force offset which was attributed to causality problems. It was found that with suitable compensation the offset could be reduced but not eliminated. Although the work reported by **Quinghe et al. (1999)** was on rotary load emulation using a servo-controlled hydraulic motor, it is interesting to note that a disturbance torque was reported. This is analogous to the dynamic force offset reported by **Nimegeers et al. (1996)**. The disturbance torque observed by **Quinghe et al. (1999)** was virtually eliminated by opening up a leakage path between the inlet and outlet ports of the loading motor and using a second servo-controlled loading motor for 'synchro-compensation'. The size of the orifice required was obtained experimentally. Unfortunately no details were given of the design of hydraulic motor used and it very likely that since different motor designs have different leakage characteristics the choice of motor would be important. The use of a second loading motor for 'synchro-compensation' also seems to work well but unfortunately scant detail is given and it is impossible to establish how the system worked.

Another paper which presents hydraulic force tracking limitations is that by **Alleyne & Liu (1999)**. The work stemmed from studies on active vehicle suspension systems and shows that although PID control is often sufficient for hydraulic position control it is inadequate for good force tracking control. Experimental work was carried out on a servovalve controlled actuator.

3.2.1 Summary

The first important conclusion to draw from this literature review is that load emulation is not a trivial matter and that an emulated load will inevitably differ from the real load. For this work it is important that the emulated load is a reasonable approximation to the real one. Causality problems have been noted in previous work, as has a dynamic force (or torque) offset. The need to retune controllers or implement load compensation strategies is something that is also common to many of the works reviewed.

3.3 Rig Design

The underlying theory behind the rig design was to recreate as much of a real injection moulding machine as possible and then emulate the parts which would have been impractical to have in the laboratory. In this case it was the molten plastic, heated barrel and mould that were impractical. The injection moulding load could then be recreated as essentially a position and velocity dependent non-linear viscous friction (filling) followed by a stiff spring (packing). This load could be created by metering flow out of a loading actuator. In previously published work such as **Nimegeers et al. (1996)** effort was devoted to emulating mass. However for this study it was felt that there was no point emulating mass when it could simply be added to the rig as required.

3.3.1 Load & Injection Actuator Simulation Study

First of all the concept of load emulation was tested in simulation using the circuit in Figure 3.2. In this instance the injection actuator was a full scale representation of the pair of actuators (with the same annulus areas) on the real injection moulding machine (detailed in section 2.0). To simplify force calculations the load actuator annulus areas were both the same as the extend side of the injection actuator.

The two actuators are connected together with a force transducer between them and instrumented with load position and velocity transducers. The actuator on the left is the injection actuator, which is controlled by an electrohydraulic valve with a supply-to-tank central position. Second order valve spool dynamics are separate from the valve because the valve model itself was instantaneous. Position and velocity signals are fed into the injection moulding load model, which then in turn acts as a reference model, producing demanded force output. The actual force, measured by the force transducer is subtracted from the demanded force and the resultant force error is amplified and fed to the load actuator servo-valve. This forms a closed loop proportional force controller. The spool dynamics are again introduced separately. The load actuator valve meters flow out of the actuator during extension (movement to the right in Figure 3.2). It was found during simulation that metering out was adequate and simpler to

control than having a pressure source connected via a spool valve to the load actuator. However with suitable valve spool flow characteristics around the closed position having a pressure source connected may be a benefit.

Simulation results for injection actuator pressure are shown in Figure 3.3 and injection actuator inject pressure is compared with experimental results in Figure 3.4. At the time these results were considered to be sufficient proof that a proportional force controller was adequate to lead on to rig design. However it was subsequently found that a proportional controller was only feasible because components were tuned to give the correct response and the dynamics of the load valve were reduced to a critically damped 20Hz 2^{nd} order response which limited the bandwidth of the system. Consequently a more complex controller was required in practice; the design of the controller is discussed later in this chapter.

Initially a symmetric valve was used as the injection control valve. However it was proposed that an industry standard injection moulding P-Q control valve should be used instead. This was because, ultimately, any new P-Q controller would be used in conjunction with such a valve. It was found that the spool cut of this valve was such that the injection actuator retract side was essentially connected to tank during injection and contributed negligible damping. This meant that the load emulation method suggested in section 3.3 (that is, the electrohydraulic circuit diagram shown in Figure 3.2) could be simplified. Actuator port B could be connected to tank and since port C was already connected to tank as well, the middle 2 actuator ports in the arrangement could be removed to form one actuator. An electrohydraulic circuit diagram of the arrangement is shown in Figure 3.5. It should also be noted that using only 1 actuator avoided possible alignment and safety problems that would have existed with a 2 actuator rig. To reduce rig size and power requirements a half-size representation was chosen using a 80mm diameter piston and 56mm rods. Again the circuit was tested in Bath*fp* simulation with a proportional controller and results were sufficiently good to initiate rig construction. However a proportional controller was again only successful because the components selected gave stable control.

Details of separate components and the reasons for selecting them is contained in the next section.

3.3.2 Hydraulic Components

The pump used was a 9 piston axial piston pump with variable swashplate angle and a pressure compensator to de-swash the pump at high pressure. The pressure compensator was set to de-swash the pump well above the pressure at which any of the tests carried out. The swashplate angle was set to give a maximum actuator velocity of 0.1m/s as on the Arburg injection moulding machine this work is based on.

Initially a single stage relief valve was used with a full flow pressure of 100bar but it was found that the cracking pressure was around 85bar which was affecting results. This was changed for a pilot operated relief valve which had a cracking pressure of 95bar with a full flow pressure of 100bar.

The actuator chosen had a piston diameter of 80mm, a rod diameter of 56mm and a 150mm stroke. The stroke of the actuator on the Arburg injection moulding machine was 100mm. The extra 50mm included in the stroke of the rig actuator was to ensure that injection could be emulated outside the cushioned zones of the stroke. The polymer stiffness to be emulated can be described by equation (3.1) and the maximum stiffness the rig can emulate is described by equation (3.2).

$$\frac{F}{Y}=\frac{A^2\beta_{poly}}{V_{poly}} \quad (3.1)$$

$$\frac{F}{Y}=\frac{A_1^2\beta_{oil}}{V_1} \quad (3.2)$$

Using the parameter values in Table 3.1 it was found that the real stiffness was 9.64×10^6N/m and that the maximum possible emulated stiffness on the rig would be 9.83×10^7N/m. Hence the maximum possible emulated stiffness was approximately ten times the real stiffness. However this maximum possible emulated stiffness relies on a hydraulic fluid (oil) bulk modulus of 15000bar and it is very common, especially in hydraulics, for the theoretical bulk modulus to be much higher (double or more) than the real bulk modulus. (This is due to entrainment of air and water and other effects.) Hence if the real oil bulk

modulus is half the theoretical bulk modulus then the rig can only be 5 times as stiff as the real system. This brief analysis also does not consider the effects of leakage past the load valve on the rig which would also lower the maximum bulk modulus that could be emulated. The effect of leakage past the screw on the Arburg injection moulding machine can be approximated as follows. The total screw travel in the experimental results (displayed in Figure 2.13) was 50.25mm. Without screw leakage this would have resulted in injection of 24.7 ml of polymer into the mould and with a full barrel of polymeric material only 40.73mm would have been required to fill the 20ml volume mould. If all the leakage is assumed to occur during the (high pressure) packing phase then 9.52mm of screw displacement at a hydraulic pressure of 100bar and a resultant nozzle pressure of 1000bar results in an equivalent bulk modulus of 4280bar. To be certain of the polymer bulk modulus used in the Arburg injection moulding machine nozzle pressure would be required. A nozzle pressure transducer was not available.

The load valve used was a MOOG servovalve, the flow rating of which was chosen with the aid of simulation results from section 3.3.1. The valve was rated at 36 l/min @ 30bar.

The P-Q valve was supplied by Vickers and was a proportional solenoid valve fitted with an industry-standard P-Q spool.

Although they are not shown in the circuit diagram in Figure 3.5, 2 filters were fitted to the rig. One was a full flow 10μm filter at pump outlet and the other was a 4μm filter upstream of the loading servovalve.

Cooling was taken care of by an offline oil-water heat exchanger controlled by a thermostat measuring tank temperature. The tank capacity was 500 litres and the tank temperature was held at 40-50°C during testing.

3.3.3 Data Acquisition and Control

To facilitate hardware-in-the-loop load emulation it was first of all decided that the data acquisition and control would be implemented digitally. A personal

computer and various data acquisition and control cards were available. Five separate solutions were considered.

1. Hand coding a program in C or C++ to control the rig via D-A and A-D cards in the rig computer.
2. Hand coding data acquisition and controller software to run on a 10 year old digital signal processor (DSP) card with suitable analogue inputs and outputs as part of a host computer.
3. Using National Instruments software and dedicated hardware to autobuild C code and an executable to either run on a personal computer (PC) processor or a dedicated processor.
4. Using MATLAB SIMULINK in conjunction with dSPACE hardware and the Real Time Workshop toolbox to run SIMULINK models on a dedicated processor with analogue inputs and outputs.
5. Using MATLAB SIMULINK, the Real Time Workshop toolbox and the Windows Target toolbox in conjunction with one of a list of supported data acquisition and control cards to create an executable from a SIMULINK model to run on a host PC processor.

Of the solutions available hand coding software to run on input and output cards in a host computer was ruled out as being too time consuming. Using the 10 year old DSP was investigated but all software and hardware was obsolete. The National Instruments software and hardware was found to be keenly priced and there is no doubt that it would have been a capable solution. However the department already had a MATLAB site licence and experience with dSPACE in automotive applications. Hence the choice was between using dSPACE hardware with a dedicated DSP or using the MATLAB real time windows target toolbox with a supported card. A supported card (Data Translation DT2811h) was already available from within the department and although the dSPACE solution would have been capable of running more complex algorithms it was decided to take the real time windows target option. This was partly because it was significantly cheaper but also because the processing power available was considered adequate.

3.3.4 Transducers

The pressure transducers used were semi-conductor strain gauge type. This type of transducer is characterised as having low hysterisis and good linearity characteristics and an overall bandwidth of 1kHz. The only problem with this type of transducer is its temperature dependency which begins to become significant above 80°C but since the hydraulic fluid used in the rig was cooled to between 40-50°C this was circumvented. This type of transducer also gives excellent performance for price which is the main reason why it was chosen.

Two displacement transducers were fitted to the rig. One an LVDT was used to measure displacement and the other, a pull wire potentiometer with a tachogenerator was used for measuring velocity. Two displacement transducers were fitted because the tachogenerator velocity and potentiometer displacement transducers were not sold separately. However the LVDT offered a more accurate displacement measurement.

3.3.5 Commissioning

During commissioning all transducers and their signal conditioning cards were calibrated. The pressure transducers were statically calibrated using a dead weight tester. The position transducers were calibrated using callipers with a vernier scale and the velocity transducer was calibrated using results from the calibrated displacement transducers. By far the most time consuming part of commissioning was flushing. This was done using a crude contaminant resistant valve to cyclically extend and retract the actuator. Then at 3-4 day intervals oil samples were taken and inspected under a microscope for contamination. This was done to rid the system of any particles that may have entered the rig during component manufacture or rig construction. After 4 weeks of flushing the rig was free of significant contamination. Unfortunately part way through experimental work one of the valves seized due to contamination. The actuator was identified as the source and a second period of flushing lasting 2 weeks was needed. While the actuator was undoubtedly more contaminated than should reasonably be expected the second period of flushing could perhaps have been avoided if the actuator had been mounted differently, with the ports underneath. Gravity would then have helped particles 'fall' out of the actuator. Also during

the 1st period of flushing a flexible pipe with more volume than that contained in the actuator was used on the injection side (as would be used for experimental work). This meant that there was little interchange between the oil in the actuator and fresh filtered oil from the tank.

3.4 Emulation & Compensation

As described in Chapter 2, the load during filling is essentially viscous friction with a dependency on position and velocity. Therefore, in order to test load emulation dynamics a viscous friction type load model was set up on the rig with a proportional gain force controller.

3.4.1 Initial Experimental Results

Pure viscous friction levels of 6.40×10^{4}Ns/m, 1.28×10^{5}Ns/m and 1.92×10^{5}Ns/m were initially set up. The injection control valve was set fully open in order to supply full pump flow to the injection side of the rig actuator. This resulted in the rig actuator extending at its maximum speed of 0.1m/s which it was calculated would lead to emulated pressures of 25bar, 50bar and 75bar. A fixed gain proportional controller was used with a gain of 4×10^{-5}. The results are shown in Figure 3.6, Figure 3.7 and Figure 3.8. The first thing to notice in Figure 3.6 is that the error is large; the demanded viscous friction should lead to a 25bar pressure load, instead 70bar load is emulated. This is an error of 280%. When the viscous friction is increased to 1.92×10^{5}Ns/m, which should lead to a load pressure of 50bar, a load of 85bar is emulated (an error of 70%). i.e. as the demand, in this case the viscosity, increases the error decreases. It may be expected that an error in demanded viscous friction would lead to emulation of a lower viscous friction and subsequently a lower-than-demanded pressure. However because of the way the load emulation was set up there was a negative error in valve displacement (the restriction through the load valve was too small) which leads to a higher-than-expected emulated pressure. This is consistent with a fixed gain proportional controller. The injection pressure overshoot at the start of load emulation in both Figure 3.6 and Figure 3.7 is due to the accumulator effect of the flexible pipe work between the pump and inject side of the actuator. Further increasing the emulated viscous friction to 1.92×10^{5}Ns/m should have led to an emulated pressure of 75bar. The results for this are shown in Figure 3.8.

Unfortunately such a level of viscous friction with a proportional gain controller leads to instability. Clearly a fixed gain controller is not adequate.

Part of the reason for the instability in these initial rig results is that the signal from the velocity transducer has a rich dynamic content. It was originally thought that this was simply noise. In order to rule out loading interference the rig actuator was extended with the load valve fully open and a fast Fourier transform (FFT) of the velocity signal was carried out. The results with a resolution of 2Hz are shown in Figure 3.9. It is clear from this that while there is some dynamic content at higher frequency, notably a peak at around 220Hz which corresponds to the pumping frequency, most of the dynamic content is below 50Hz. For comparison an FFT of equivalent velocity data from the real injection moulding machine used in Chapter 2 of this thesis is included in Figure 3.10. Again the results have a resolution of 2Hz. It is important to note that again the highest dynamic content is at low frequency but that there is also much more dynamic content at high frequency. The height of the low frequency peak in the real injection moulding machine results is nearly double that in the results from the rig. Hence although the dynamic content of the velocity transducer signal on the rig causes load emulation problems a velocity signal from a comparable real injection moulding machine is likely to contain higher amplitude dynamic content at low frequency and significantly more dynamic content at high frequency. The load emulation has therefore been successful in recreating the low frequency dynamic component from a real injection moulding machine. It is also worth noting that the low frequency component is far more important as it is of a sufficiently low frequency to be a real phenomenon rather than noise and as such would be difficult to filter out.

The cause of the low frequency dynamic content in the velocity signal is unclear and has not been actively pursued. However it is strongly suspected that such a velocity oscillation is caused by a flow oscillation in the pipework between the pump and the pressurised side of the actuator. One possible cause of this is highly non-linear actuator piston friction. Another candidate for flow oscillation initialisation is an oscillating system relief valve.

3.4.2 Meter-Out Pressure Control Analysis

To aid load emulation controller design a small perturbation analysis of meter-out pressure control was carried out. A diagram of the system considered is shown in Figure 3.11. The assumptions used are:

- The valve spool response is instantaneous (2^{nd} order dynamics will be introduced later).
- There is no actuator piston leakage.
- Actuator friction (viscous, stiction and Coulomb) is negligible.
- Oil bulk modulus is constant.
- Flow metered by a fully annular area.

Lower case symbols denote small changes in variables.

Original Equations	Linearised Equations
$Q = A_1 Ys - \frac{V_1 P_1}{\beta_{oil}} s$ (3.3)	$q = A_1 sy - \frac{V_1 s}{\beta_{oil}} p_1$ (3.3a)
$Q = X_1 X C_q \sqrt{\frac{2P_1}{\rho}}$ (3.4)	$q = X_1 C_q \sqrt{\frac{2P_1}{\rho}} x + \frac{X_1 X C_q}{2} \sqrt{\frac{2}{\rho P_1}} p_1$ (3.4a)
$F - A_1 P_1 = ms^2 Y$ (3.5)	$-A_1 p_1 = ms^2 y$ (3.5a)
	$y = \frac{-A_1}{ms^2} p_1$ (3.5b)

Let (3.3a) equal (3.4a)

$$A_1 sy - \frac{V_1 s}{\beta_{oil}} p_1 = X_1 C_q \sqrt{\frac{2P_1}{\rho}} x + \frac{X_1 X C_q}{2} \sqrt{\frac{2}{\rho P_1}} p_1 \quad (3.6)$$

Substitute for y from (3.5b)

$$A_1 s\left(\frac{-A_1}{ms^2}\right) - \frac{V_1 s}{\beta_{oil}} p_1 = X_1 C_q \sqrt{\frac{2P_1}{\rho}} x + \frac{X_1 X C_q}{2} \sqrt{\frac{2}{\rho P_1}} p_1 \quad (3.7)$$

Multiply through by ms and rearrange gives

$$\frac{p_1}{x} = \frac{-X_1 C_q m \sqrt{\frac{2P_1}{\rho}} s}{\frac{V_1 m}{\beta_{oil}} s^2 + \frac{X_1 X C_q m}{2} \sqrt{\frac{2}{\rho P_1}} s + A_1^2} \quad (3.8)$$

It is interesting to note that the transfer function has a negative gain. This is because increasing valve opening (x) will act to decrease the pressure in the actuator. Using a positive proportional controller gain would lead to instability. Instead a negative proportional gain is required.

For the purposes of analysis the overall system in Figure 3.12 is better described in block diagram form in Figure 3.13. This can then be re-arranged to show force as an input and velocity as an output, Figure 3.14. The block diagram in Figure 3.14 can then be reduced to equation (3.9)

$$\frac{v}{F} = \frac{1 + G_v(s) G_c(s)}{(m + m G_v(s) G_c(s)) s + C G_v(s) G_c(s)} \quad (3.9)$$

Since

$$G_v(s) = \frac{p_1}{x} \quad (3.10)$$

equation (3.6) can now be substituted in for $G_v(s)$. This gives

$$\frac{v}{F} = \frac{\frac{V_1 m s^2}{\beta_{oil}} + \left(\frac{X_1 X C_q m}{2} \sqrt{\frac{2}{\rho P_1}} - G_c(s) X_1 C_q m \sqrt{\frac{2P_1}{\rho}} \right) s + A_1^2}{s \left[\frac{V_1 m^2}{\beta_{oil}} s^2 + \left(\frac{X_1 X C_q m^2}{2} \sqrt{\frac{2}{\rho P_1}} - G_c(s) X_1 C_q m^2 \sqrt{\frac{2P_1}{\rho}} \right) s + \left(A_1^2 m - C G_c(s) X_1 C_q m \sqrt{\frac{2P_1}{\rho}} \right) \right]}$$

(3.11)

Taking the parameter values listed in Table 3.1 and setting $G_c(s) = -1$ (i.e. a unity gain proportional controller) the resulting root locus diagram, Figure 3.15 shows a stable system. However if 2nd order valve dynamics (critically damped, 50Hz natural frequency) with the same form as equation (3.12) are added the unstable root locus in Figure 3.16 is formed. (In all root locus diagrams in this

thesis crosses denote poles, circles denote zeroes and squares denote closed loop roots.)

$$G(s)=\frac{k\omega_n^2}{s^2+2\zeta\omega_n+\omega_n^2} \quad (3.12)$$

So far the analysis has involved a linearisation of the true non-linear system. In order to check that the inclusion of valve dynamics does lead to instability a more realistic non-linear simulation of the circuit in Figure 3.5 was set up and run using Bath*fp*. Emulation pressure and velocity results without valve dynamics are shown in Figure 3.17. As predicted by the root linear analysis the system is stable. Results with critically damped, 50Hz natural frequency 2nd order valve dynamics included are shown in Figure 3.18. As in the linear analysis the system is unstable.

Since the 2nd order valve dynamics are causing the stability problem it would seem very convenient to cancel them out with a 2nd order lead. If a 2nd order lead is designed to cancel out the valve dynamics and accompanied by a fast 2nd order lag (to achieve a realisable transfer function) then the same problem arises with the fast 2nd order lag. In fact if the 50Hz 2nd order valve dynamics are replaced by a 100Hz 2nd order term then the unstable poles are moved further right in the root locus diagram. This can be seen by comparing Figure 3.16 with Figure 3.19.

On inspection of the inner pressure control loop it was found that the proportional gain was set far too high. Reducing the proportional controller gain to -5×10^{-9} forced the root locus to that in Figure 3.20 where it is clear to see that the closed loop roots are stable. The corresponding closed loop Bode plot in Figure 3.21 showed a phase of 90° at low frequency. It was therefore decided that integral control would be more appropriate. A suitable integral controller was found to be $\frac{-3.1\times10^{-6}}{s}$. Whilst the gain of the controller may appear low it must be remembered that this is to offset the very high gain of the valve actuator system (a small change in valve displacement results in a large change in

pressure). The root locus using this controller is shown in Figure 3.22. From the position of the closed loop roots near the imaginary axis it is clear that the system is close to instability. This is mirrored by the resonant peak at 200Hz in the accompanying Bode plot in Figure 3.23. It should be noted that if the case considered here is the 'worst case' (i.e. the least stable) then this inner pressure control loop response is acceptable. However if it is not then further stabilisation will be required, in which case the integral controller gain will need to be reduced. This is covered in the parameter sensitivity analysis in section 3.4.3.

Using an integral-only controller for the inner pressure control loop and a feedback path compensator gain of 1 for the outer force control loop resulted in the overall root locus diagram in Figure 3.24. Although the position of the closed loop roots in the right hand side of the imaginary axis would lead to instability this could be rectified by reducing the pressure control loop feedback compensator gain. However it was found that this gain had to be set quite low at 0.04 and that the Bode plot of the closed loop system, displayed in Figure 3.25 had 140° phase lag at 200Hz. This was improved upon significantly by incorporating a 2nd order lead-lag compensator in the feedback path with a steady state gain of 0.15. (This replaced the previous compensator which was a simple gain of 0.04.) The transfer function of the compensator was $\frac{4s^2+1457s+3.036\times10^6}{s^2+1727s+2.057\times10^7}$ and the resulting root locus is shown in Figure 3.26. Because of differences in scales it is not immediately obvious how the uncompensated root locus in Figure 3.24 relates to the one in Figure 3.26. In brief the zeros of the compensator have been placed near to the poles closest to the imaginary axis. This had the effect of forming a stable locus between these poles and zeros. The poles of the compensator were then placed outside the other pole pair to force the locus closer to the real axis allowing a higher gain to be used. The Bode plot of the compensated system is shown in Figure 3.27. Clearly this is an improvement on uncompensated overall system Bode plot in Figure 3.25. It is important to note that the low frequency amplitude ratio of the overall system is lower at -83dB compared to –79dB without compensation (Figure 3.25). From this it can be concluded that on the rig the gain of the pressure control loop feedback compensator may need adjusting to attain the correct pressure.

As can be seen in the experimental results for the valve used on the rig in Figure 3.28, at constant flowrate valve pressure gain increases by a factor of approximately 10 with pressure. Consequently the overall gain of the load emulation circuit will increase with load pressure. To ensure stability it is likely that this will have to be compensated for on the rig. The spike in all the results is due to experimental error and is repeated because results were taken for only 1 flowrate and then calculated using the orifice equation for the 3 others.

3.4.3 Parameter Sensitivity Analysis

While the inner pressure loop and outer force loop compensators designed in the previous section have been shown to work well for one set of conditions it was not clear if the solution would work over an injection moulding load emulation cycle. Hence a parameter sensitivity analysis was required. The parameters varied included: 2^{nd} order valve dynamics, valve mean spool position, mass, volume of trapped oil and oil bulk modulus.

With the compensators as set in the previous section it was found that if the 2^{nd} order valve dynamics were increased above 75Hz this would lead to instability. However this could be compensated for by reducing the inner pressure control loop integral gain from -3.1×10^{-6} to -2×10^{-6}. (The minus sign is only present to cancel the minus sign in equation (3.2)).

In the analysis so far the valve spool position has been set to give the same actuator pressure as that used in calculations at the specified velocity, i.e. parameters have been set as they would be found in steady state. This is not what will happen dynamically in the real system. To investigate the potential effects of this actuator pressure was held at 50bar while the valve spool displacement was set to 10 times the steady state position and to 1/10 of the steady state position. In both cases it was found that to ensure stability the inner pressure control loop gain needed to be reduced from -3.1×10^{-6} to -2×10^{-6}.

It was also found that doubling or halving the mass using the inner pressure control loop gain of -3.1×10^{-6} led to instability but that reducing the gain magnitude to -2×10^{-6} made the system stable.

The volume of trapped oil between the meter-out valve and actuator piston was increased 10 times and reduced by 1/10. Reducing the volume of trapped oil improved stability and increasing it led to instability. Once again this instability could be compensated for by changing the inner pressure control loop gain to -2×10^{-6}.

The bulk modulus was originally set at 15000bar. In practice it is likely to be lower and so it was reduced to 8000bar. Again this had the effect of causing instability but this could again be compensated for by reducing the inner pressure control loop gain.

3.4.4 Conversion to Discrete Time

For the compensator ($\frac{4s^2+1457s+3.036\times10^6}{s^2+1727s+2.057\times10^7}$) to be implemented on the rig with a sampling frequency of 1kHz it had to be converted from continuous to discrete time. This was done using the Tustin approximation giving ($\frac{0.78z^2-0.93z+0.58}{z^2+1.18s+0.75}$).

Bode plots of the continuous time and discrete time implementations of the compensator are shown in Figure 3.29 and Figure 3.30 for comparison.

3.5 Rig Results

The inner pressure control loop was stabilised by an integral-only controller. The gain was set as high as possible to retain stability during injection moulding load emulation. In root locus terms the closed loop zeroes were set as close to the imaginary axis as possible. The 2nd order lead/lag overall system compensator was also implemented. It was found that the load pressure had a large steady state error and that the gain of the 2nd order force control loop compensator had to be raised. It was also necessary to pass the velocity transducer signal through a 2nd order low pass filter with a cut off frequency of 30Hz.

Load emulation pressure results from the rig (load pressure on the graph) are displayed in Figure 3.31 alongside the original injection moulding machine results. The first thing to notice is that the rig load emulation pressure starts from 22bar rather than 0bar as on the real injection moulding machine. This is because the rig actuator was extended from 0mm but the load valve was held open until load emulation was initiated at 30mm. This was done for two main reasons. Firstly it was important to carry out load emulation outside the cushioned part of the actuator stroke and secondly, starting load emulation with the actuator already moving and with the load valve fully open was found to be the best way of avoiding pressure peaks at startup. Hence 22bar load pressure is the lowest pressure that can be emulated at full actuator velocity. The next thing to notice comparing the two sets of results is how closely the emulated pressure follows the real injection moulding pressure. Even the pressure peaks at the end of injection are similar. Admittedly the rig pressure peaks 20bar lower at 110bar but the height and shape of pressure decay are certainly governed by the relief valve dynamics and, in the case of the injection moulding results the actuator cushioning arrangement. While it was never intended to reproduce this part of the injection moulding results it is encouraging that such agreement exists.

The same load emulation results are then displayed again in Figure 3.32 with the corresponding velocity and load reference model data. Firstly, despite filtering, the velocity signal still fluctuates considerably and these fluctuations are mirrored in the reference model pressure results during filling (filling is complete after 0.75s). Secondly the model following is adequate during the filling phase (up to 0.75s) but there is a significant phase lag during the packing phase and the load reference model pressure is oscillatory at the end of *packing*. Undoubtedly some of the load reference model oscillations are caused by the dynamic content of the filtered velocity signal. However since this was of such a low frequency, low frequency oscillations in the load reference model output were to be expected. As previously mentioned the relief valve dynamics were also having an effect at the end of *packing*. In order to minimise the effects of relief valve dynamics the same test was run with the injection valve restricting the flow into the loading actuator. By doing this not all flow would pass into the actuator and the relief valve would be open throughout emulated *filling* and *packing*. This

would avoid the relief valve dynamics affecting *packing* emulation so much. The results for this test are shown in Figure 3.33. Unfortunately the load reference model output is again oscillatory at the end of *packing*. The reason for this is that much as there is a minimum pressure that can be emulated there is also a maximum stiffness that can be emulated. This is because compressible oil was trapped between the rig actuator piston and the load valve. The oil had a bulk modulus of around 8000bar and without leakage this system was in theory 5 times as stiff as the stiffness it was required to emulate. Clearly it is important when emulating a stiffness to do this using a system that is stiffer than that to be emulated. What is unclear is how much stiffer the emulating system has to be. In this instance the leakage is hard to determine and nothing can be done to minimise it. Reducing the trapped oil volume would also increase stiffness. However the load valve was already mounted on top of the rig actuator and it was not desirable to change the actuator emulation initialisation position as this may begin to impede on the cushioning on the load side. Another solution considered was to run the rig actuator on 2 different hydraulic fluids – standard fluid for the injection side and a less compressible hydraulic fluid for the load side. Unfortunately this was ruled out because contamination between the 2 fluids due to cross-piston leakage was bound to occur. Also using 2 different fluids would require a second hydraulic pump in order to retract the actuator and this was considered too complicated a solution.

Hence the bulk modulus (of the polymeric material) to be emulated was lowered from 8000bar to 2000bar. It had also been noted during testing on the rig that if the inner pressure control loop integral gain was raised this improved low pressure tracking performance but lead to instability at high pressure. As suggested earlier it is likely that this was due to the increase in valve gain with pressure. Therefore a gain scheduling multiplier was also added to the inner pressure control loop after the integral controller. Gain was scheduled on pressure and was lowered from 1 to 0.1 linearly over the range 0-100bar. Load emulation results using this more advanced controller for an emulated bulk modulus of 2000bar are shown in Figure 3.34. Comparing the results to those in Figure 3.33 it is clear that packing emulation has been improved.

While it is unfortunate that emulating a bulk modulus of 8000bar is not possible, as previously mentioned, it is very common, especially in hydraulics, for the theoretical bulk modulus to be much higher than the real bulk modulus. This is due to entrainment of air and water and other effects. Hence it is quite possible that the 8000bar bulk modulus stated in the literature for polypropylene is higher than that encountered experimentally. Also, as previously stated, if all the barrel leakage is considered to have occurred during packing then this leakage had the effect of lowering the bulk modulus from 8000bar to 4280bar during packing. Hence a maximum emulated bulk modulus of 2000bar is still of the correct order for injection moulding and the emulation is still reasonable. Assuming that that load valve seals well in the closed position then the maximum stiffness that the rig can emulate is approximately 5 or 10 times stiffer than that required to emulate injection of polymer with a bulk modulus of 8000bar. The reason why a bulk modulus of only 2000bar can be emulated is a limitation of the load emulation control strategy developed. Essentially the inclusion of packing phase replaces the viscosity term (C) in Figure 3.14 with a lead integrator term as in equation (3.13). Unfortunately this has not explicitly been compensated for and limits the maximum stiffness that can be emulated. However it was decided early on in this work that the load emulation controller would be a single controller strategy rather than 2 controllers linked with a bumpless transfer mechanism. This decision was taken in order to avoid designing a P-Q emulator and an analogous P-Q controller.

$$\frac{Cs + \frac{A^2 \beta_{poly}}{V_{poly}}}{s} \quad (3.13)$$

3.6 Concluding Remarks

Load emulation of the *filling* and *packing* stages of injection moulding has been accomplished by metering flow out of an actuator. Unfortunately the maximum stiffness that can be emulated is a quarter of that specified for the real load.

Table 3.1 Parameter Values

Parameter	**Value**
Mass	60kg
Actuator pressure	50bar
Oil density	870kg/m^3
Valve flow coefficient	0.7
Valve flow area	$3.16\times10^{-6}m^2$
Actuator annulus area	2.56×10^{-3}
Actuator velocity	0.1m/s
Trapped volume of oil	0.1l
Oil Bulk modulus	15000bar
Polymer Bulk modulus	8000bar
Screw area	$4.91\times10^{-4}m^2$
Volume of polymer in the mould	$2.0\times10^{-5}m^2$

Figure 3.1 Load Simulator

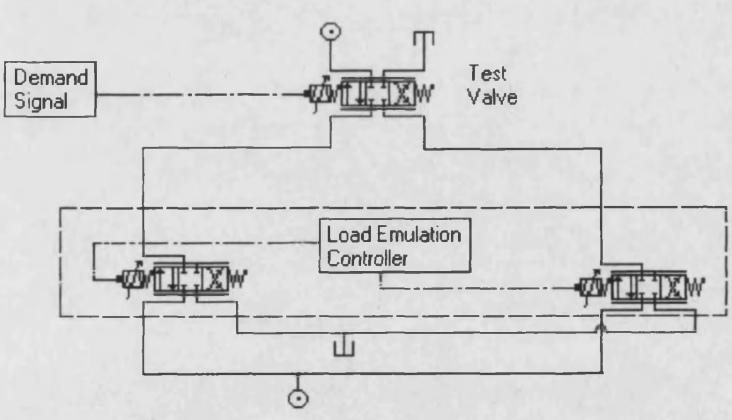

From **Ramdén et al. (1997)**

Figure 3.2 Hydraulic Load Emulator Circuit Diagram

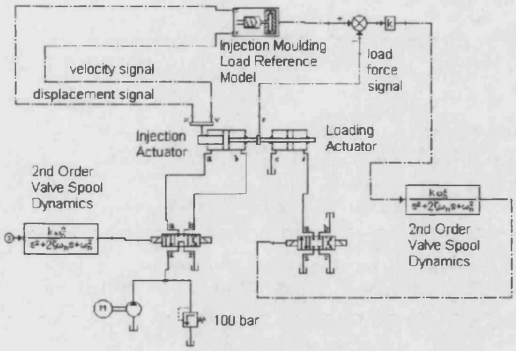

Figure 3.3 Load Emulator Simulation Using 20Hz Load Control Valve

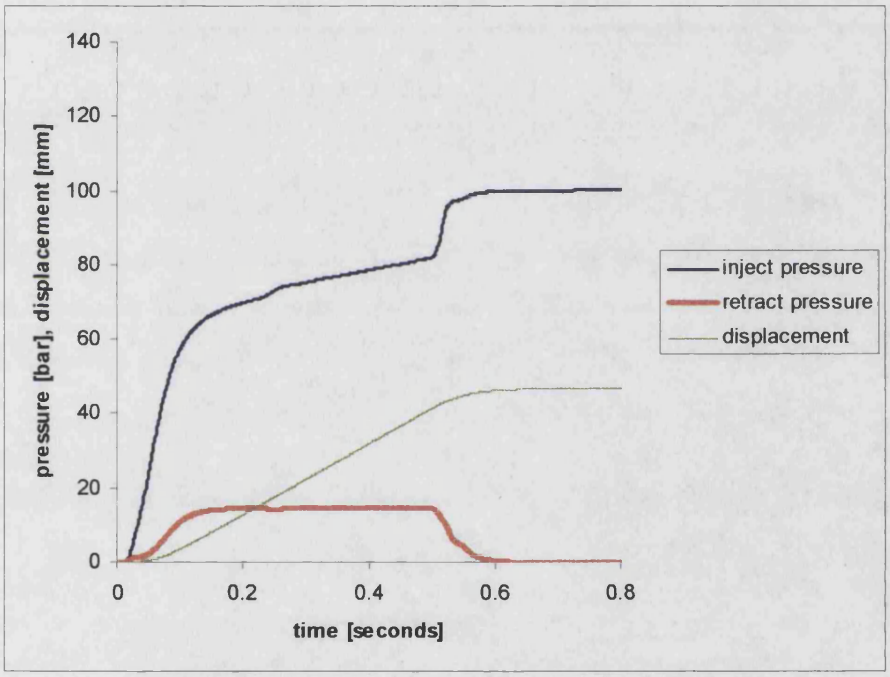

Figure 3.4 Experimental & Load Emulation

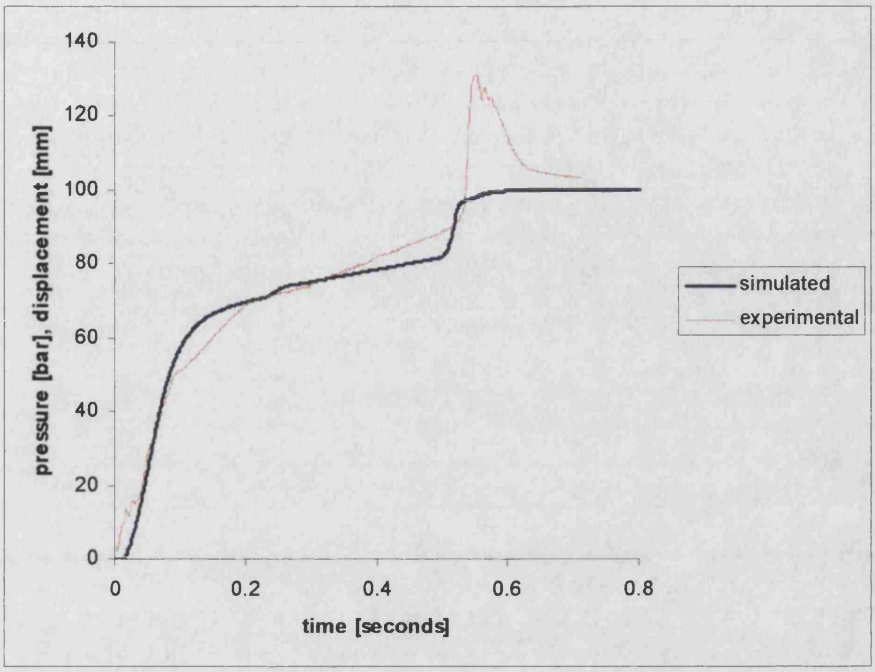

Figure 3.5 Electrohydraulic Rig Circuit Diagram

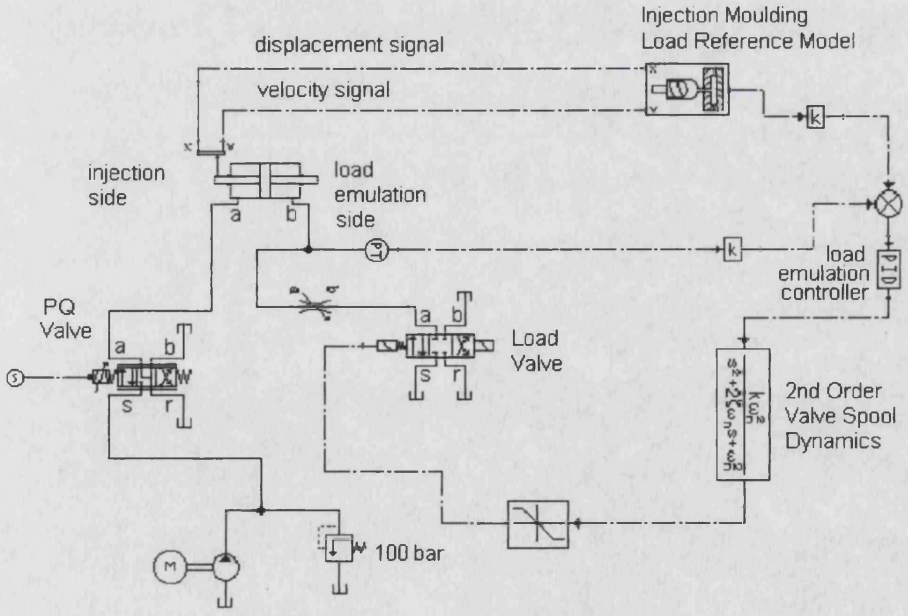

Figure 3.6 25bar Viscous Friction Load Emulation

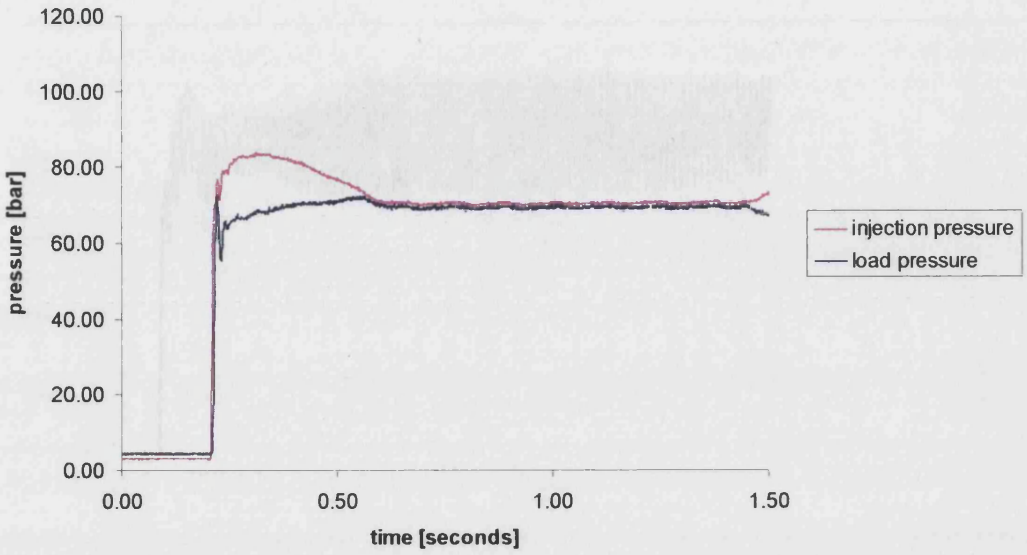

Figure 3.7 50bar Viscous Friction Load Emulation

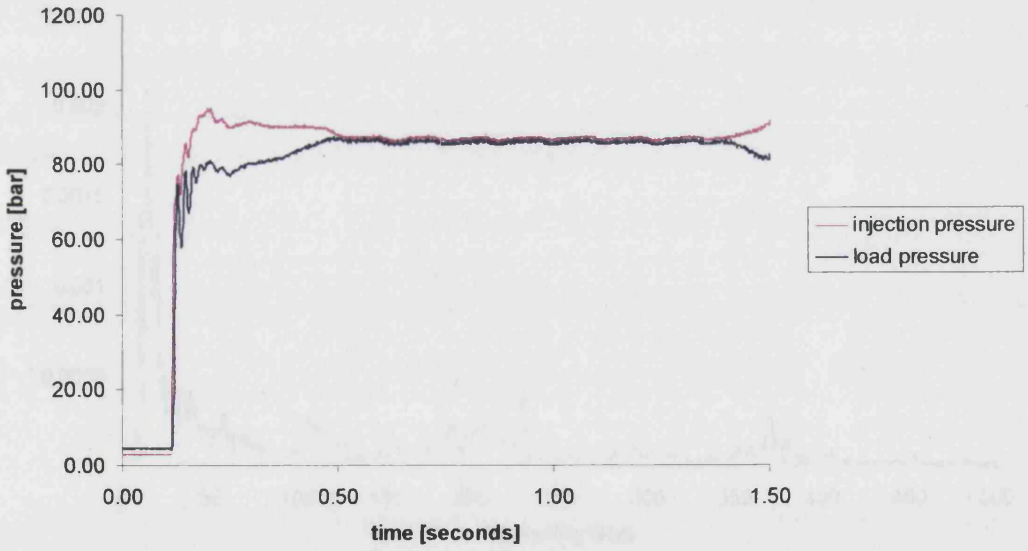

Figure 3.8 75bar Viscous Friction Load Emulation

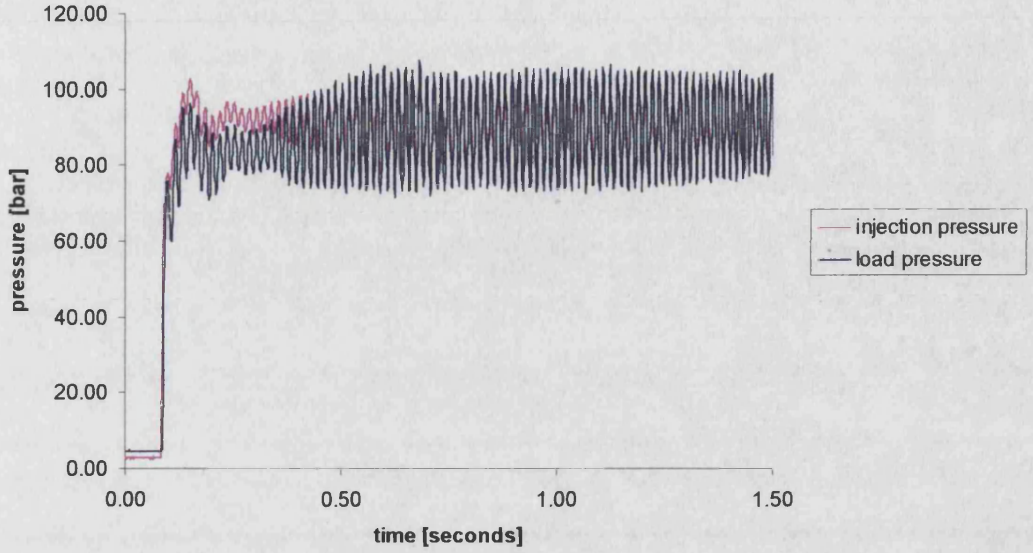

Figure 3.9 Rig Velocity FFT

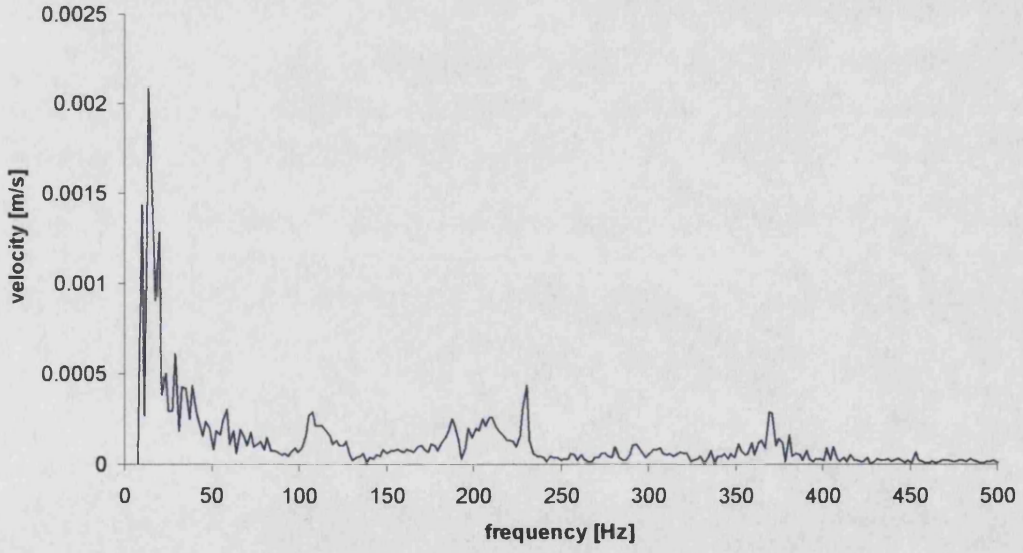

Figure 3.10 Experimental Velocity Results FFT

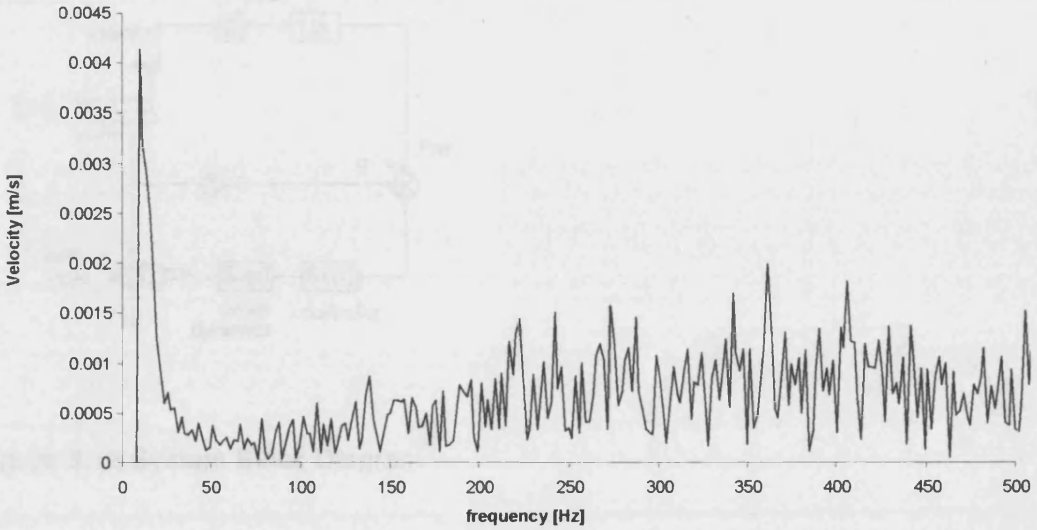

Figure 3.11 Valve Actuator System Diagram

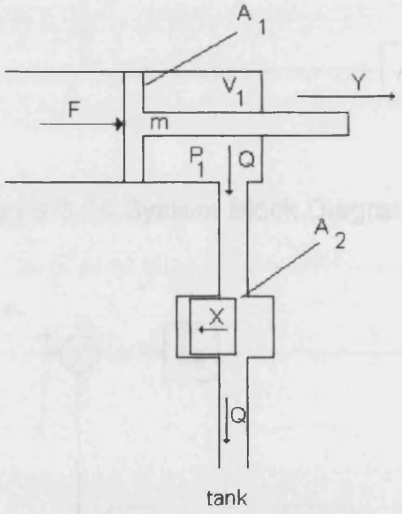

Figure 3.12 System Electrohydraulic Circuit Diagram

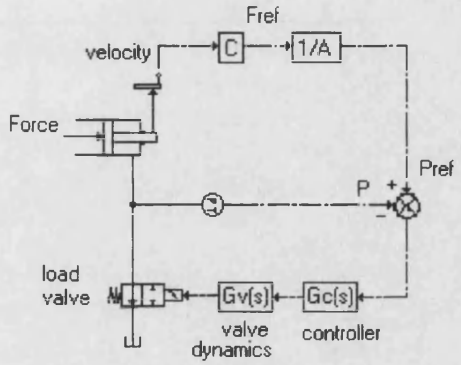

Figure 3.13 System Block Diagram

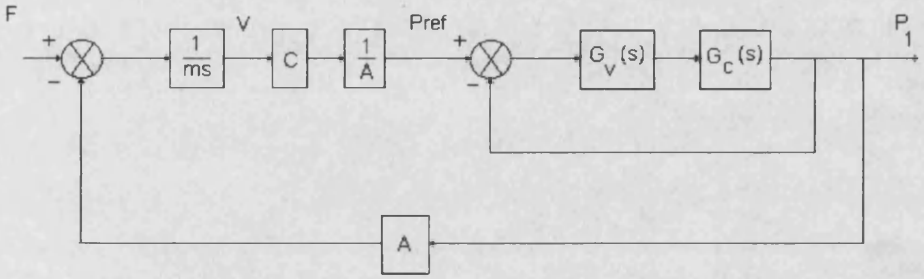

Figure 3.14 System Block Diagram (re-arranged)

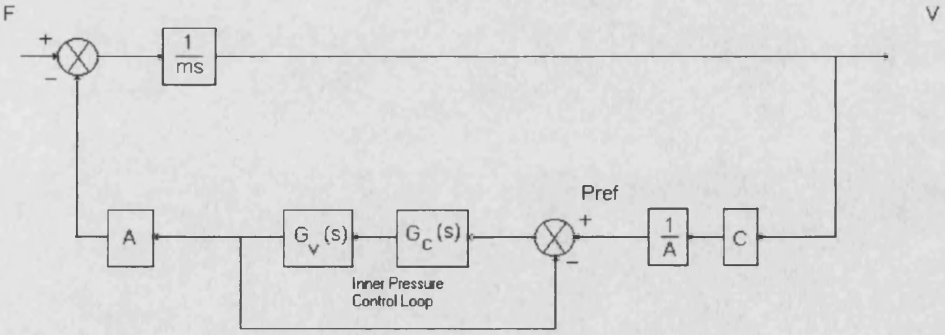

Figure 3.15 System Root Locus, Without Valve Dynamics

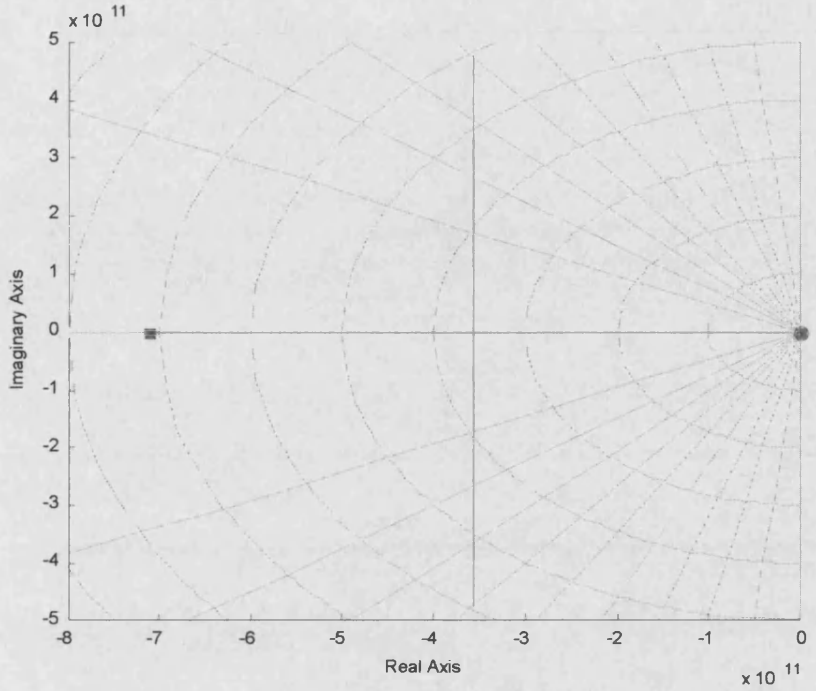

Figure 3.16 System Root Locus, With Valve Dynamics

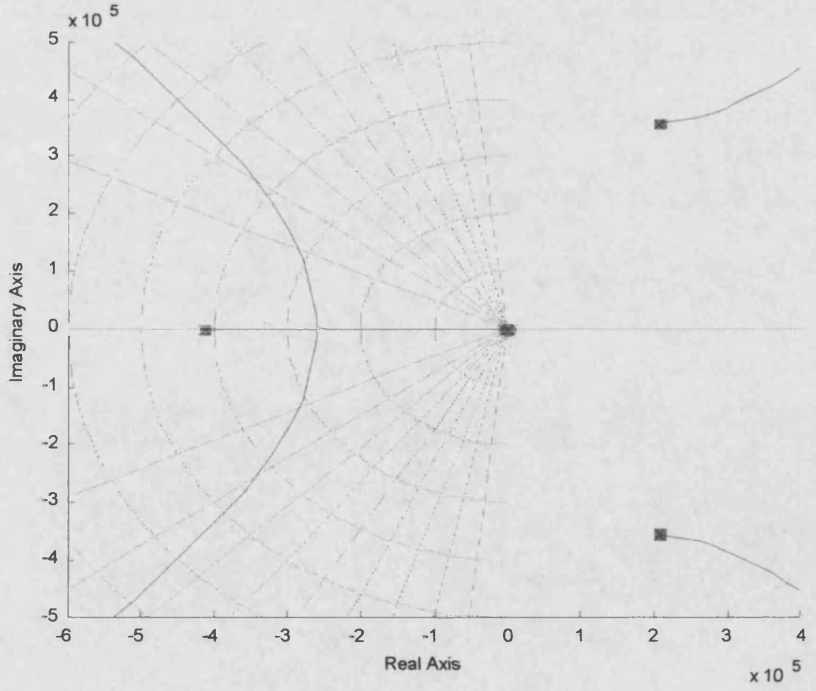

Figure 3.17 Bath*fp* Non-Linear Simulation Results, Valve Dynamics Not Included

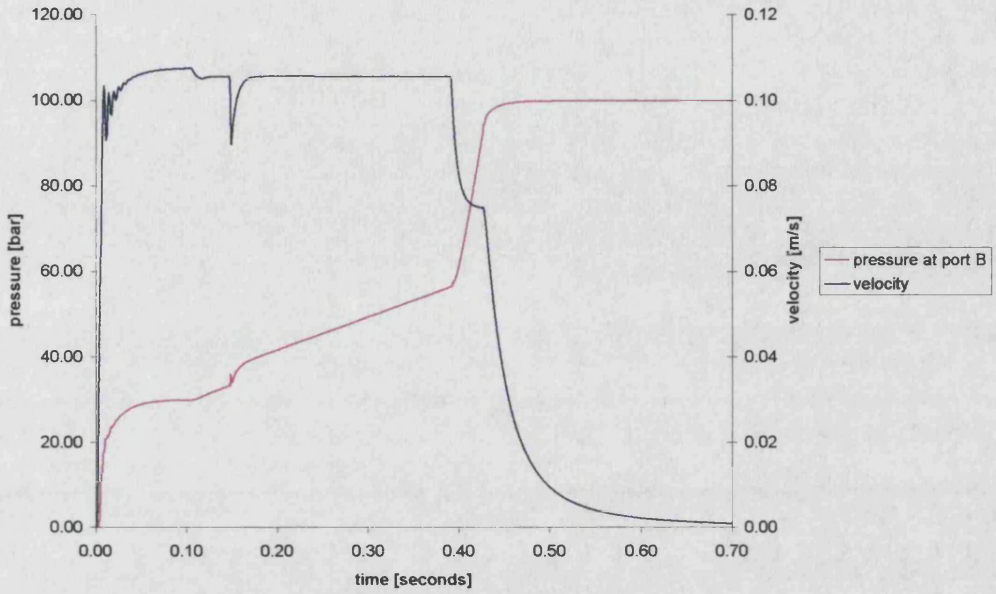

Figure 3.18 Bath*fp* Non-Linear Simulation Results, Valve Dynamics Included

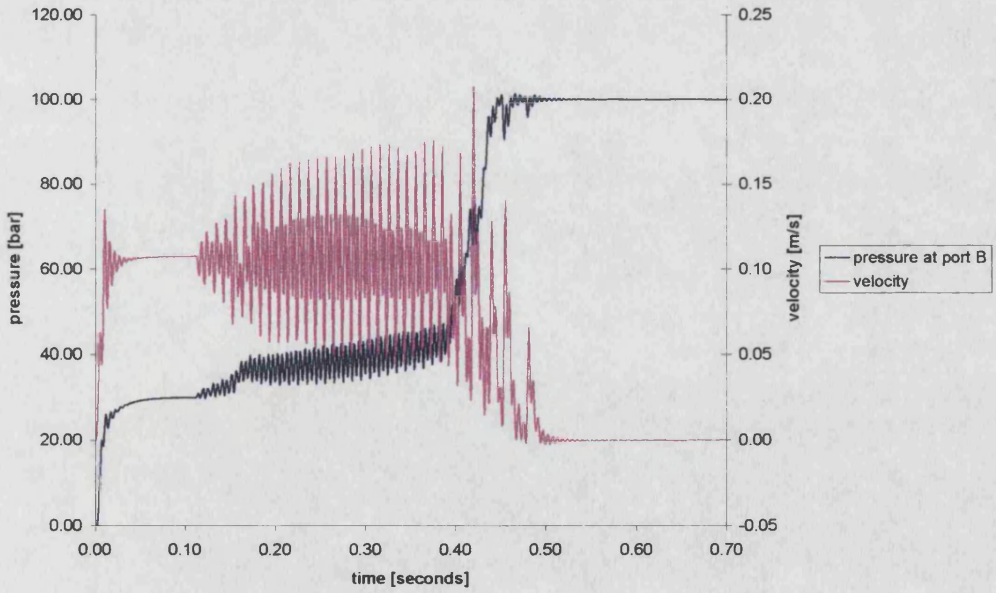

Figure 3.19 100Hz Valve Dynamics Root Locus

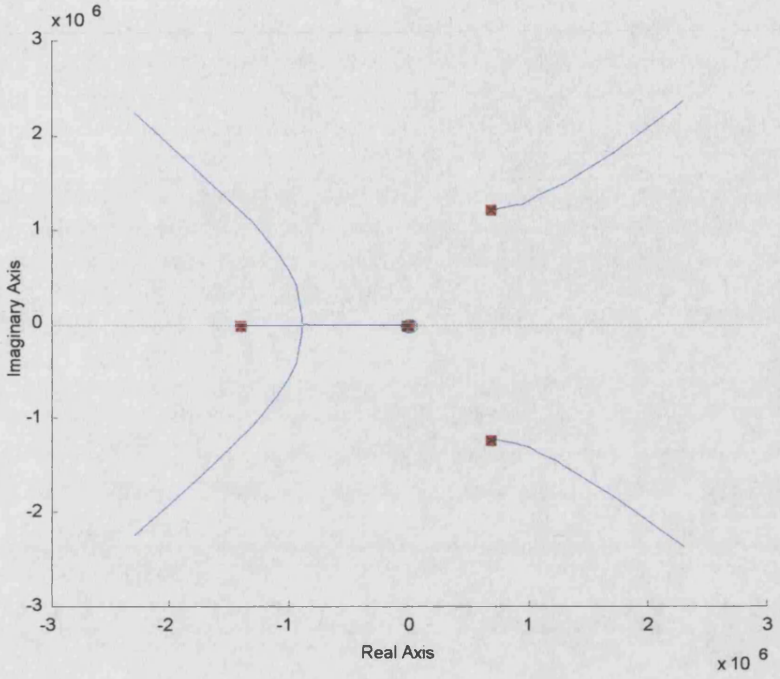

Figure 3.20 Low Proportional Gain Pressure Control Pressure Control Loop Root Locus

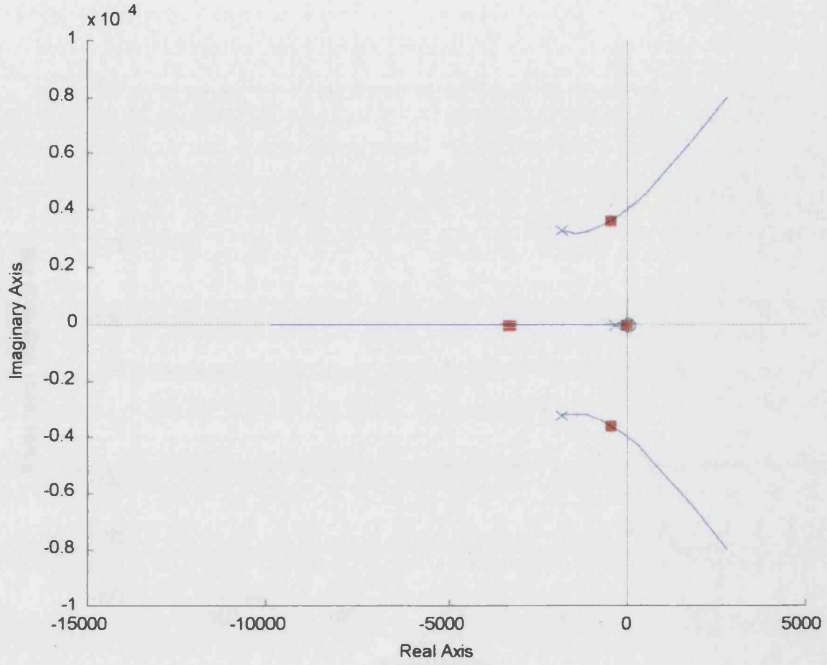

Figure 3.21 Low Proportional Gain Pressure Control Closed Loop Bode Plot

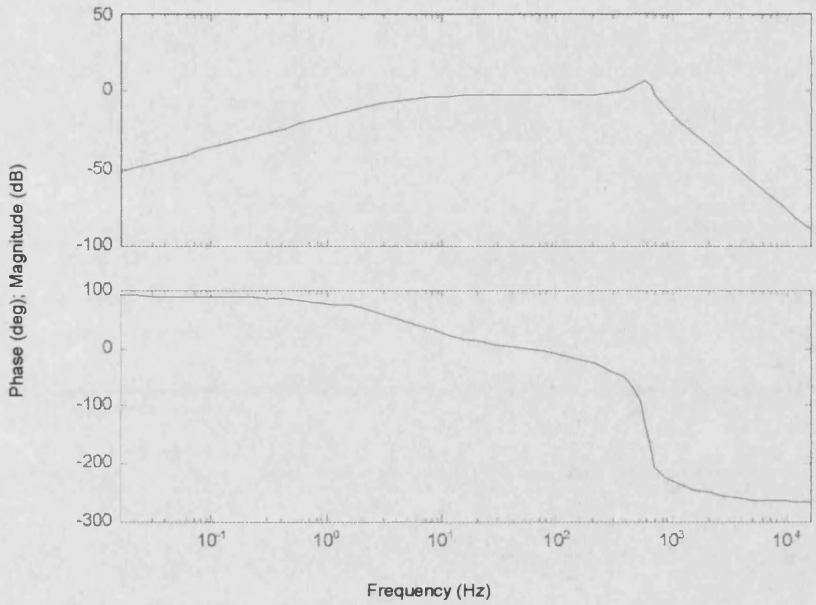

Figure 3.22 Integral Control Pressure Control Root Locus

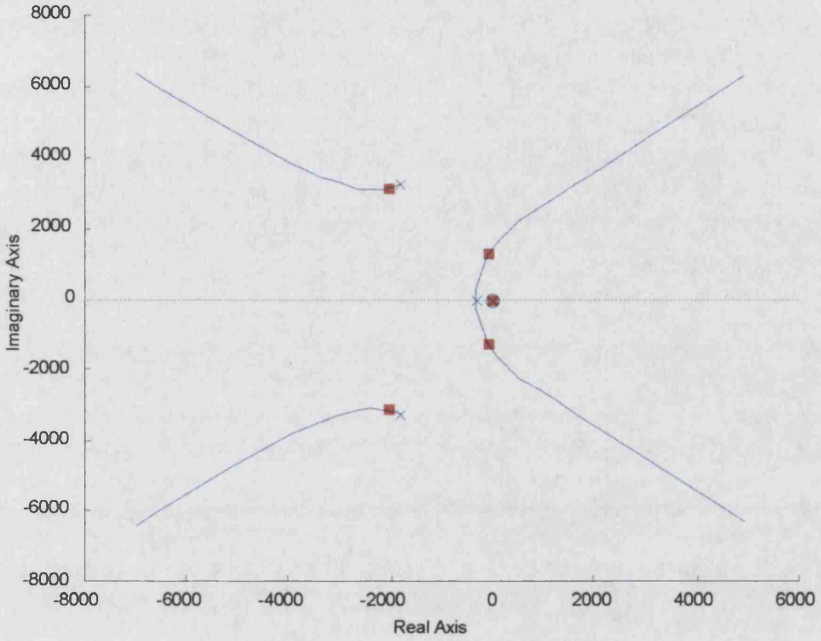

Figure 3.23 Integral Control Pressure Control Loop Bode Plot

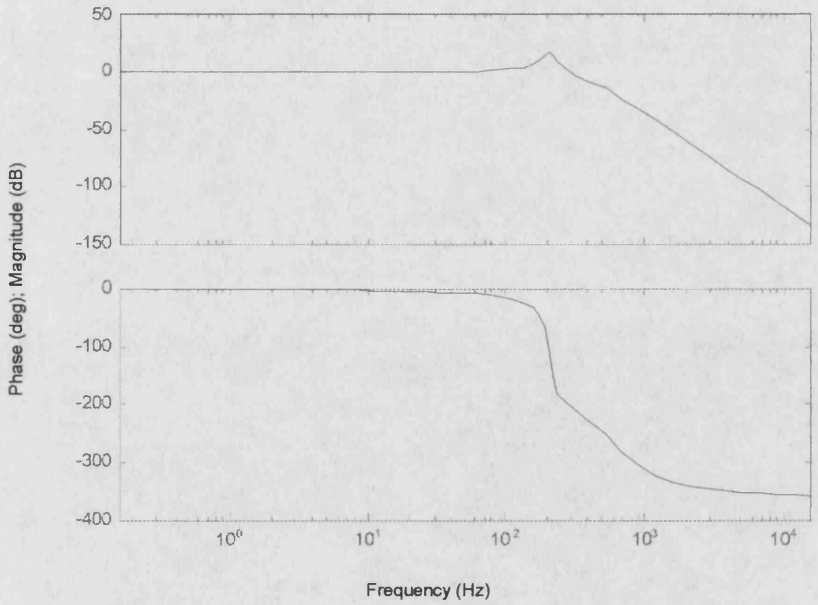

Figure 3.24 Uncompensated Overall System Root Locus

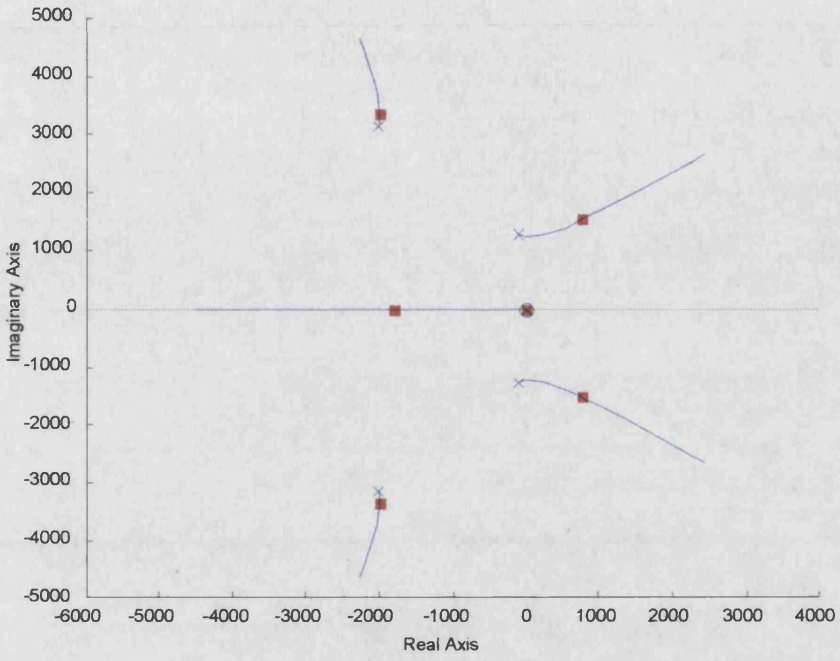

Figure 3.25 Uncompensated Overall System Bode Plot

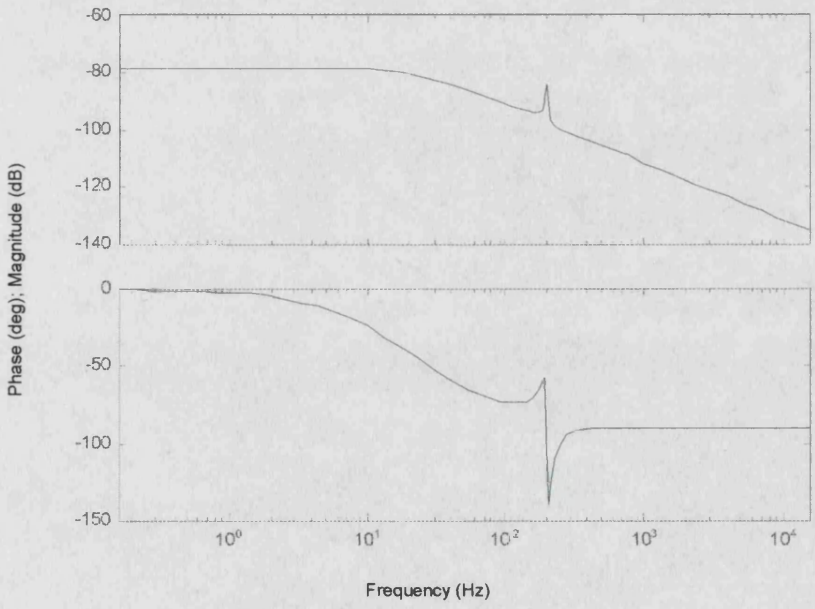

Figure 3.26 Compensated Overall System Root Locus

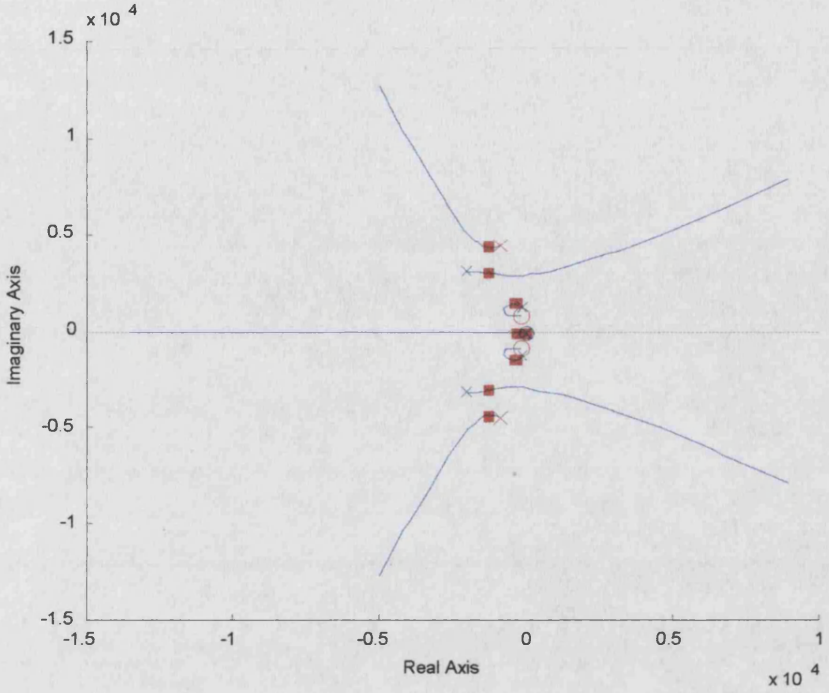

Figure 3.27 Compensated Overall System Closed Loop Bode Plot

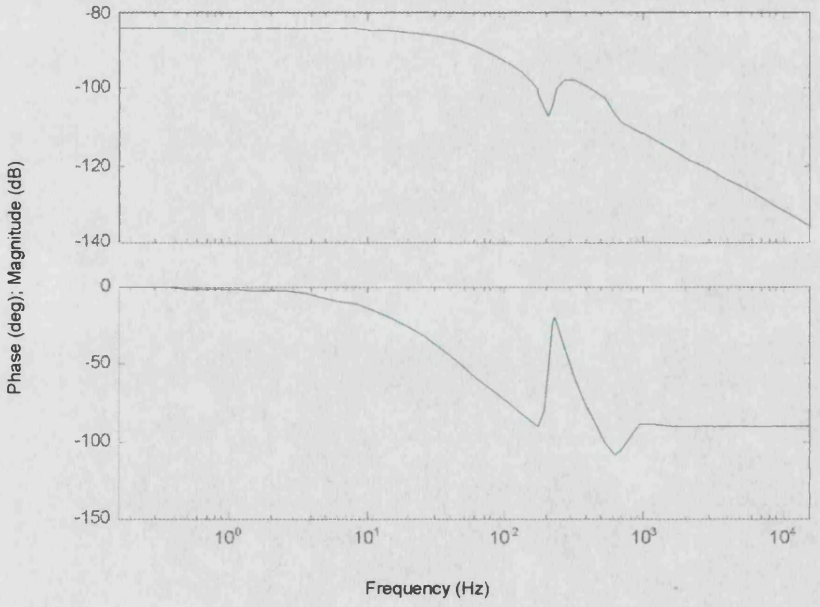

Figure 3.28 Load Emulation Valve Pressure Gain Results

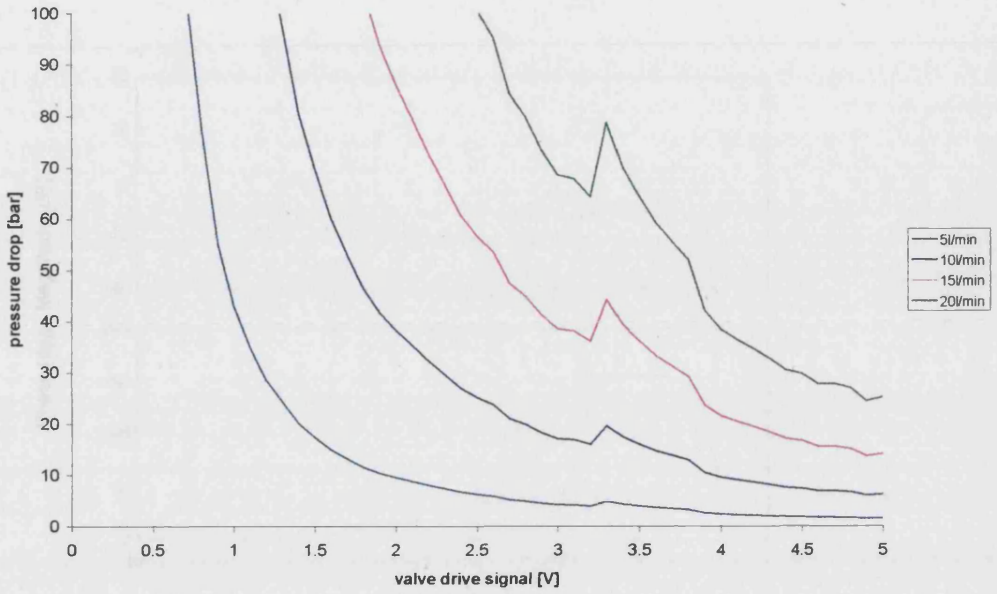

Figure 3.29 Continuous Time Compensator Bode Plot

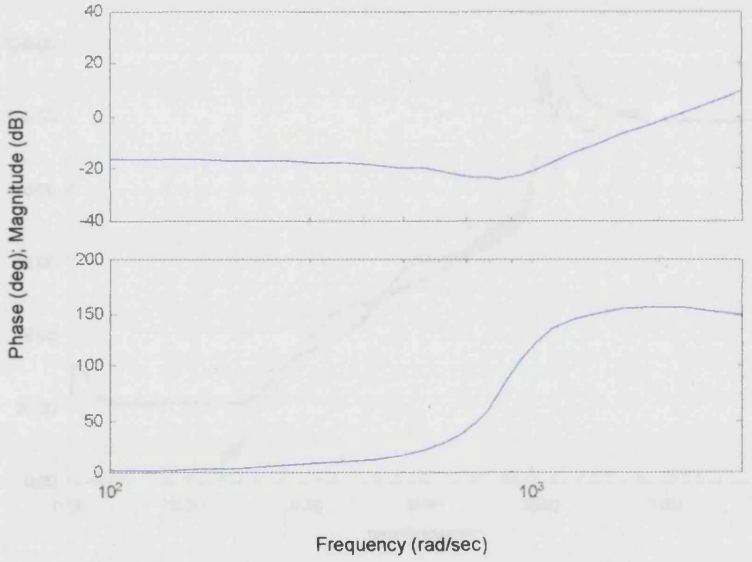

Figure 3.30 Discrete Time Compensator Bode Plot

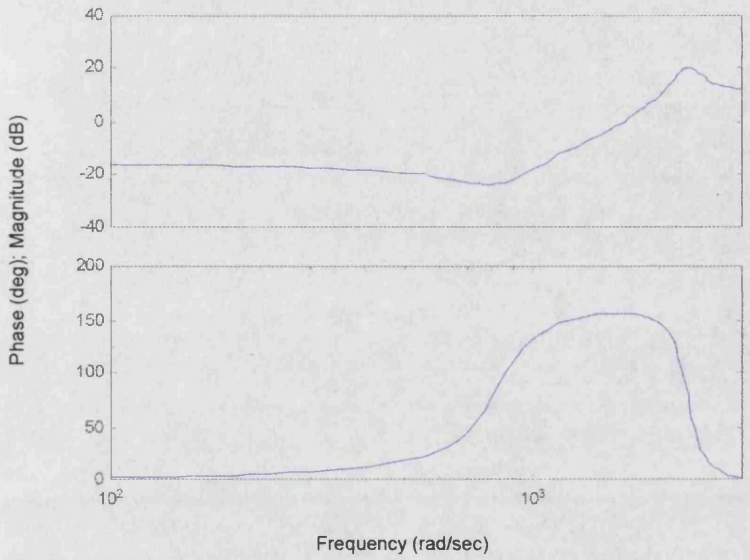

Figure 3.31 Injection Moulding Load Emulation Rig Results

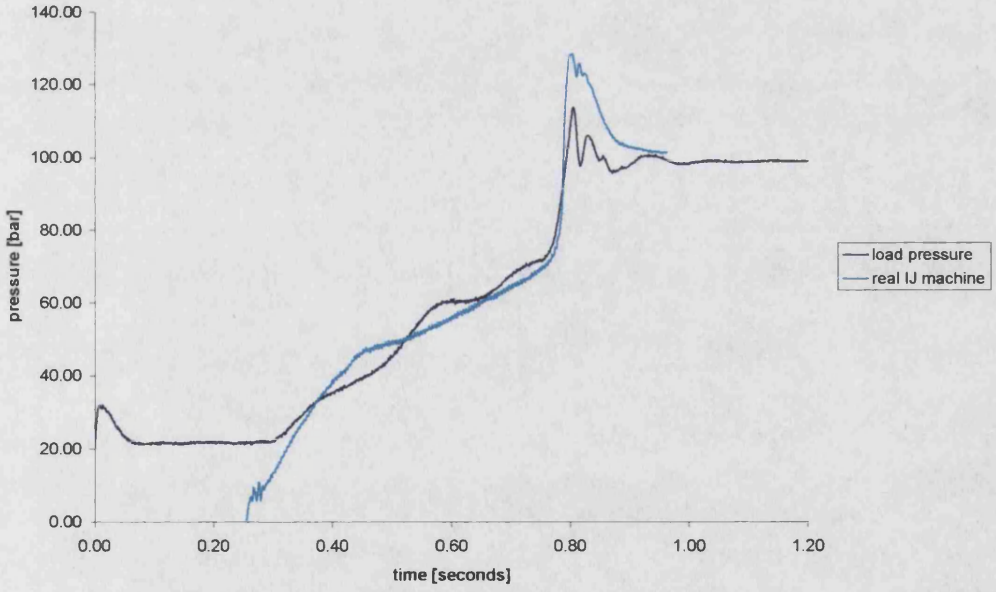

Figure 3.32 Rig Results, Reference Model Included

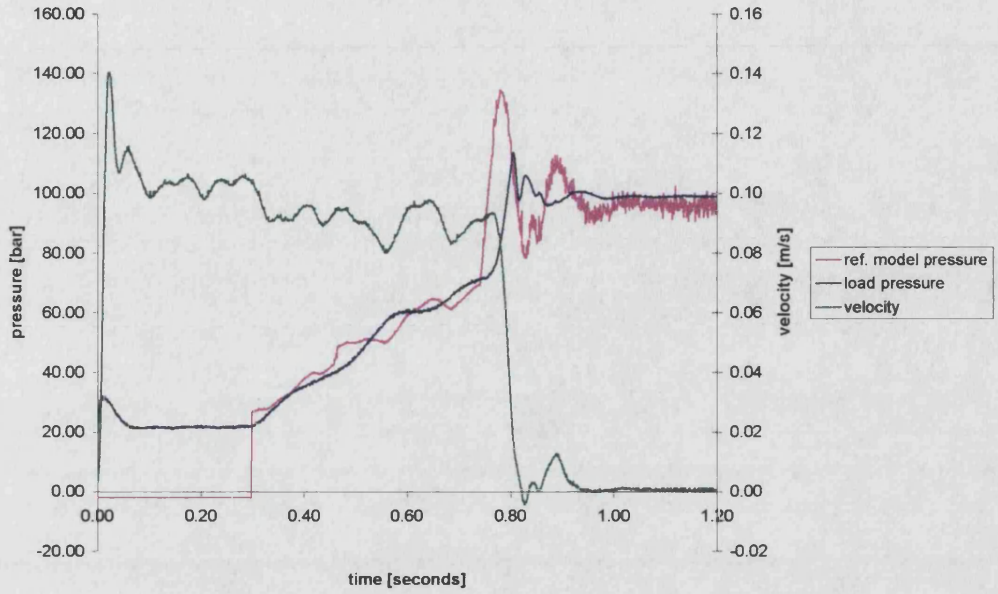

Figure 3.33 Rig Results, Slower Injection

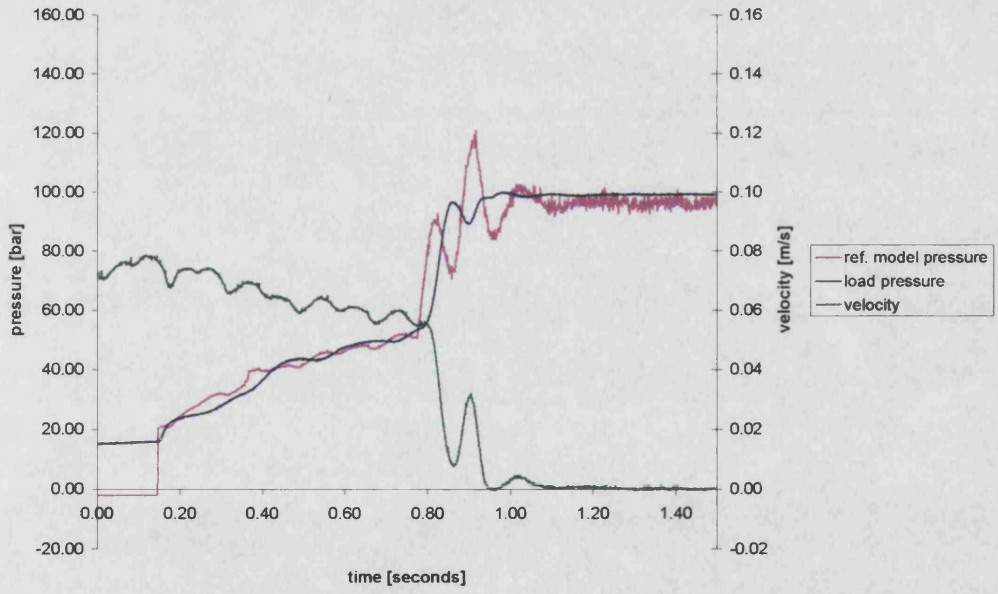

Figure 3.34 Rig Results, Reduced Emulated Bulk Modulus

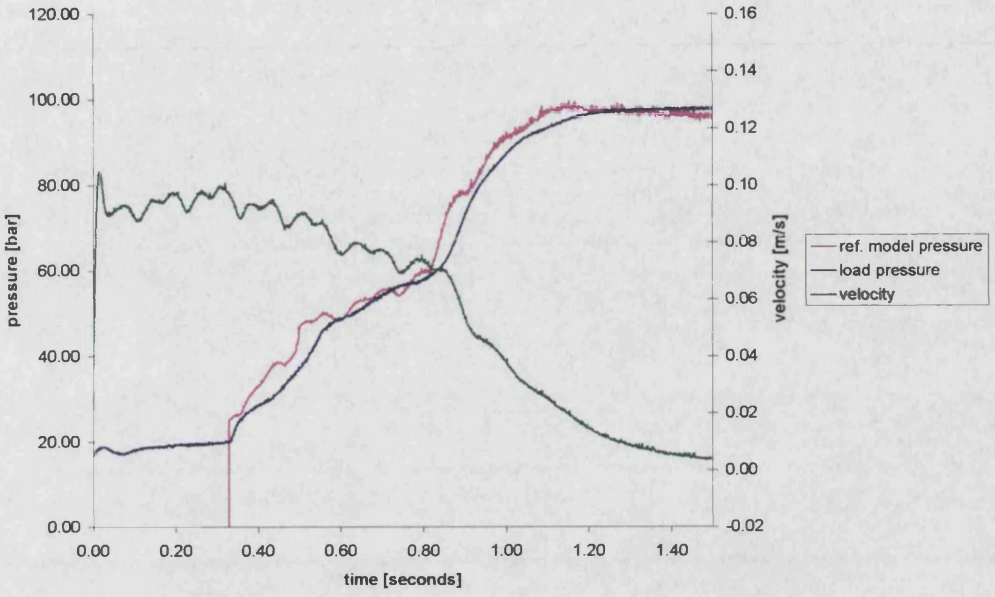

4.0 Controller Evaluation & Choice

4.1 Introduction

This chapter describes the current industry standard P-Q controller and highlights the problems associated with its use in injection moulding. Alternative solutions are discussed and the implementation of the most promising one is then covered in the next chapter. The work detailed in this chapter resulted in a paper presented at the 2000 ASME Winter Annual Conference, a copy of this work is included in Appendix A.

4.2 Traditional P-Q Control

The industry standard P-Q controller considered in this work is a fixed gain closed loop (or open loop) velocity controller which is linked by a P-Q switch to a closed loop proportional plus integral (PI) pressure controller. Since this research was primarily interested in the switch from flow control and subsequent pressure control, velocity was open loop controlled. Switching between flow and pressure control is generally initiated on either: actuator position, pressure (injection pressure) or time. The general consensus is that switching on injection pressure is the most reliable method and this was the one used in this study. The switch from flow to pressure control is irreversible during a cycle and the output of the pressure controller integrator is held at zero until the controller is activated. The switch to pressure control was set to occur at an injection pressure of 70bar, with a final target of 90bar. The goal was to achieve the smoothest pressure response without overshoot.

There are many ways to tune a PID controller and controller performance can be considerably altered by the tuning method employed. Manual tuning by a commissioning engineer is undoubtedly the most commonly used method for tuning the PI pressure controller in the field. Clearly the skill and experience of the commissioning engineer will affect the efficacy of the controller. In order that the results of the PI pressure controller in this work can be compared with other controller results it is important that a standard tuning method is used. The method chosen was the Ziegler-Nichols frequency response method detailed in **Åström & Hägglund (1988)**. Such a controller was implemented on the rig and using this method the integral gain was set 7 times higher than the proportional

gain. A variety of manually tuned controllers were also implemented but none were significantly better than the one tuned using the Ziegler-Nichols frequency response method.

4.2.4 Discussion of Results

The experimental injection pressure results from the rig are shown in Figure 4.1. The initial sharp pressure rise is due to an accumulator effect in the flexible pipework between the pump and injection actuator, pressure then falls as the actuator extends under zero load conditions until filling emulation begins at 0.4s. Injection pressure then rises as the emulated mould is filled up at 0.8s when the mould is full and packing begins. The pressure when the mould is filled is 68bar and with the switch from filling to packing control set to occur at 70bar it can be considered to be 2bar late. On a real injection moulding machine it is very difficult to know the exact point in time when the mould is full without the aid of expensive cavity pressure or ultrasonic transducers. In this instance it is only possible to know the exact point in time when the mould is filled from the load valve control signal. This simply helps to illustrate one of the problems with the standard controller.

The 1st pressure oscillation after switchover has an amplitude of 25bar and the oscillations continue for 0.25s with a frequency of 22Hz. While these injection pressure results look less than satisfactory it is important to point out that this injection cycle sounded and appeared smooth and controlled. It is only with the aid of transducers that the true behaviour can be revealed. It is also interesting to note that the overall response is typically 3rd order with fast underdamped 2nd order dynamics. The fact the response is 3rd order is linked to the 2nd order valve dynamics coupled with meter-in pressure control of a fixed volume of oil which is 1st order (a small perturbation analysis confirming this is included later in this chapter).

One claim from commissioning engineers is that if shorter pipes are fitted between the injection control valve and the actuator the PI pressure controller becomes more difficult to tune. This is because the volume of trapped oil between the valve and actuator piston is reduced and the system stiffness

increased. Retaining the same PI pressure controller set-up this was tested by changing the pipe between the injection valve and the actuator on the rig from 1.8m to 1.1m. The subsequent results are shown in Figure 4.2 and are very similar to those in Figure 4.1. Clearly the change in volume was not sufficiently significant to unduly affect performance. Hence the pipe was changed for a 3m (the pipe connecting the injection control valve to the actuator on the real injection moulding machine was 2.5m long) and the results are presented in Figure 4.3. By increasing the trapped volume of oil the pressure fluctuations after switchover from velocity to pressure control have been significantly reduced compared to those in Figure 4.1. The results support the claim from commissioning engineers that shorter pipes make the PI pressure controller more difficult to tune.

4.2.5 Problems

The main problems with traditional P-Q controllers controlling injection moulding machines are:

- The selection of the control gains relies on significant knowledge and skill of the commissioning engineer.
- The switch from flow to pressure control may lead to a short oscillatory pressure transient. Ideally a smooth critically damped or overdamped increase in pressure up to the packing pressure is required at the onset of packing.
- If short pipes are used between the P-Q valve and the actuator, the PI pressure controller tends to be particularly difficult to tune.
- Once the PI pressure controller gains are set by the commissioning engineer they will remain fixed until a machine overhaul is undertaken. The controller gains are not re-tuned for new moulds or operating conditions.

These problems arise essentially for the same reason. The velocity controlled filling phase is a low gain system and the pressure controlled packing phase is a high gain system.

Currently a commissioning engineer has to tune and test each closed loop PI pressure controller separately. Great cost savings could be made if a more advanced self-commissioning P-Q controller could be implemented.

4.3 Alternative Control Strategies

Alternative P-Q control strategies can be conveniently sub-divided into 2 main groups. These are single controller solutions and hybrid controller solutions. Single controller solutions cover both velocity and pressure control embodied within a single structure with both velocity and pressure demand inputs and a single output. Hybrid controller solutions are those with separate controllers for velocity and pressure control and some form of transfer mechanism between the two. The industry standard P-Q controller detailed earlier in this chapter is a hybrid controller. Work has also been reported by **Gao et al. (1996a)** on a (pressure only) self-tuning single controller solution using cavity pressure as the controlled variable. This will be discussed with the P-Q single controller solutions.

Firstly, single controller solutions will be considered. Besides the cavity pressure control solution two other candidates are considered here: neural networks and fuzzy logic. Hybrid solutions are then considered, with discussions of adaptive controllers, fuzzy logic velocity control, linearised valve velocity control, sliding mode pressure control and learning control. Bumpless transfer, which may be required to link control strategies in a hybrid solution is also considered.

4.3.1 Neural Network Pressure & Flow Control

The potential benefits of using artificial neural networks for the control of non-linear systems are identified by **Suykens et al. (1996)**. Stability issues aside, one possible method of control using a neural network is the inverse model method. A neural network is set up and trained to be an accurate model of the system to be controlled. The model is then inverted and the required system outputs fed into the model. The neural network model returns the system input necessary, which is then fed into the real system to be controlled. This might be a good method of controlling a complex highly non-linear system but would only work if the system parameters were fixed or did not change significantly. While it is

very possible that a neural network could be devised and trained for a *particular* injection moulding machine, the system characteristics can change quite significantly. For example if a mould or material is changed this would certainly require retraining and might even require a different neural network structure.

Even if a neural network solution were employed satisfactorily it may be practically impossible to guarantee stability at all operating conditions. This stems from the fact that the non-linear equations describing a neural network of any significant complexity are very difficult to obtain. As such it is difficult to construct an analytical proof of stability. The legal implications of this may be such that a neural network controller would be unmarketable. Of course an analytical proof of stability for a simple neural network should be possible.

A further reason why a neural network solution is inappropriate is that they can only be trained from data that exists. To retain the same level of performance each new mould, material, or control valve encountered would very likely require a new controller. This would then constitute a new controller, which would require testing before it could be guaranteed to perform correctly. It would be a very time consuming exercise to test as many moulds and materials as possible to be able to supply a family of trained controllers. Also since new mould designs and to a lesser extent new materials are continually being developed there would be a continuing requirement to test and retrain new controllers.

As a single controller a neural network solution is therefore eliminated on the grounds that it is inappropriate for controlling a system with an unknown range of parameter variations.

4.3.2 Fuzzy Logic Pressure and Flow Control

As explained in **Pedrycz (1993)** fuzzy logic is typically very useful for constructing controllers from human experience of controlling a system manually. Mathematical models are not required. This is because fuzzy logic is used to create a controller from a set of rules. Consequently fuzzy logic controllers are often found in process control applications where they replace

human operators. In such cases fuzzy logic is a suitable solution because little information is required about the system plant. All that is required is a set of rules describing how the system input signal should be regulated to give the correct system output.

The work by **Yang & Chang (1998)** details the implementation and testing of a fuzzy logic controller on an electrohydraulic materials testing machine. The main conclusion arrived at is that a fixed rule base fuzzy logic controller is not sufficiently robust for fatigue testing over a wide range of frequencies. Instead the authors argue that a self-organising fuzzy logic approach needs to be used to give sufficient robustness. While this appears to work adequately, a stability proof for such a controller would be extremely difficult to carry out. Again the legal implications of this may be such as to make the controller unmarketable. It is also worth noting that although the controller detailed in the work by **Yang & Chang (1998)** was successful this is not always the case with self organising fuzzy logic controllers. The work by **Pannett et al. (1999)** on self-organising fuzzy control states that 'performance and robustness are not predictable'. Work by **Tsoi & Gao (1999)** on an injection moulding *speed* controller showed that a fixed rule base fuzzy logic gave good performance and was more robust than a fixed gain PID controller. Three different moulds were tested with 2 different materials and 2 different barrel temperature settings (12 different configurations in all). However there was no mention of either the implications of making the controller commercially available or linking it to a pressure controller.

While it may be possible to construct a fuzzy logic P-Q controller it is likely that it would be complex and necessary to have a self-organising element to take account of plant (mould or polymeric material) changes. Analysis to guarantee stability would be difficult. For this reason a fuzzy logic P-Q controller has been discounted.

4.3.3 Cavity Pressure Filling and Packing Control

In the work by **Gao et al. (1996a)** an on-line recursive system identification with forgetting factor was performed to tune a self-tuning regulator (see section 4.3.5). This was done by supplying a square wave to the servovalve controlling the

injection actuator which varied the demanded valve spool position between 20% and 80% of its maximum with a frequency of 5Hz. A sample time of 20ms was used and the transfer function relating valve opening to cavity pressure was found to be of the form:

$$\frac{b_1 z + b_2}{z(z^2 + a_1 z + a_2)} \qquad (4.1)$$

During the system identification tests the packing pressure oscillated, with servovalve position, about an increasing mean pressure. Consequently the transfer function varied between equation (4.2) during pressure overshoot caused by large valve openings and equation (4.3) during pressure undershoot caused by small valve openings.

$$\frac{0.8z - 0.2}{z(z^2 + 1.2z - 0.2)} \qquad (4.2) \text{ overshoot}$$

$$\frac{0.3z - 0.5}{z(z^2 + 2z - 1)} \qquad (4.3) \text{ undershoot}$$

The authors failed to mention that unfortunately both transfer functions have poles outside the unit circle which means that both systems are unstable. This in itself demonstrates the difficulty associated with performing an on-line parameter identification necessary for self-tuning regulators. Despite this the pressure tracking performance demonstrated by **Gao et al. (1996a)** was quite good. However as a strategy cavity pressure control can be discounted as it relies upon a cavity pressure transducer. These transducers are still not commonly fitted to moulds and the intention of this work has always been to avoid relying on any more transducers than those already fitted to an injection moulding machine.

4.3.4 Linearised Valve Velocity Control

One of the fundamental non-linearities of hydraulic systems is the relationship between valve position and the flow rate through the valve, equation (4.4) below. This arises from the relationship between valve position and the pressure drop across the valve.

$$Q = kX\sqrt{\Delta P} \qquad (4.4)$$

If the force required to inject molten polymeric material into a mould was constant, and independent of position and velocity then the flow through the valve would be proportional to valve position. However, it has previously been established in chapter 3 that the force required to inject molten polymeric material into a mould increases non-linearly with injection actuator position. Therefore in injection moulding the function relating valve position to flow rate will be non-linear and dependent on actuator position.

Since a pressure transducer in the inject side of the injection actuator will be necessary for closed loop pressure control it seems attractive to use the pressure information during velocity control to linearise the valve characteristic. One application where this has been used successfully is in the acceleration control of hydraulic actuators for flight simulators. A good paper on the subject is by **Plummer (1997)**. However, system simulations have shown that the supply pressure from the pump is not constant during the injection moulding cycle. During filling the total pump flow is used and the pump supply pressure depends on the injection actuator velocity and the position of the melt front in the mould. Hence if the valve characteristics were to be satisfactorily linearised a second pressure transducer would be required, upstream of the injection control valve, to measure pump supply pressure. This would increase the cost and complexity of the P-Q controller but not so much as to rule this method out.

4.3.5 Adaptive Velocity Control

Because the relationship relating injection moulding force to position and velocity is non-linear it would seem sensible to adjust the controller gain during injection to reflect the melt front position. One possible way to do this is by using an adaptive controller. Various strategies are available. A good introduction to three of the main types (gain scheduling, self-tuning regulation, model reference adaptive control) is found in **Åström (1983)** and a more detailed account of current progress is given by **Iserman et al. (1992)**. Diagrams of each of the 3 strategies are shown in Figure 4.4, Figure 4.5 and Figure 4.6. An excellent survey of continuous time gain scheduling controller analysis and design is given in **Leith & Leithead (2000)**. It is envisaged that any advanced P-Q control strategy will require a minimum of displacement, velocity and pressure measurement.

Hence the common problem of a gain scheduling solution requiring one or more measurable parameters with which to vary the regulator does not arise. It is very likely that gain would be scheduled against injection pressure and actuator position with actuator velocity as a useful addition. The construction of a gain scheduling map is not a trivial task and the design of such a map would be feasible for an injection moulding machine that was only ever going to be used with one particular mould, one material and the same temperature set point. Such a map would be at the very least be mould and material specific and require redesign for new moulds and/or materials. In light of this gain scheduling is not appropriate. Since the scheme relies, to a large part, on suitable interpolation methods it is surprising that **Leith & Leithead (2000)** report that this part of the problem is not yet resolved.

Self-tuning regulation is another possible candidate as an adaptive controller. The biggest problem likely to be encountered is that of obtaining an accurate system model and then performing a parameter identification. Another problem commonly encountered is that the transducer signals derived from measuring the process must be sufficiently rich which implies that the process has to be persistently excited. This will not pose a problem when the controller is badly tuned but as performance improves excitation decreases. This can be viewed as a tuning problem in that if tuning is stopped too soon then the regulator will not be optimised but more importantly if tuning is not stopped when the process has reached a steady state regulator gains can drift and provide excitation. Hence In some cases perturbation signals also have to be added to the input signal to ensure good estimation. In the case of injection moulding where part quality is paramount it would not be possible to include a perturbation signal.

Since self-tuning regulators and model reference adaptive controllers (MRAC) have a similar structure it is not surprising that they can have similar problems. The key components of an MRAC controller are the reference model and the regulator adaptive gain or gains. The reference model is usually defined to give an achievable output for the plant output to track, with dynamic characteristics similar to those of the plant. The scheme then works by trying to minimise the error between the plant output and the reference model output by varying the

regulator adaptive gain. While the concept of MRAC itself may not seem to have many advantages over gain scheduling or self-tuning control, certain types do. This is because an accurate reference model is not always needed. An adaptive *velocity* controller for injection moulding has already been designed and tested with some success, as described by **Zhang et al. (1996)**. Unfortunately only scant detail is given.

One problem that can be encountered with adaptive control is gain drift. If no safeguards are put in place, adaptive gains can change until they saturate. At this point the system output would deviate from the demand until sufficient information is available to re-tune the adaptive gains. The cycle would then start again forming a type of limit cycle. If an MRAC controller were to be implemented on an injection moulding machine then this issue would have to be addressed.

4.3.6 Fuzzy Logic Velocity Control

Although fuzzy logic has already been considered for a single controller solution work on fuzzy logic *velocity* control has been reported by **Huang & Lee (2000)**. The article includes experimental results for the hybrid fuzzy logic controller that was designed and implemented. In both sets of results the injection velocity was set at 15mm/s and the second set of results was used to demonstrate the robustness of the strategy to a new mould. The controller was successful but an injection velocity of 15mm/s is rather slow which trivialises the problem. It is also true the commercialisation issues raised previously still holds for a hybrid controller with an element of fuzzy logic control.

4.3.6 Bumpless Transfer

Considering the alternatives, a hybrid strategy appears to be the most promising. With this approach a bumpless transfer strategy may be required to avoid the problem of an unacceptable pressure transient when switching from flow to pressure control. A good overview of anti-windup and bumpless transfer schemes is given by **Edwards & Postlethwaite (1998)**. A general anti-windup and bumpless transfer method is presented by **Hanus et al. (1987)**. However by far the most useful work for this application is that by **Graebe & Ahlén (1996)**.

Their scheme, reproduced in Figure 4.7, acts to make the output of the latent (offline) controller track the output of the active controller. This means that on transfer the system input will have the correct initial conditions. The bumpless transfer strategy was devised to change between 2 controllers controlling the same plant output. This is not the same as bumpless transfer of flow to pressure control but the principle of forcing the latent controller to track the output of the active one can still be applied. In the case of flow and pressure control the flow controller would be the active controller and the pressure controller the latent one.

4.3.7 Learning Control

Since injection moulding is a repetitive process it is attractive to try to harness this fact and implement a scheme which takes account of past controller performance. This type of controller is generally referred to as a *learning controller* or an *iterative controller.*

One of the earlier publications to use the term *learning control* is that by **Arimoto et al. (1984)**. In this work a *betterment process* for the control of a mechanical robot is presented. While this work is important in that it defines and explains the concept and some of the practicalities of learning control, one major disadvantage is that the conclusions are entirely based on theory and simulation rather than experimental work. Another major problem is that the method is only applied to a linear system and proof of convergence for the controller has only been derived for the linear case. Possible problems identified by the authors include the need for clean and continuous transducer signals and the choice of a suitable function for determining the changes that are made to the system input, based on the error between demanded and actual system output. It was also concluded that the rate of convergence varies as this function is altered.

Sugie & Ono (1991) prove in theory that certain types of non-linear system can be controlled by a controller with an iterative structure, without knowledge of the system being controlled. Even so the point that the derivative of the controlled variable error is important for stability is again raised as it was for the linear plant case considered by **Arimoto et al. (1984)**. In the case of P-Q control this

means the use of the derivative of velocity and the derivative of pressure. While the derivative of velocity could be obtained without too much difficulty it is notoriously difficult to obtain a useful derivative of pressure. This is because the measured pressure signal usually contains a pump pressure ripple and filtering the signal introduces an unacceptable phase lag.

The paper by **Kirecci & Gilmartin (1998)** reveals some practical problems. The system being controlled was a robot with 2 degrees of freedom; the learning controller used positional error and was set up to give good position tracking performance. The main problem reported was a high frequency ripple on the command signal from the controller. This occurred during high speed robot movement after a few iterations of the controller's learning cycle. The solution used by **Kirecci & Gilmartin (1998)** was to add a digital filter to the learning controller algorithm. Such controller instability, occurring after good performance has been achieved, can be considered analogous to gain drift in adaptive control.

The work presented in the paper by **Kim & Kim (1996)** is also based on experimental results. In this case a PID controller with the addition of a learning gain-changing element was implemented. The aim was to improve CNC machine tool position demand tracking and was carried out without full knowledge of plant parameters and with the knowledge that there were non-linear external disturbances. In this study the disturbances were repeatable which is one reason why the controller was successful. Since the tool was following a circular trajectory cutting through the same depth of material the controller gains did not vary during each cycle. However fixing gains for an entire cycle may not be appropriate for injection moulding filling control. Overall the controller developed was successful in halving the tracking error within 5 cycles, although this is not so instructive since there is no mention of initial gain estimation.

Results for separate learning velocity and learning pressure controllers have been published by **Havlicsek & Alleyne (1999)**. However the initial estimate of the controller output had to be quite good for convergence. This is not to say that an learning element could not be incorporated into an adaptive scheme, which

would have certain advantages. Velocity and pressure control aside, in a fully automatic P-Q injection moulding controller there is still a requirement to switch from velocity to flow control at the correct point in the cycle. This task is perhaps best suited to iterative control. One possible way of doing this is to monitor the derivative of pressure, which should indicate the onset of packing as the pressure rises rapidly. However as mentioned previously, a useful derivative of pressure can be difficult to obtain.

4.3.8 Sliding Mode Pressure Control

One promising pressure control strategy is sliding mode control. This is a robust control strategy and there is no doubt that in the case of hydraulic spool valve position control, it is superior to PID control as demonstrated by **Gamble & Vaughan (1996)**. As explained by **Gamble (1992)** the design of a sliding hyperplane is not a trivial task. Hence for pressure control, it is possible that a sliding mode controller would need an observer to instigate a hyperplane change for different mould volumes. The work by **Hwang et al. (1993)** showed that a fixed gain sliding mode controller was suitable for the position control of a valve actuator system but the parameter changes the system had to cope with were relatively small. In contrast, in injection moulding, while the plant structure will remain the same, parameters will change significantly with new moulds or materials. One way of coping with this would be to use a gain-scheduling observer sliding mode controller much like the one for electrohydraulic motor speed control detailed in **Yanada & Shimahara (1997)**. This would be more robust than a fixed gain method.

While the strategy cannot be ruled out, a sufficiently short sample time cannot be achieved on the rig and so it was not possible to test the strategy. This was a fundamental limitation of implementing a controller under the WINDOWS environment where a minimum slice time of 1ms is imposed.

4.3.9 Adaptive Pressure Control

The arguments for using any one of the 3 broad classes of adaptive controller (gain-scheduling, self-tuning regulator and model reference) are similar to those for adaptive velocity controlled filling. Gain scheduling is inappropriate not

through lack of measured variables on which to schedule control but because any gain scheduling map would be mould specific and the construction of such a map is a fairly lengthy task. The successful implementation of a self-tuning regulator has recently been reported by **Yang & Gao (1999)** for packing pressure tracking control. However it is important to note that no results were presented showing how the controller dealt with the *onset* of packing. The issue of parameter estimation windup was addressed by fixing controller gains once pressure error was sufficiently low. As such a self-tuning approach has been shown to work for the latter stages of packing pressure control. While it would be unfair to say that the self-tuning regulator implemented by **Yang & Gao (1999)** was over complex, MRAC solutions do exist that are much more compact. One such scheme is the Minimal Control Synthesis (MCS) MRAC. MCS has a number of advantages over other possible controllers. Firstly it has already been used successfully on hydraulic valve actuator systems e.g. in the force control of a servo-hydraulic materials testing machine, reported in **Stoten (1992)** or more recently in energy efficient control of a valve actuator system with a variable displacement pump, detailed in **Beard (1998)**. Secondly a large amount of research has been done using the MCS algorithm and it is fair to say that a solution incorporating MCS could be commercialised. Therefore MCS was chosen for packing pressure control. The next section on MCS explains the algorithm and issues surrounding its use.

4.4 Minimal Control Synthesis

The MCS controller is suitable for both single input single output (SISO) and multi-input multi-output (MIMO) systems and has been shown to be effective for both (**Stoten & Hodgson (1991)** and **Stoten et al (1994)**). Using conventional state-space notation for the plant dynamics in equation (4.5) then the continuous time implementation of the MCS algorithm for MIMO and SISO systems can be summarised by equations (4.5)-(4.11).

$$\dot{x}(t) = Ax(t) + Bu(t) + d(t) \qquad (4.5)$$

$$u(t) = K(t)x(t) + K_r r(t) \qquad (4.6)$$

$$K(t) = \int_0^t \alpha y_e(\tau) x^T(\tau) d\tau + \beta y_e(t) x^T(t) \qquad (4.7)$$

$$K_r(t) = \int_0^t \alpha y_e(\tau) r^T(\tau) d\tau + \beta y_e(t) r^T(t) \qquad (4.8)$$

$$y_e(t) = C_e x_e(t) \qquad (4.9)$$

$$x_e(t) = x_m(t) - x(t) \qquad (4.10)$$

$$\dot{x}_m(t) = A_m x_m(t) + B_m r(t) \qquad (4.11)$$

A block diagram of this is shown in Figure 4.8. Essentially the state feedback gain (K) and the forward loop gain (K_r) are varied to minimise the difference between the system output (x) and the reference model output (x_e).

Apart from system state values, for an MCS controller to be implemented there are 4 parameters that need to be supplied.

- The order of the reference model (In this work only critically damped reference models were used.)
- The reference model settling time
- Output error matrix, often set to 1 in SISO systems
- Integral adaptive gain, α
- Proportional adaptive gain, β (α and β are often quoted in the literature as being a decade apart i.e. if $\alpha = 10$ then $\beta = 1$, this is covered in more detail later in this chapter.)

While the list above may appear long in comparison to other model reference adaptive schemes, for a successful implementation, MCS requires little information. This is the main advantage of MCS.

4.4.1 Stability

Since one of the central intentions of this work has been that suggested controllers are eventually commercialised, guaranteeing stability and robustness are important concerns. In the case of a fixed gain controller such as PID the analysis is relatively simple. However in the case of adaptive control this is not so simple. Fortunately this work has already been carried out and is detailed in **Stoten & Benchoubane (1990b)**. The important results detailed in this work are that

- Provided that system parameters vary slower than the adaptive laws in an MCS controller then MCS ensures an asymptotically hyperstable closed loop system.
- MCS control is robust to changes in plant parameters, external disturbances, effects of non-linearities and modelling inaccuracies.

With reference to **Astrom & Wittenmark (1984)** and **D'Azzo & Houpis (1988)** asymptotically stability means that the error between the plant and reference model tends to zero as time tends to infinity. This is distinctly different from Lyapunov stability which means that error will tend to a maximum and minimum value and then limit cycle between the 2. Practically this will mean that to guarantee the stability of a commercially available MCS controller it will have to be implemented at a sampling frequency faster than changes in plant parameters.

A pragmatic solution to any MCS stability concerns might be to lock the adaptive gains after 1 or 2 injection moulding cycles. This would mean that the proof of stability in **Stoten & Benchoubane (1990b)** would be rendered irrelevant. Unfortunately tests have shown that locking the adaptive gains does not work and for injection packing pressure control the system response using the final adaptive gain values from the previous cycle is sluggish. This is because MCS is an adaptive control strategy whose success is determined by its ability to change its gains to minimise the error between the reference model and the plant output.

4.4.3 Reference Model Choice

When selecting a reference model the first thing to decide is the reference model order. This choice is principally dependent on the order of the system being controlled and the transducer signals available. For MCS control the order of the reference model dictates the maximum order of the plant output required. (e.g. for a 2nd order reference model the 1st derivative of plant output is required, for a 3rd order reference model the 2nd derivative of plant output is required.) However in the case of hydraulic pressure control it is generally acknowledged that due to pump pressure ripple the unfiltered derivative of pressure is of little or no use for control. Since pump pressure ripple is due to the discrete pumping action of the hydraulic pump it is possible to minimise the effects by synchronising pressure measurement with pump shaft angle. However this was considered too complicated for commercialisation and was not implemented. Hence from the implementation standpoint it was preferable to use a 1st order reference model.

4.4.3.1 Meter-In Pressure Control Of a Fixed Volume: Small Perturbation Analysis

Ignoring screw leakage, from the point of view of packing pressure control the problem can be simplified to the control of pressure in a fixed volume of oil using an underlapped valve. In order to help in the choice of reference model a small perturbation analysis of this system was carried out. A diagram of the system considered is shown in Figure 4.9.

The assumptions made were:

- The flow coefficient is considered constant.
- The bulk modulus is considered constant.
- Flow past the valve spool is metered by two 90° spool notches in each flow path and is the same as an industry standard P-Q spool used in injection moulding control.
- The compliance of the pipe connecting the valve to the volume is ignored.
- The 2nd order valve dynamics are neglected.

The equations can then be written as:

Original Equations	Linearised Equations	
$Q_S = 2(X_u + X)^2 C_q \sqrt{\frac{2(P_s - P_1)}{\rho}}$ (4.12)	$q_S = 4(X_u + X)C_q \sqrt{\frac{2(P_s - P_1)}{\rho}} x - (X_u + X)^2 C_q \sqrt{\frac{2}{\rho}} \frac{1}{\sqrt{P_s - P_1}} p_1$	(4.12a)
$Q_R = 2(X_u - X)^2 C_q \sqrt{\frac{2P_1}{\rho}}$ (4.13)	$q_R = -4(X_u - X)C_q \sqrt{\frac{2P_1}{\rho}} x + (X_u - X)^2 C_q \sqrt{\frac{2}{\rho}} \frac{1}{\sqrt{P_1}} p_1$	(4.13a)
$Q_1 = \frac{P_1 V_1 s}{\beta_{oil}}$ (4.14)	$q_1 = \frac{V_1 s}{\beta_{oil}} p_1$	(4.14a)
$Q_S = Q_1 + Q_R$ (4.15)	$q_S = q_1 + q_R$	(4.15a)

Where lower case symbols denote small changes in variables

Substituting (4.12a), (4.13a) and (4.14a) into (4.15a) gives

$$4(X_u + X)C_q \sqrt{\frac{2(P_s - P_1)}{\rho}} x - (X_u + X)^2 C_q \sqrt{\frac{2}{\rho}} \frac{1}{\sqrt{P_s - P_1}} p_1 = \frac{V_1 s}{\beta_{oil}} p_1 - 4(X_u - X)C_q \sqrt{\frac{2P_1}{\rho}} x + (X_u - X)^2 C_q \sqrt{\frac{2}{\rho}} \frac{1}{\sqrt{P_1}} p_1 \quad (4.16)$$

let

$$K_{x1} = 4(X_u + X)C_q \sqrt{\frac{2}{\rho}} \quad (4.17)$$

$$K_{x2} = 4(X_u - X)C_q \sqrt{\frac{2}{\rho}} \quad (4.18)$$

$$K_{p1} = (X_u + X)^2 C_q \sqrt{\frac{2}{\rho}} \tag{4.19}$$

$$K_{p2} = (X_u - X)^2 C_q \sqrt{\frac{2}{\rho}} \tag{4.20}$$

then substituting into (4.16) with (4.17), (4.18), (4.19) and (4.20) gives

$$K_{x1}\sqrt{P_s - P_1}x - \frac{K_{p1}}{\sqrt{P_s - P_1}}p_1 = \frac{V_1 s}{\beta_{oil}}p_1 - K_{x2}\sqrt{P_1}x + \frac{K_{p2}}{\sqrt{P_1}}p_1 \tag{4.21}$$

rearranging (4.21)

$$\frac{p_1}{x} = \frac{K_{x1}\sqrt{P_s - P_1} + K_{x2}\sqrt{P_1}}{\frac{V_1 s}{\beta_{oil}} + \frac{K_{p1}}{\sqrt{P_s - P_1}} + \frac{K_{p2}}{\sqrt{P_1}}} \tag{4.22}$$

The system is 1st order and depending on the rig operating point the –3dB bandwidth is between 0.1Hz and 10Hz. The bandwidth is so low because of the large volume of trapped oil between the actuator piston and the injection control valve. Most of this volume is in the flexible pipe as in the real system. The –3dB bandwidth of the injection control valve is approximately 30Hz. Hence if the valve dynamics are now included the system is overall 3rd order with a 1st order dominant root. Neither 3rd or 2nd order MCS controllers are desirable. The next section elaborates on the topic of reference model choice.

4.4.3.2 MCS Reference Model & Plant Order Investigation

A simple circuit including an MCS controller controlling a 2nd order lag in series with a 1st order lag was set up in MATLAB, the circuit block diagram is shown in Figure 4.10. The 2nd order lag was critically damped and both lags had a steady state gain of 1. To make sure that the 3rd order plant was either 1st or 2nd order dominant the break frequencies of the lags were set to 1Hz (1st order) and

100Hz (2^{nd} order) or 100Hz (1^{st} order) and 1Hz (2^{nd} order). These 2 systems were then controlled using MCS controllers with 1^{st} and 2^{nd} order critically damped reference models with break frequencies of 1Hz, 5Hz, 20Hz, 50Hz and 100Hz. The output from the MCS controller was limited to ±100. All the different plant and reference model configurations are summarised in Table 4.1.

The demand signal was kept the same for all tests and was set as a 0-10 step input after 1s. It was also decided for simplicity to set the adaptive weights α and β to 0.1 and 0.01 respectively. Clearly changing the adaptive weights has an effect on system performance and this will be discussed later.

The results are included in Figures 4.11-4.20 in the same order as the configurations are set out in Table 4.1 and a brief summary of the results is set out in Table 4.2. Each figure contains results for plant output, 'controller output' which is the output from the MCS controller and 'reference output' which is the output from the reference model. Briefly looking through all the results it is clear that for all the configurations the plant achieves the required steady state level. However there is a clear distinction between the 1^{st} and 2^{nd} order dominant plant results. The 2^{nd} order dominant plant output results are much less well damped than the 1^{st} order dominant ones. On closer inspection there is much greater overshoot in the cases when the plant is 2^{nd} order dominant (1Hz natural frequency).

Now looking at all the results when the plant was 1^{st} order dominant in Figure 4.11, Figure 4.13, Figure 4.15, Figure 4.17 and Figure 4.19. It can be seen that once the reference model is 5Hz or faster it continues to take the same amount of time for the plant output to reach its final value. In fact increasing the reference model natural frequency above 5Hz has no effect on system performance when the 3^{rd} order plant is 1^{st} order dominant.

Consider again the results in Figure 4.12, Figure 4.14, Figure 4.16, Figure 4.18 and Figure 4.20. When the plant was 2^{nd} order dominant it is clear that overshoot remains the same at 140% when the reference model is 5Hz or quicker. Also

increasing the reference model natural frequency above 5Hz has no effect on the plant output oscillations that follow the overshoot. From this it can be surmised that 1st order MCS controllers are more suitable for controlling 1st order dominant 3rd order plants as opposed to 2nd order dominant ones.

Again all the configurations for 2nd order MCS controllers tested are set out in Table 4.1 and a summary of the results is given in Table 4.3. The results themselves are presented in Figures 4.21–4.25 and set out in the same order as the configurations in Table 4.1. Again each figure contains results for plant output, 'controller output' which is the output from the MCS controller and 'reference model output', which is the output from the reference model. The first observation is that not all the controller and plant configurations are stable. All the 1st order dominant plant configurations (1st order lag break frequency 1Hz) show controller output instability. All of the configurations tested were unstable with a reference model of 50Hz or more.

Now looking more closely at the plant 2nd order dominant results in Figure 4.22 and Figure 4.24. It is clear that the controller output becomes increasingly oscillatory as the reference model natural frequency is increased and that the system output actually settles faster with the slower 5Hz reference model as opposed to the 20Hz one.

Compared to an MCS controller with a 2nd order critically damped reference model an MCS controller with a 1st order reference model can achieve better control of a 1st order dominant 3rd order plant. Also, if controller output stability is used as a measure then better control of 2nd order dominant 3rd order plants can be achieved by an MCS controller with a 2nd order reference model. It is also clear that an MCS reference model can be too fast for a system and cause instability. Hence, from the results it can be concluded that as a general rule the MCS reference model should be set as slow as the slowest root of the plant being controlled. It must not be forgotten that all the plants used in all the tests were linear and continuous which is not the case for injection moulding control. Even so the results still clearly suggest the use of a 1st order reference model and that

to guarantee stability the reference model settling time should be longer than that of the system being controlled.

4.4.4 Adaptive Gain Weights

Since the output error matrix was set to 1 the only parameters remaining to tune on an MCS implementation are the adaptive gain weights α and β. This section contains an explanation of the adaptation mechanism underpinning MCS and a literature review of other reported implementations including the adaptive gain weights chosen.

The MATLAB SIMULINK block diagram of a 1st order MCS controller is shown in Figure 4.26. From this diagram it is clear that adaptive gain k is calculated by multiplying the plant output with the error between the reference model output and plant output. This signal is then fed simultaneously into a proportional gain (β) and an integrator with a gain of α the outputs of which are summed to give the adaptive gain. In Figure 4.26, as on the rig, the integrator is a discrete time implementation running at 1kHz. In this work this can be considered fast enough to be the same as a continuous time integrator. The adaptive gain calculation is the same as a PI controller the dynamics of which are described by equation (4.9).

$$\frac{\alpha+\beta s}{s} \qquad (4.9)$$

Adaptive gain k_r is calculated by multiplying the reference model input with the error between the reference model output and plant output. This is then fed into an exact copy of the PI controller used to calculate k. Equation (4.9) is a 1st order lead and an integrator. So far the ratio of adaptive weights used in this work has been, $\alpha = 10\beta$. The ratio of $\alpha:\beta$ sets the break frequency of the 1st order lead term which decides the frequency at which the controller action changes from dominantly integral to dominantly proportional. With the adaptive weight ratio set to 10 the break point is 1.59Hz, α sets the high frequency (above 1.59Hz) gain of the controller. A discrete time Bode plot with a sampling time of 1ms of equation (4.9), using the ratio of adaptive weights $\alpha = 10\beta$ and with $\alpha = 2\times10^{-5}$ is shown in Figure 4.27.

With the ratio of adaptive gains set to 10, changing the adaptive weights does not alter the plot in Figure 4.27 nor does it alter the shape of the amplitude ratio plot. Changing the adaptive gains shifts the amplitude ratio line up or down the amplitude ratio axis.

Using $\alpha = 10\beta$ sets the frequency below which the integral action is dominant and as such it seems that the ratio should be linked to plant dynamics. It seems unlikely that a very slow plant with time constants measured in minutes can best be controlled with the same adaptive weights ratio as a plant with time constants measured in tenths of seconds. With this in mind a literature review of all the published work on MCS control was carried out.

Over 10 papers published on MCS control have been found and this section considers 6 of these where plant details are given and adaptive weights have been chosen. The first was by **Stoten & Benchoubane (1990a)** and detailed MCS speed control of a dc motor and MCS control of a reservoir level. The DC motor plant was 1st order with a break frequency of 0.08Hz and the reservoir level had a settling time of around 100s. The adaptive weights used for dc motor speed control were $\alpha = 4$, $\beta = 1$ and for reservoir level control the adaptive weights were $\alpha = 0.003$, $\beta = 0.03$ Neither of these used the ratio $\alpha = 10\beta$ and the break frequencies for the adaptive gains PI controllers are 0.64Hz for the dc motor control and 16mHz for the reservoir level control.

The next work considered is that by **Stoten (1992)** on the MCS force control of a servo-hydraulic materials testing machine. Although the plant dynamics change during materials testing a Bode plot for a representative plant is shown in Figure 4.28. This plant is 2nd order and faster than the 2 previous examples with a natural frequency of around 18Hz. Consequently a different adaptive weights ratio was used with $\alpha = 100$, $\beta = 10$. Thus the ratio $\alpha = 10\beta$ was used.

The control of a web tension and speed during tape winding was also tackled using MCS control and detailed in **Stoten & Webb (1994)**. The plant controlled was both highly non-linear and time dependent. While plant transfer function

time constants were not given, the MCS controller reference model settling times were all set to 0.5s. Assuming that the reference models were set slower than the plant dynamics, this indicates that the plant dynamics were around 8Hz or more. Again in this example of MCS control the adaptive weights ratio of $\alpha = 10\beta$ was used.

Aziz & Thomson (1996) detail MCS control of a rotatable beam using a reference model with a time constant of 0.5s. Once again the adaptive weights ratio of $\alpha = 10\beta$ was used.

As part of a study into gain-bounded MCS control **Stoten & Sebusang (1998)** detail the results of MCS control of a ball and beam rig. The beam pivots in the middle like a see-saw and the ball runs along the length of the beam. Beam angle is controlled by an actuator offset to one side of the pivot. The transfer function relating ball position to actuator output was given and a Bode plot of this is shown in Figure 4.29. The system was open loop unstable and had a –3dB bandwidth of around 0.1Hz. Yet again the adaptive weights ratio of $\alpha = 10\beta$ was used with α set to 0.01 and β set to 0.001.

Finally **Hodgson & Stoten (1998)** reported on MCS control of 2 trolleys linked by 3 springs, one between them and the other 2 to anchoring points either side. Details of the transfer function relating the input signal to one of the trolley's position were given. The system was 2nd order, slightly underdamped with a natural frequency of around 0.8Hz. To control this the adaptive weights ratio of $\alpha = 10\beta$ was again used with α set to 0.3 and β set to 0.03.

Of the seven separate systems in this brief review in five cases the adaptive weights ratio of $\alpha = 10\beta$ was used. In these case all plants natural frequencies were in the range 0.1Hz-18Hz. In the control of the dc motor in the work by **Stoten & Benchoubane (1990a)** the plant had a natural frequency of 0.08Hz which is only just outside the range 0.1Hz-18Hz. The adaptive weights ratio used in this case was $\alpha = 4\beta$ which seems curious. However it is worth pointing out that the work by **Stoten & Benchoubane (1990a)** was one of the first on MCS

control and it is likely that an adaptive weights ratio of $\alpha = 10\beta$ may work almost as well. The other case in which a different adaptive weights ratio was used in the control of a reservoir level, detailed in **Stoten & Benchoubane (1990a)**. In this case the ratio $10\alpha = \beta$ was used. This had the effect of reducing the adaptive gain PI controller break point to 16mHz from the more usual 1.59Hz (when $\alpha = 10\beta$). Considering that the reservoir level plant had a settling time of 100s and is much slower than any other MCS controlled system in this review this is as one would expect. It has previously been reported that the adaptive weights ratio $\alpha : \beta$ should always be set to $\alpha = 10\beta$. More precisely, in similar servo applications the adaptive weights ratio $\alpha : \beta$ should usually be set to $\alpha = 10\beta$. In the case of slower plant control the ratio should be reduced (e.g. $10\alpha = \beta$) and conversely it is highly likely that in the case of faster plants the ratio should be increased.

4.5 Concluding Remarks

Fuzzy logic or neural network control of injection moulding filling and packing P-Q control can be discounted on the grounds that, with a controller of medium complexity, stability would be hard to prove. Hence a hybrid solution for P-Q control seems appropriate. Overall adaptive control of filling and packing with a bumpless transfer strategy connecting the pair appears to be the best solution. Of the adaptive solutions available the MRAC controller MCS shows considerable promise. From a small perturbation analysis packing pressure control is a 1^{st} order dominant 3^{rd} order system. Analysis of MCS control of different 3^{rd} order systems has shown that a 1^{st} order reference model should be sufficient. A review of previous implementations of MCS control has also been carried out and shown that there is scope to match the adaption mechanism dynamics to those of the plant by altering the adaptive gain weight ratio.

Table 4.1 MCS Controller and Plant Details

Ref. Model Break Frequency [Hz]	1st order lag Break Frequency [Hz]	2nd order lag Break Frequency [Hz]
1	1	100
1	100	1
5	1	100
5	100	1
20	1	100
20	100	1
50	1	100
50	100	1
100	1	100
100	100	1

Table 4.2 1st Order Reference Model Results Summary

Reference Model Break Frequency [Hz]	Break Frequency of 1st Order Part of Plant [Hz]	Break Frequency of 2nd Order Part of Plant [Hz]	Comments
1	1	100	No overshoot
1	100	1	80% overshoot
5	1	100	5% overshoot
5	100	1	140% overshoot
20	1	100	5%overshoot
20	100	1	140% overshoot
50	1	100	5% overshoot
50	100	1	140% overshoot
100	1	100	5% overshoot
100	100	1	140% overshoot

Table 4.3 2nd Order Reference Model Results Summary

Reference Model Break Frequency [Hz]	Break Frequency of 1st Order Part of Plant [Hz]	Break Frequency of 2nd Order Part of Plant [Hz]	Comments
1	1	100	8% overshoot
1	100	1	8% overshoot
5	1	100	Control Output saturates
5	100	1	Control Output saturates
20	1	100	Instability
20	100	1	Control output saturates
50	1	100	Instability
50	100	1	Instability
100	1	100	Instability
100	100	1	Instability

Figure 4.1 Tuned Industry Standard P-Q Controller Results

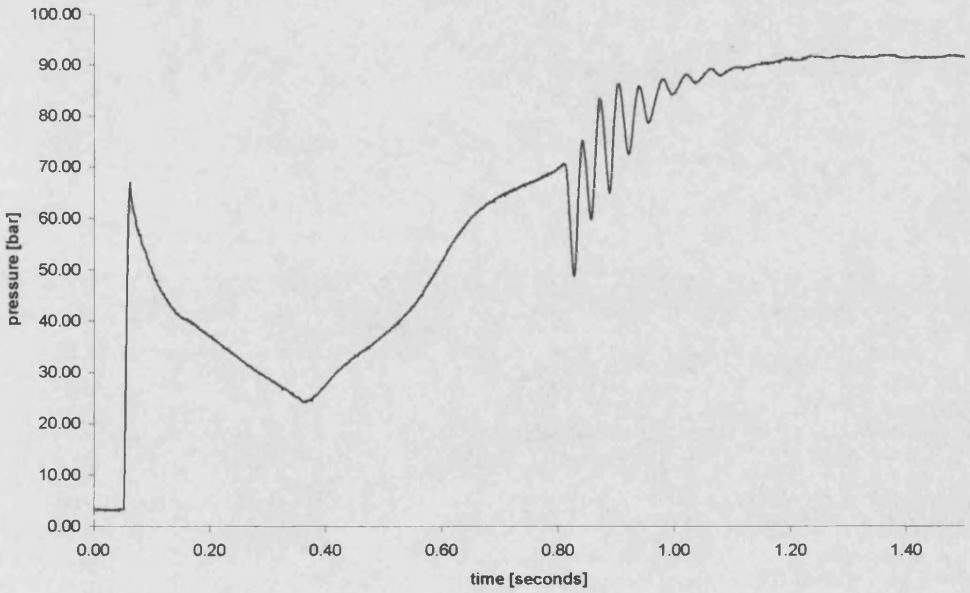

Figure 4.2 Tuned Industry Standard P-Q Controller Results, Short Pipe

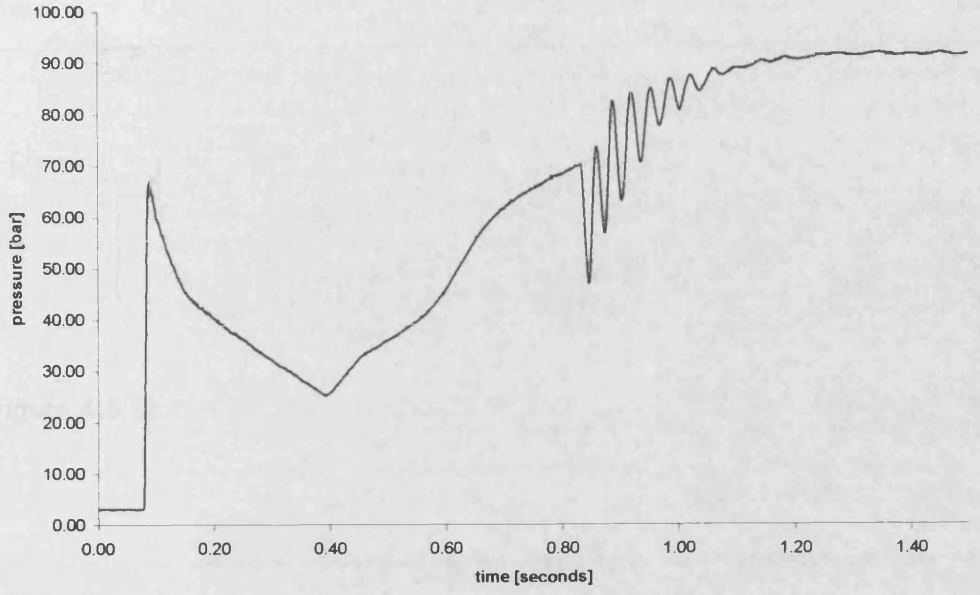

Figure 4.3 Tuned Industry Standard P-Q Controller Results, Long Pipe

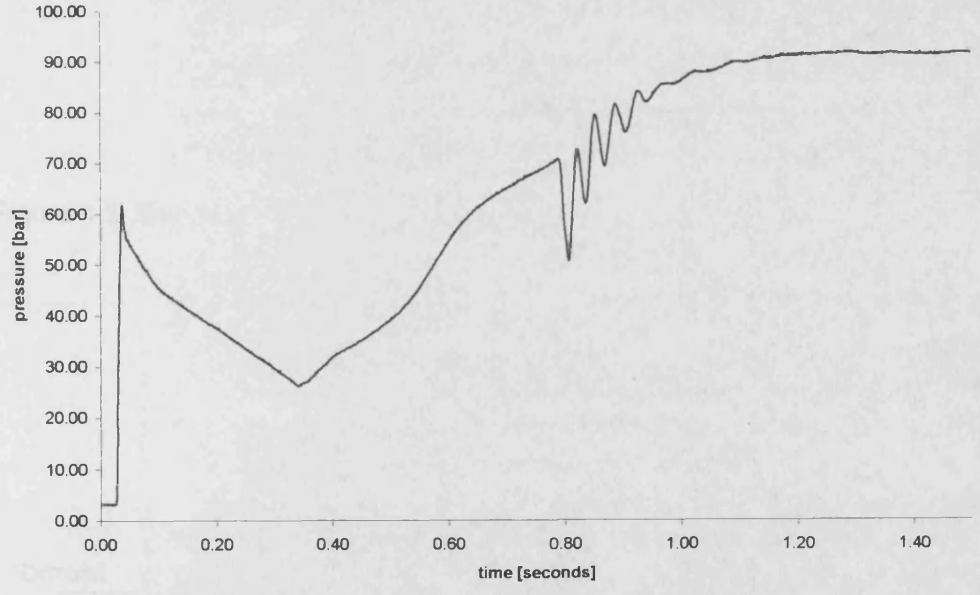

Figure 4.4 Block Diagram of a Gain Scheduling System

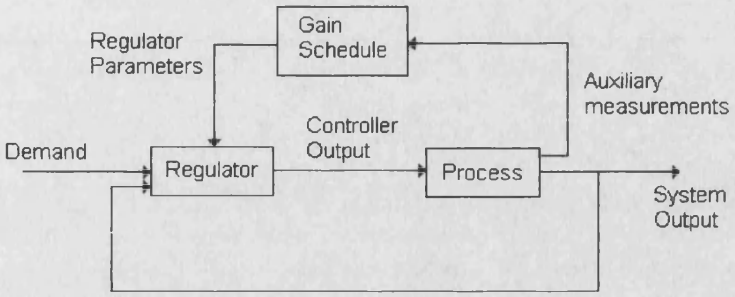

Figure 4.5 Block Diagram of a Self Tuning Regulator

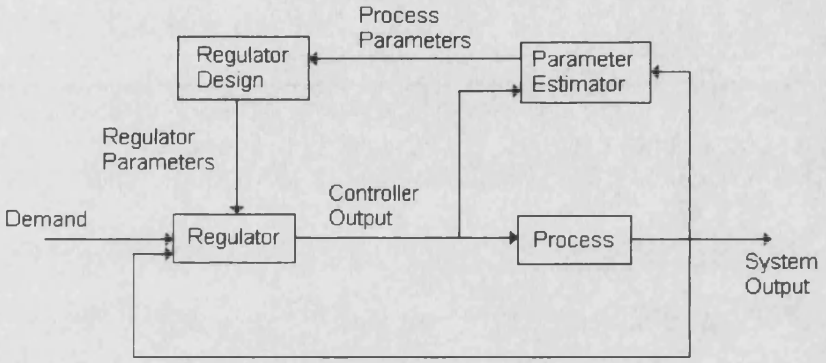

Figure 4.6 Block Diagram of a Model Reference Adaptive System

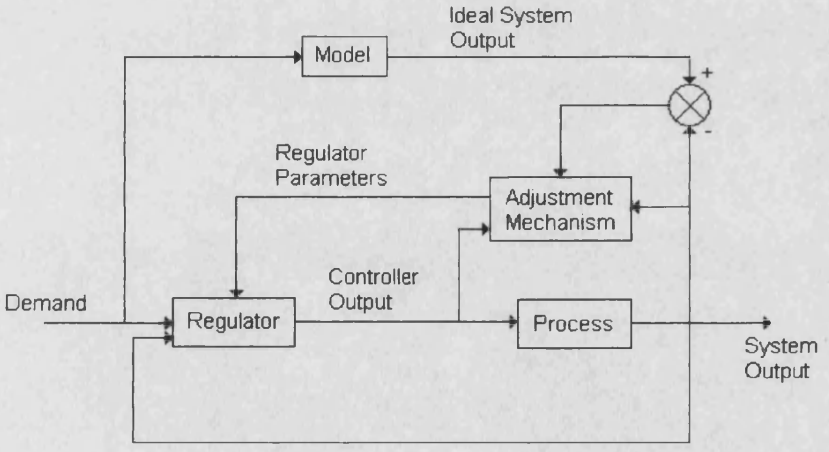

Figure 4.7 Bumpless Transfer Block Diagram

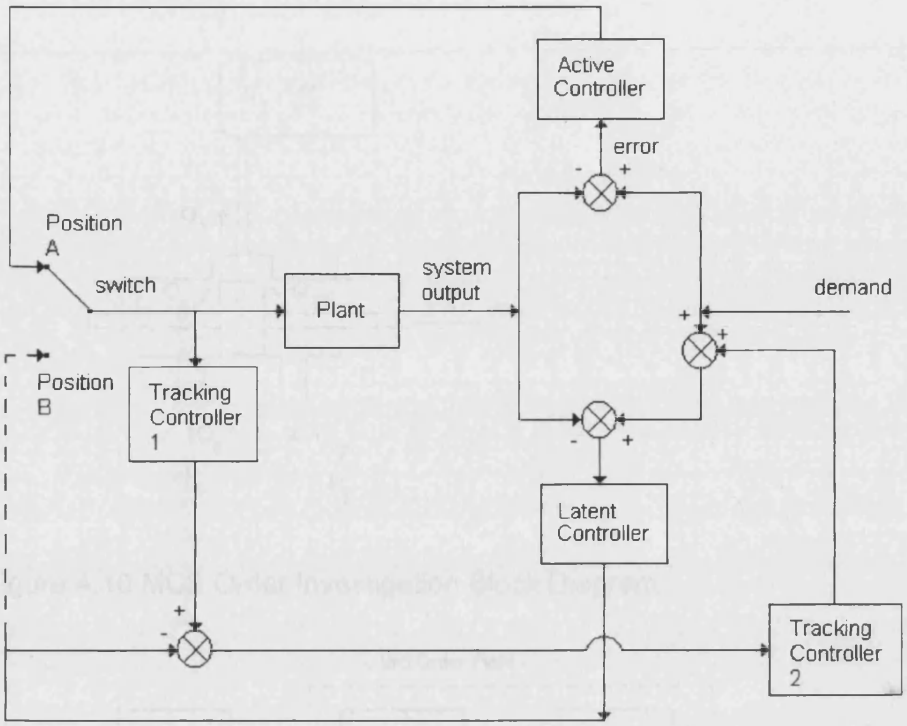

reproduced from **Graebe & Ahlén (1996)**

Figure 4.8 Block Diagram of the MCS Algorithm

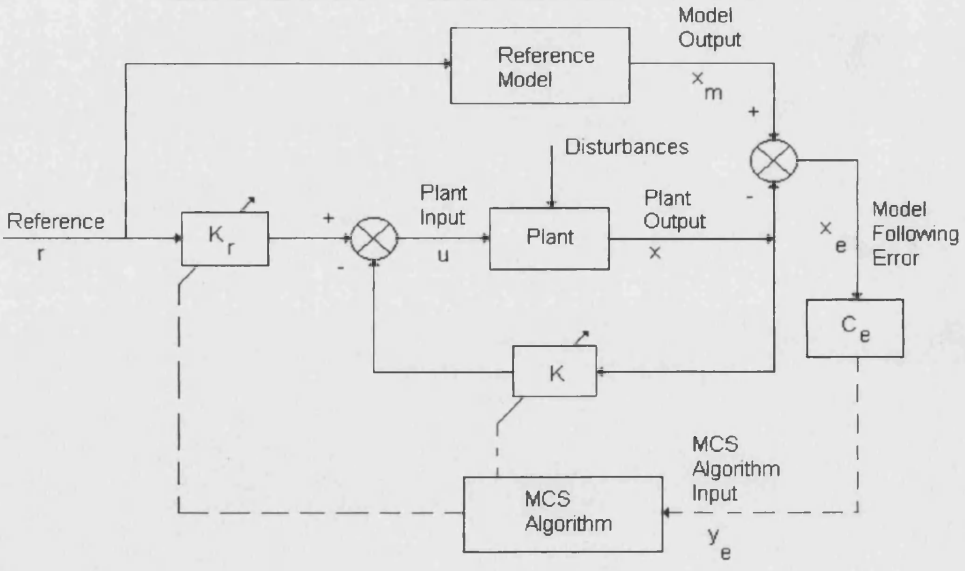

reproduced from **Stoten & Sebusang (1998)**

Figure 4.9 Meter-In Pressure Control of a Fixed Volume

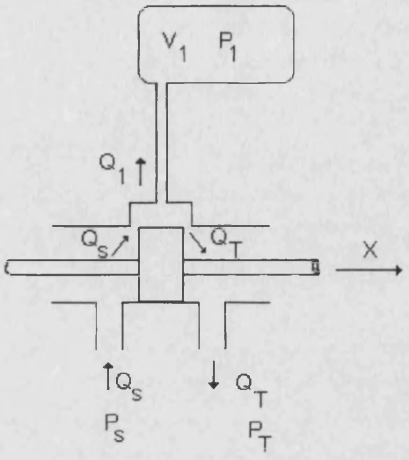

Figure 4.10 MCS Order Investigation Block Diagram

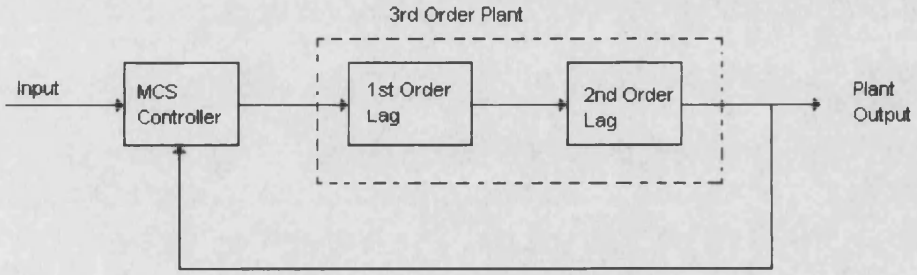

Figure 4.11 1st Order 1Hz Ref. Model, 1Hz 1st Order & 100Hz 2nd Order Plant

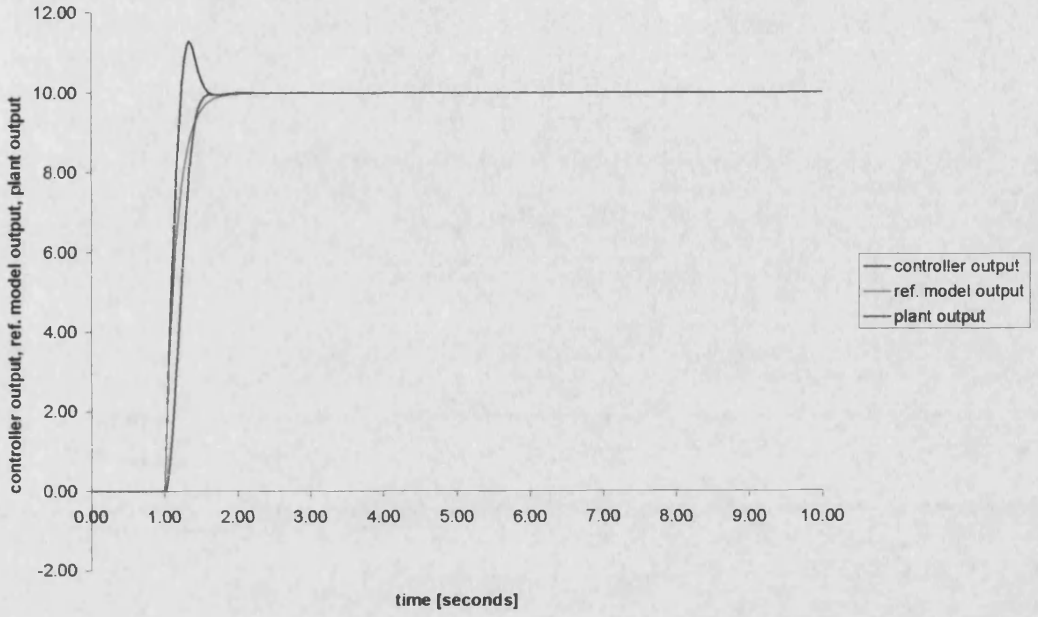

Figure 4.12 1st Order 1Hz Ref. Model, 100Hz 1st Order & 1Hz 2nd Order Plant

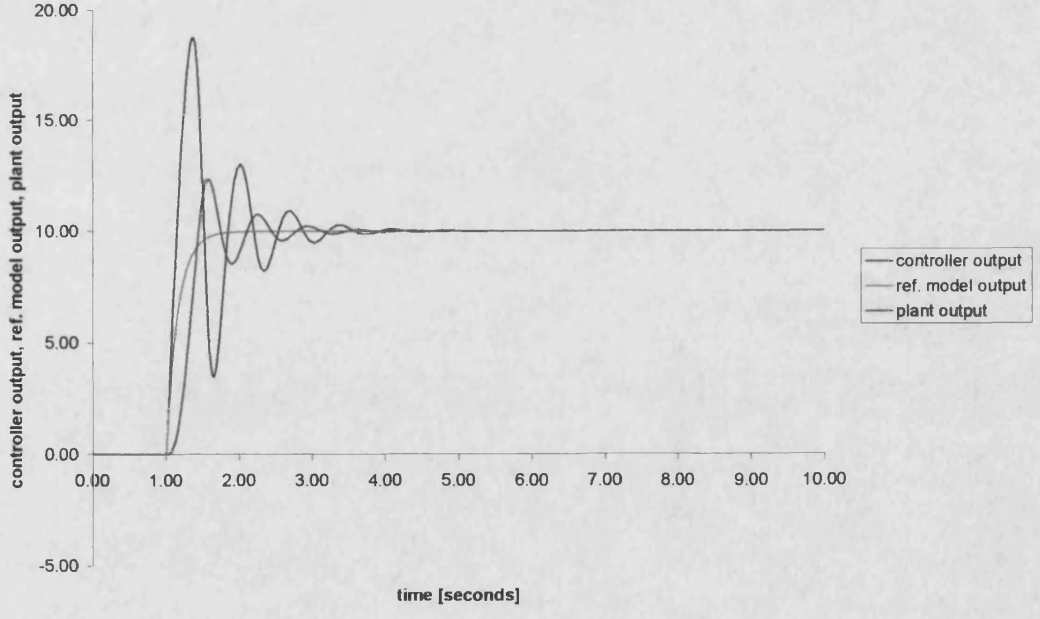

Figure 4.13 1st Order 5Hz Ref. Model, 1Hz 1st Order & 100Hz 2nd Order Plant

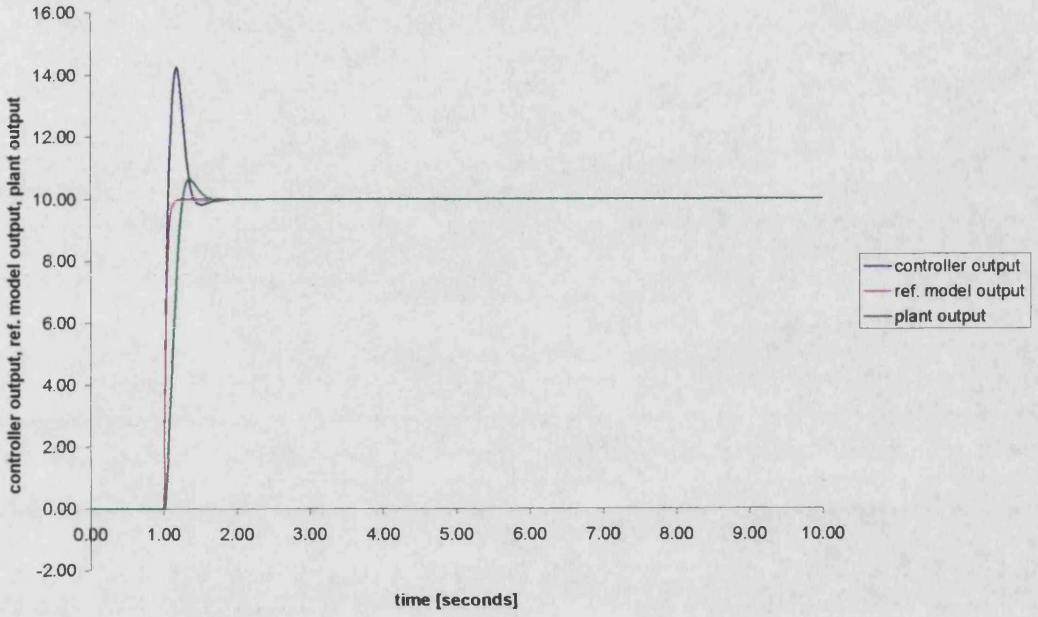

Figure 4.14 1st Order 5Hz Ref. Model, 100Hz 1st Order & 1Hz 2nd Order Plant

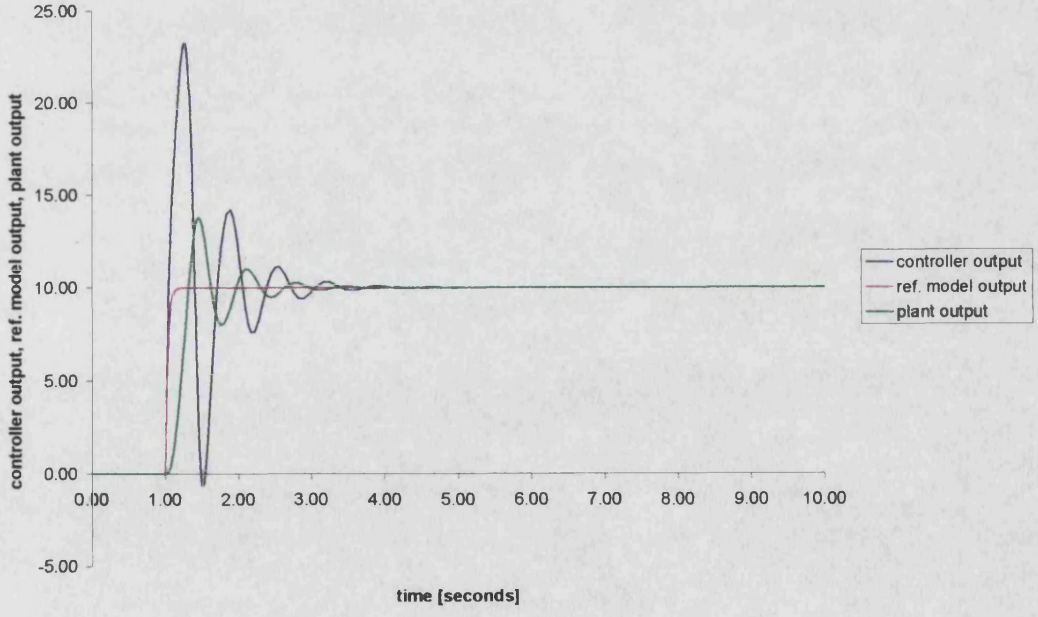

Figure 4.15 1st Order 20Hz Ref. Model, 1Hz 1st Order & 100Hz 2nd Order Plant

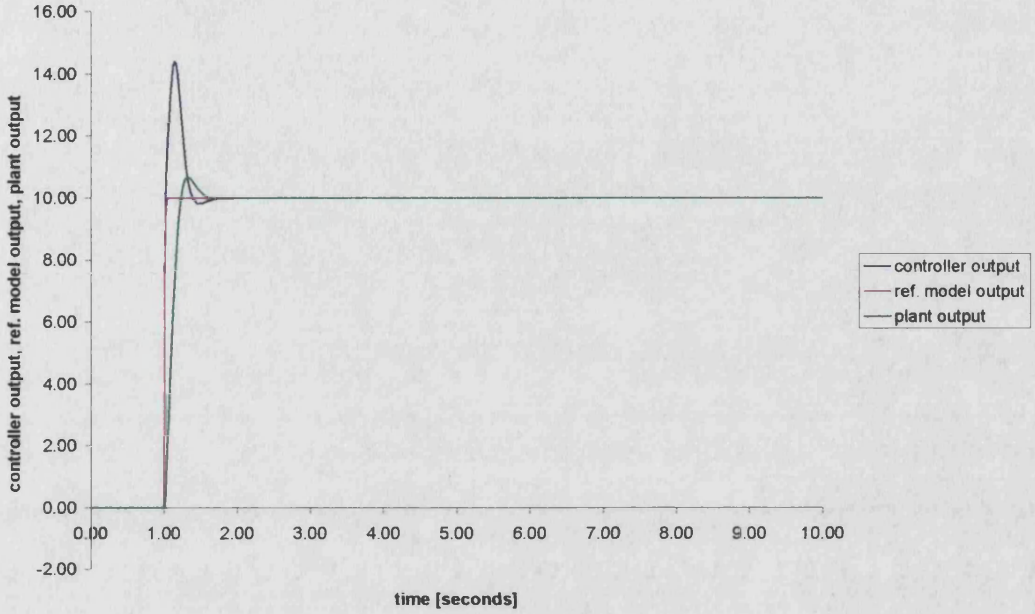

Figure 4.16 1st Order 20Hz Ref. Model, 100Hz 1st Order & 1Hz 2nd Order Plant

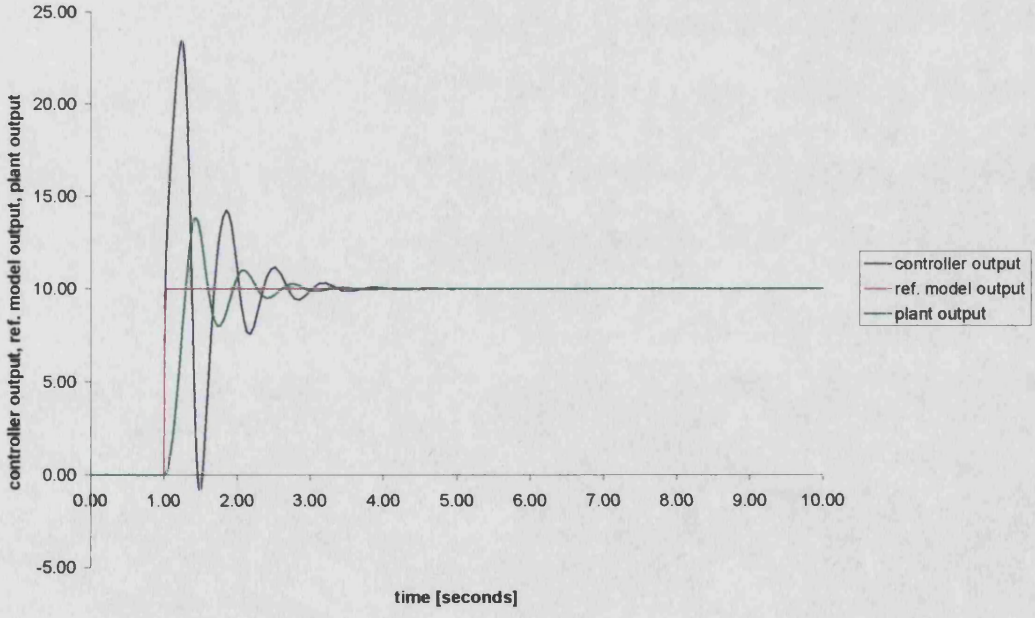

Figure 4.17 1st Order 50Hz Ref. Model, 1Hz 1st Order & 100Hz 2nd Order Plant

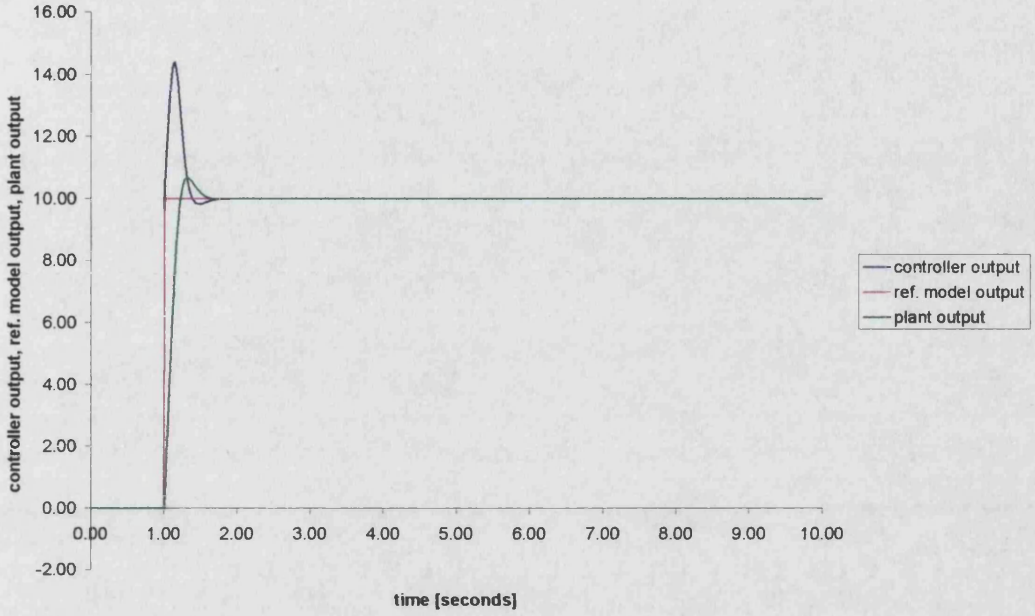

Figure 4.18 1st Order 50Hz Ref. Model, 100Hz 1st Order & 1Hz 2nd Order Plant

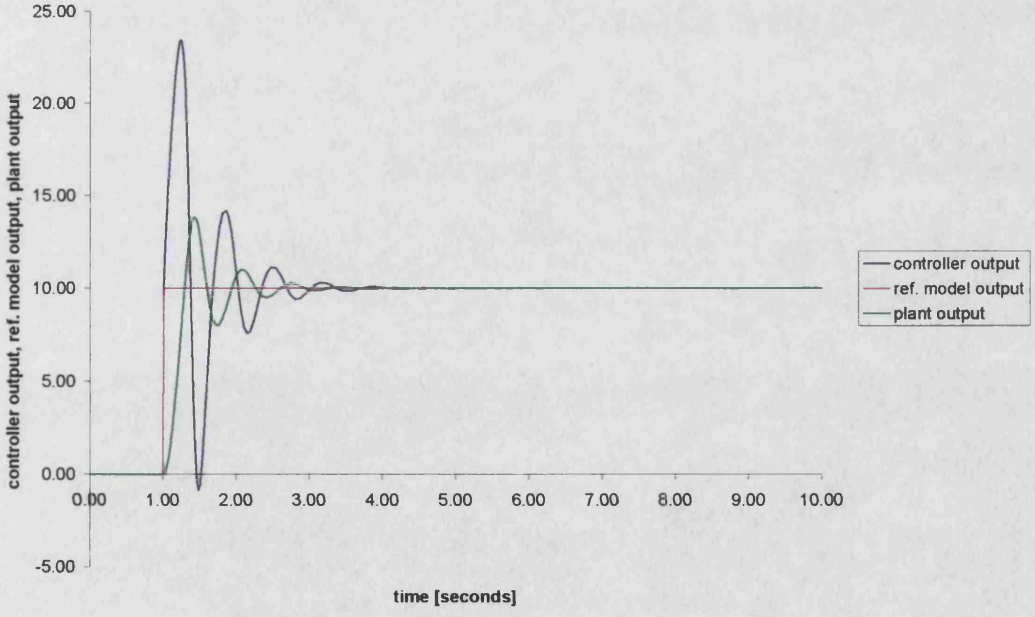

Figure 4.19 1st Order 100Hz Ref. Model, 1Hz 1st Order & 100Hz 2nd Order Plant

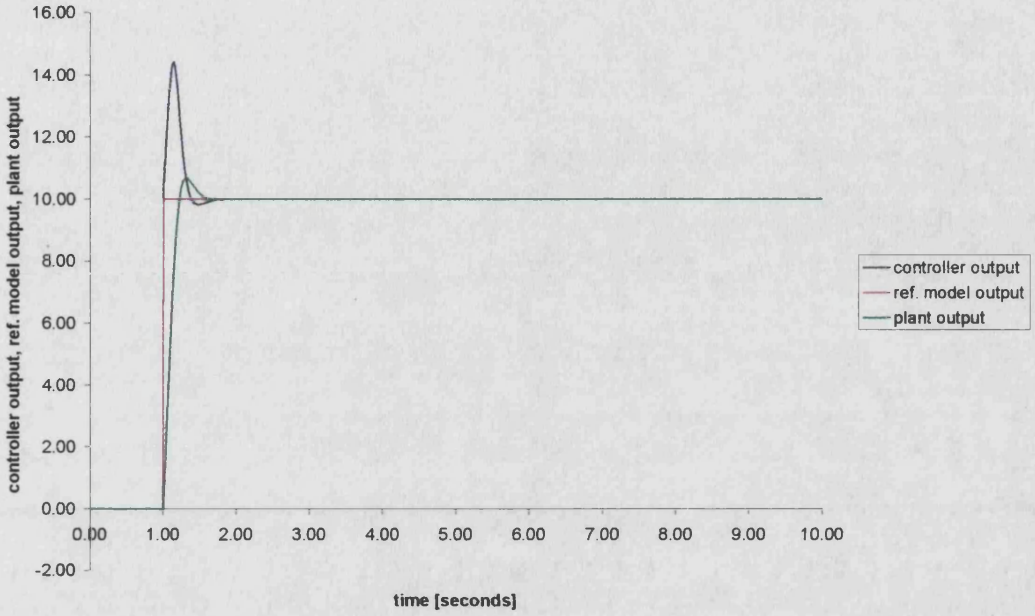

Figure 4.20 1st Order 100Hz Ref. Model, 100Hz 1st Order & 1Hz 2nd Order Plant

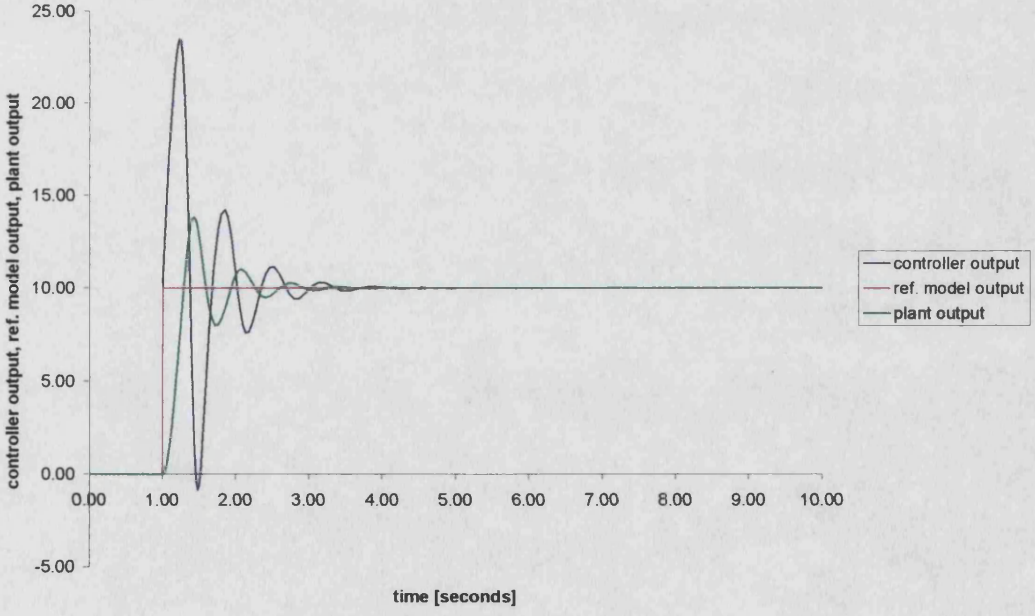

Figure 4.21 2nd Order 1Hz Ref. Model, 1Hz 1st Order & 100Hz 2nd Order Plant

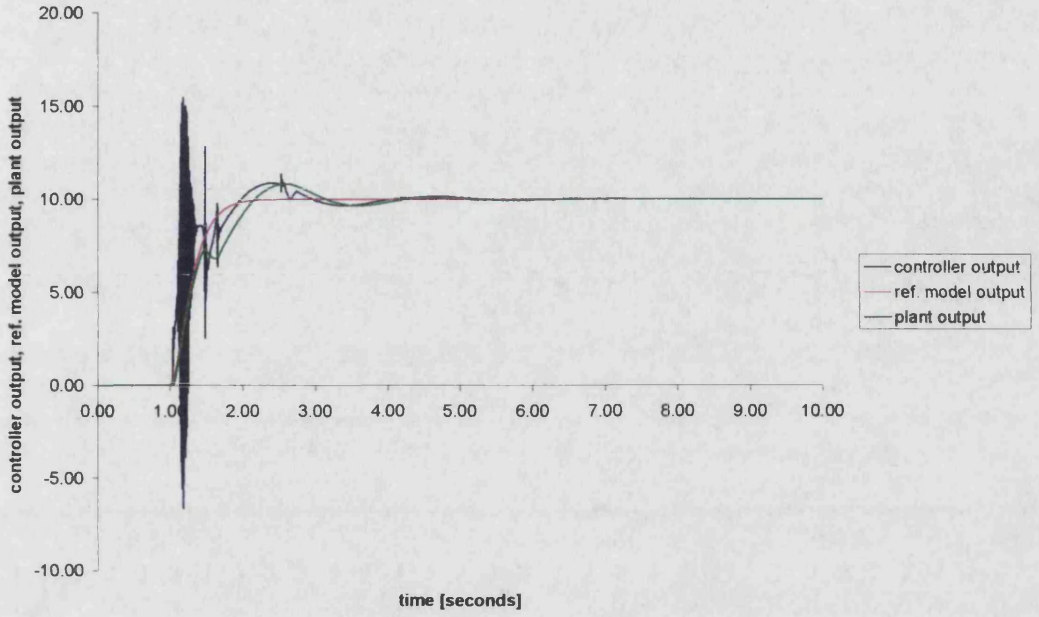

Figure 4.22 2nd Order 1Hz Ref. Model, 100Hz 1st Order & 1Hz 2nd Order Plant

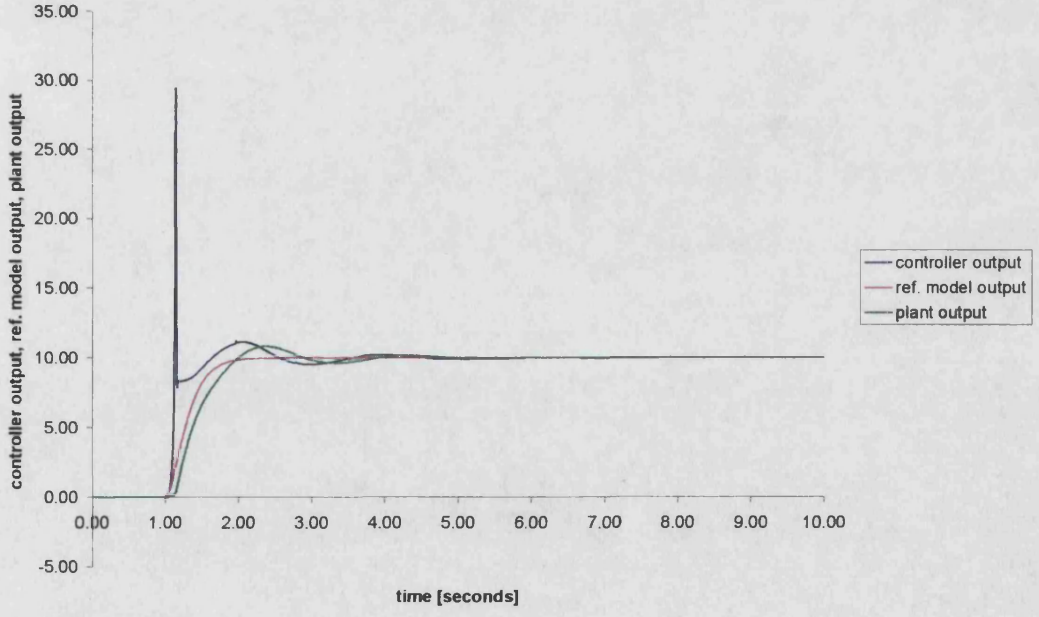

Figure 4.23 2nd Order 5Hz Ref. Model, 1Hz 1st Order & 100Hz 2nd Order Plant

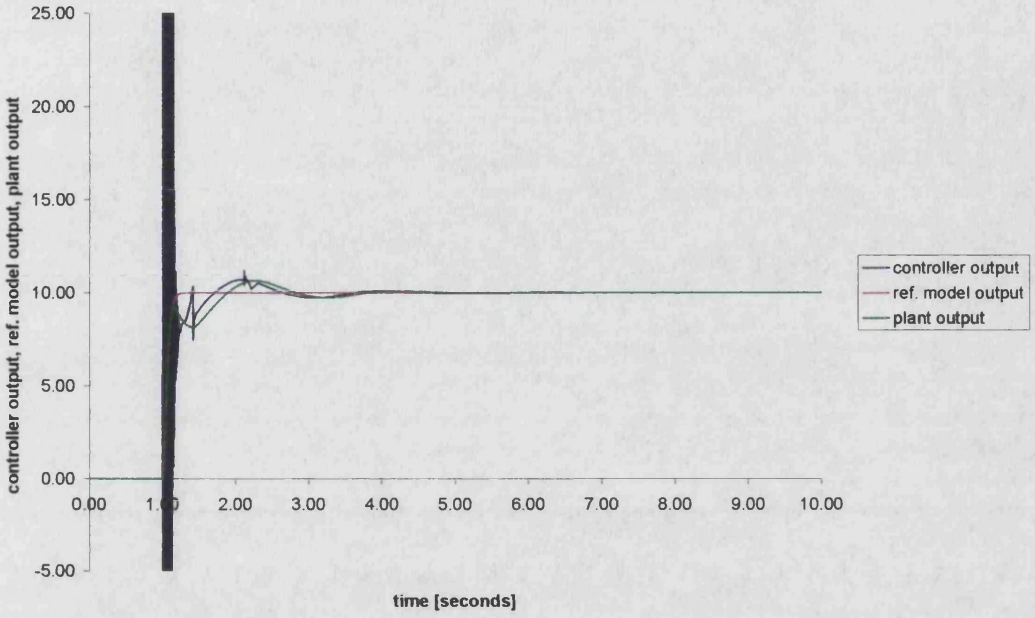

Figure 4.24 2nd Order 5Hz Ref. Model, 100Hz 1st Order & 1Hz 2nd Order Plant

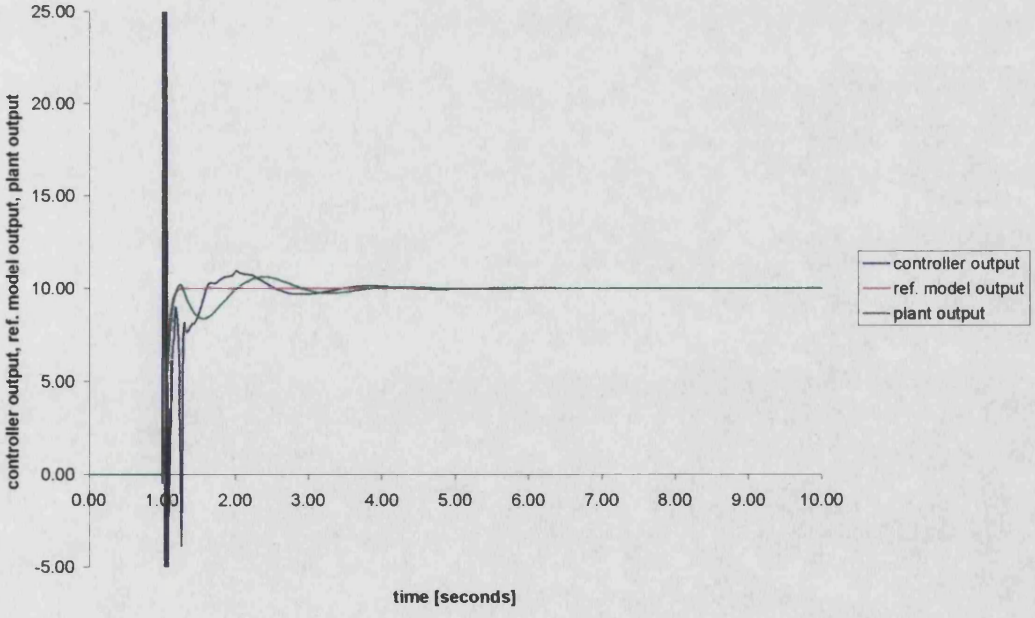

Figure 4.25 2nd Order 20Hz Ref. Model, 1Hz 1st Order & 100Hz 2nd Order Plant

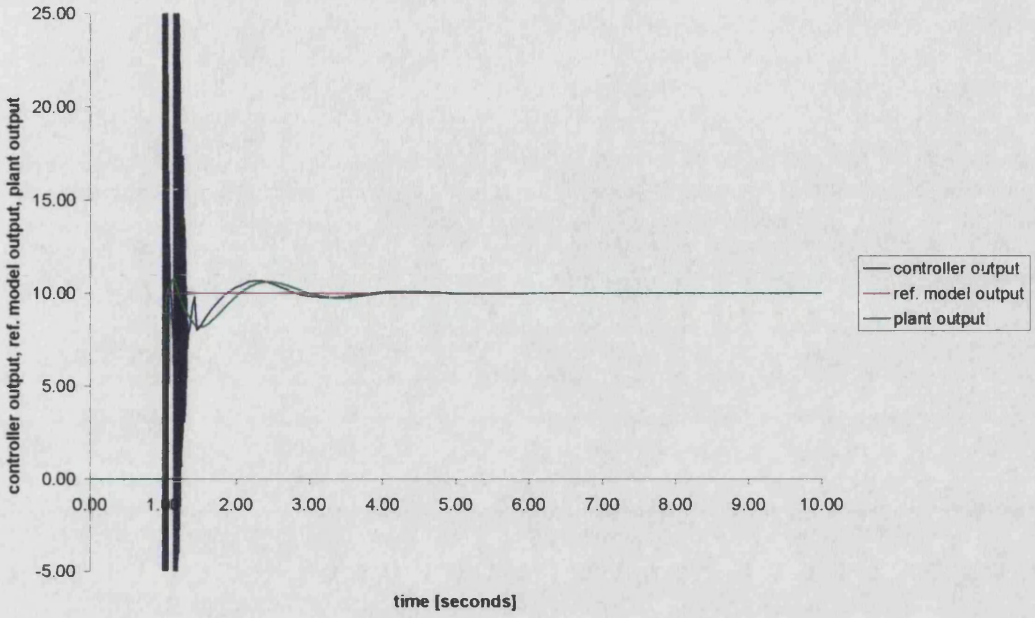

Figure 4.26 MATLAB SIMULINK 1st Order MCS Controller Implementation

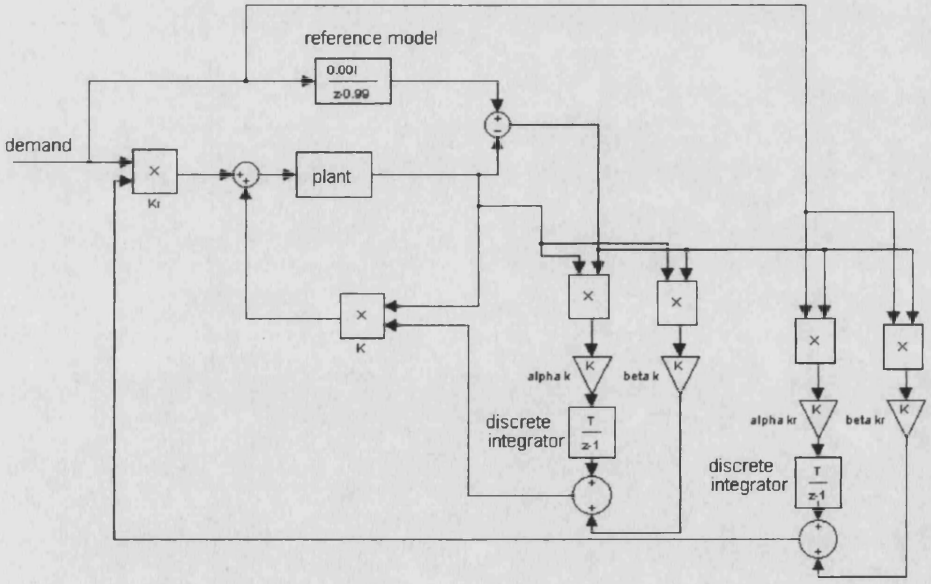

Figure 4.27 MCS Adaptive Gains Discrete Time Frequency Response

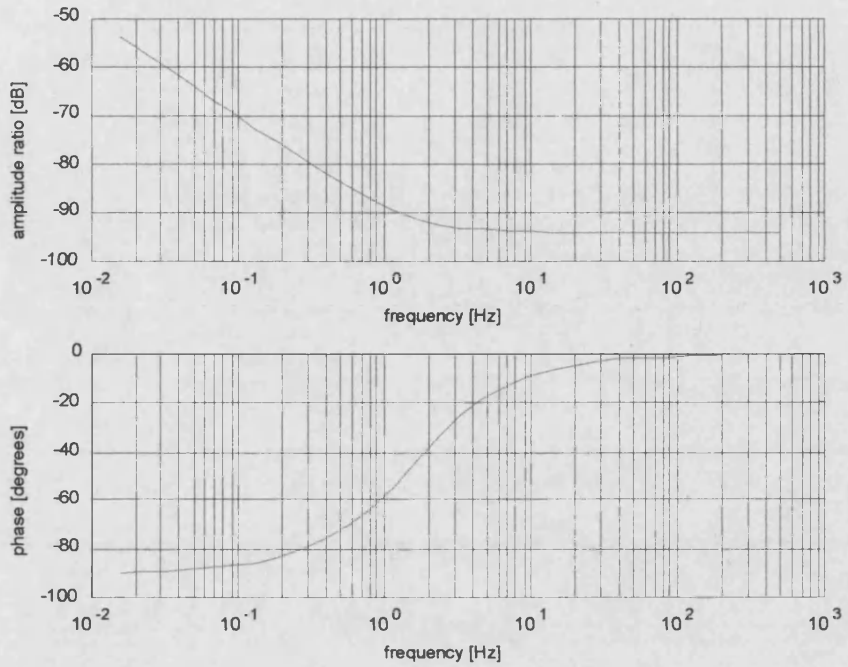

Figure 4.28 Materials Testing Machine Bode Plot

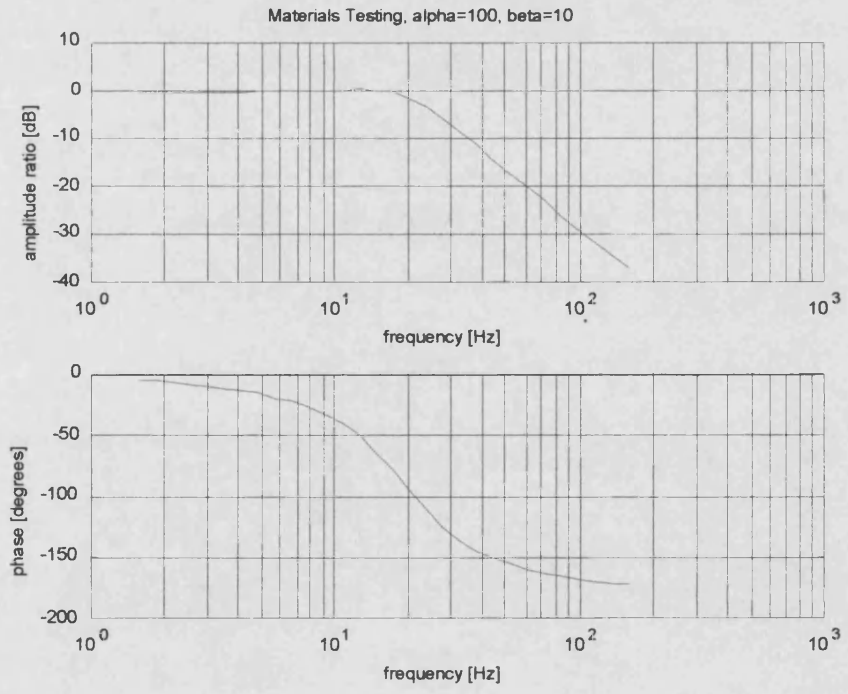

Figure 4.29 Ball & Beam Rig Bode Plot

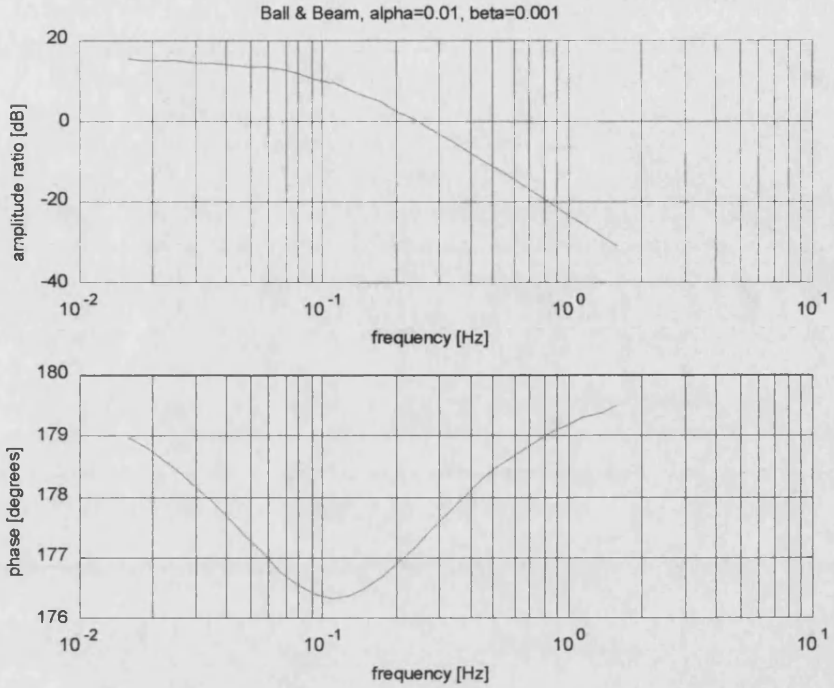

5.0 MCS Pressure Control & Bumpless Transfer

5.1 Introduction

This chapter details the results obtained from the test rig using a 1st order MCS controller for packing pressure control. Improvements in MCS pressure control are made by altering adaptive weights and resetting the integrators to appropriate values.

5.2 Initial MCS Pressure Control Results

As in chapter 4 the irreversible switch from flow to pressure control is initiated after an injection pressure of 70bar is reached and pressure is then controlled to 90bar. The medium length pipe (1.8m) was fitted between the injection control valve and actuator in all the MCS controller tests and the reduced bulk modulus of 2000bar was emulated. In all initial MCS controller work the integrators in the adaption mechanism were initialised at zero and the adaptive weight ratio of $\alpha = 10\beta$ was used. The effect of changes to both these parameters will be discussed later in this chapter. Since the reference model had already been fixed as 1st order the reference model, the break frequency was chosen as the first parameter to tune.

5.2.1 Reference Model Choice

Discrete time reference models with break frequencies of between 0.1-15Hz were tested on the rig. Since the break frequencies were so much lower than the 1kHz sampling frequency the frequency responses of the continuous and discrete time implementations of the reference models were identical. It was found that the fastest reference model that could be tracked had a break frequency of 3Hz. This may seem rather slow. However it should be remembered that the –3dB bandwidth of the injection valve actuator system (section 4.4.3.1) was predicted to be 0.1-10Hz. Results using such a reference model and adaptive gain weights of $\alpha = 1\times10^{-5}$ and $\beta = 1\times10^{-6}$ are presented in Figure 5.1 and can be compared with equivalent PI pressure controlled results in Figure 4.1. The first thing to note is the huge drop in injection pressure as MCS pressure control is switched in. This is an initial condition problem and due to maintaining the two integrator outputs at zero until the controller is switched in. This is covered in the next

section. The second thing to notice is that overall the MCS pressure controlled response is much less oscillatory than the equivalent PI controlled one.

5.2.2 MCS Integrator Initial Conditions

In any application of MCS control the values of the integrator outputs in the algorithm when the controller is enabled will to an extent determine the initial controller output. In the particular case of MCS pressure control when switching to pressure control, triggered by injection pressure then the integral terms alone will determine the initial controller output. This can be seen by looking at the block diagram in Figure 5.2 for a 1st order MCS pressure controller just after switchover from flow to pressure control. The controller has been switched in at a packing pressure of 70bar with the demand increasing from 70bar to 90bar. This means that in the instant after switchover the input to the reference model will be 90bar and the output from it will be 70bar. The system (plant) output will also be 70bar. Consequently the difference between the reference model output and the system output will be zero. Following this through the rest of the block diagram it is evident that the values of the adaptive gains (K and K_r) depend solely upon the discrete integrator outputs. In practise this means that just after switchover from velocity to pressure control the initial demanded valve spool position depends solely upon the discrete integrator outputs.

It was initially thought that the problem of setting the discrete integrator outputs just after switchover could be simplified by maintaining the discrete integrator determining the value of K at zero. Thus just after switchover the MCS controller could be simplified to an open loop controller with the value of K_r and the demanded pressure determining the controller output and the valve spool position. A study was therefore carried out on the rig to determine values of K_r which gave the same pressure as that demanded for demanded pressures of 25bar, 50bar and 75bar. This was done by leaving the actuator on its endstop (in the extended position in relation to the injection valve) and setting up the same open loop controller as that formed by MCS just after switchover with K set to zero. The demanded pressure was set and the forward path gain was then varied while measuring the pressure in the actuator. It was observed that the pressure in the actuator took time to rise from zero and reach a constant value and so 3 tests

were carried out. The first test was to find the values of K_r that gave zero steady state error. The second test was to determine the values of K_r for actuator pressure, starting from 0bar, to reach demanded pressure within 5 seconds. The third test was the same as the second except that the time for actuator pressure to reach demanded pressure was reduced to 1s. Using these results it was possible to estimate suitable initial values for the MCS integrator determining the value of K_r just after switchover.

The discrete integrator determining the value of K just after switchover was then set to zero and the results from the open loop pressure control tests to determine suitable values for the discrete integrator determining K_r just after switchover were then used during injection moulding emulation tests. Firstly these tests showed that better performance is obtained if K is initialised to a nonzero value. Secondly it was noted that there is a preferred ratio between the integral terms of K and K_r. In general during emulated injection moulding packing pressure control K/K_r tends to -0.03 with K negative and K_r positive. Thirdly it was also originally thought that the value of K_r would have to be scheduled with switchover pressure. However, results from the rig have shown that for a limited range of switchover pressures this is not the case. Instead a single value for K and a single value for K_r have proven to be sufficient.

Results with the MCS K integrator maintained at -1.6×10^{-4} until just after switchover and the K_r integrator maintained at 5.5×10^{-3} until just after switchover are shown in Figure 5.3. Firstly, compared to the results in Figure 5.1, the pressure undershoot has been reduced from 50bar to 7bar. However the improved performance at switchover has highlighted the slight overshoot and fairly poor reference model tracking. This is indicative of the adaptive weights being set too low. Unfortunately, when the adaptive weights were increased whilst maintaining $\alpha = 10\beta$ led to a more oscillatory response. To improve the response further it was therefore necessary to vary the adaptive weights ratio.

5.2.3 Adaptive Weights Choice

Different adaptive weight ratios were tested and the ratio of $\alpha = 100\beta$ was found to work best. Bearing in mind the previous work done using MCS control (detailed in section 4.4.4) and the adaptive weight ratios chosen this implies that the controlled system has a bandwidth of more than 18Hz. This seems to contradict the small perturbation analysis meter-in control of pressure in a fixed volume which predicted a 1st order response with a natural frequency of 1-10Hz. However the injection control valve (a prototype P-Q valve with a high performance spool position controller) has, for small displacements a bandwidth greater than 18Hz. The adaptive weight ratio has therefore been set to allow the adaptive gains to respond to the fastest dynamics of the controlled system.

Using this ratio allowed α to be increased from 1×10^{-5} to 5×10^{-5}. The K_r integrator was also maintained at a higher value of 7×10^{-3} (until just after switchover) which produced the results in Figure 5.4. The initial pressure undershoot after the controller was switched in at 70bar has been reduced to 4bar and overall reference model tracking is improved. However the pressure transient just after the pressure undershoot has increased and pressure overshoots to 91bar before being controlled back to the reference model trajectory. Even so this is still a great improvement on the results using a fixed gain PI pressure controller displayed in Figure 4.1.

5.2.4 MCS Pressure Control Robustness

Of course one of the desired advantages of MCS pressure control over a fixed gain strategy is that it should be robust to a change in operating conditions. To test this the filling injection velocity was reduced from 0.1m/s to 0.04m/s. This lowered the pressure at which packing began to approximately 45bar. Packing pressure control was therefore set to commence at 45bar and control to 65bar. Industry standard fixed gain PI pressure control was tested first and the results for this are in Figure 5.5. These can be compared with the MCS implementation results in Figure 5.6. In both cases the controller settings were identical from those used previously. Using PI control the amplitude of the pressure oscillations after switchover are slightly lower at 18bar compared to those with a higher

injection velocity at 23bar (in Figure 4.1) but the response is more oscillatory. However this is not so important, what is important is whether MCS control is better or not. The MCS results show a pressure undershoot after switchover of 0.5 bar which can be compared to a pressure undershoot of 8bar in the PI controller results. The MCS results also show only 2 major pressure oscillations with an amplitude of 8bar before reference model tracking is approached at 2s. The PI results show 7 large pressure oscillation before the demanded pressure is approached at 2.4s.

The only worrying problem with the MCS results in Figure 5.6 is that just as the error between the reference model and the plant output is being reduced to a small value at 2.2s a limit cycle takes over. It might be concluded that this is due to gain drift and is an adaptive gain limit cycle appears. However the instability is in part due to a problem with load emulation and it also affects the PI pressure control results, although the limit cycle began much later than in the MCS controlled case. This can be seen in Figure 5.7.

Or course a change in injection velocity from 0.1m/s to 0.04m/s is quite a severe change in operating conditions. Therefore a further comparative study at an injection velocity of 0.08m/s was carried out using both the PI and MCS controller. Again the same settings were retained as had been used with an injection velocity of 0.1m/s. The PI and MCS results are shown in Figure 5.8 and Figure 5.9 respectively. First of all reducing the injection velocity from 0.1m/s to 0.08m/s lowered the initial packing pressure to around 60bar. Consequently the 2 controllers were set to switch in at a pressure of 60bar and control to a pressure of 80bar. The PI pressure controller results show an undershoot of 15bar and an overshoot of 1.5bar with considerable pressure oscillation, as in previous results. The MCS controller results show a pressure overshoot of 2bar with zero undershoot and significantly less oscillation, although there is significantly more than that with a 0.1m/s injection velocity. A 2 bar amplitude limit cycle also starts after the injection pressure has reached the reference model pressure of 80bar. The limit cycle has a much smaller amplitude than that in Figure 5.6 but a limit cycle exists nonetheless. The limit cycle can be eliminated by simply

reducing α from 5×10^{-5} to 4×10^{-5}. The results for this are shown in Figure 5.10. While there is still no undershoot and the overshoot is small overall the response is less oscillatory. This is the same as one would expect from reducing the proportional gain of a similar fixed gain controller.

From the results presented it is clear that MCS packing pressure control outperforms fixed gain PI packing pressure control. The pressure responses in both sets of results are rather oscillatory. However this is in part due to load emulation stability problems rather than injection controller stability problems. Also with good choice of MCS integrator initial conditions a form of bumpless transfer has been implemented.

5.3 Concluding Remarks

MCS has outperformed PI pressure control of an emulated injection moulding load and been shown to be more robust. By correctly selecting the initial MCS integrator values an element of bumpless transfer has also been incorporated. In this respect an improved control strategy for injection moulding has been identified and shown to be an improvement on the current industry standard. There is still testing to be done before commercialisation of this solution can be contemplated. However, full scale testing of MCS packing pressure control should most definitely be the next stage and if successful there should be no fundamental reason why the controller cannot be commercialised.

Figure 5.1 MCS Pressure Control, Initialised at Zero

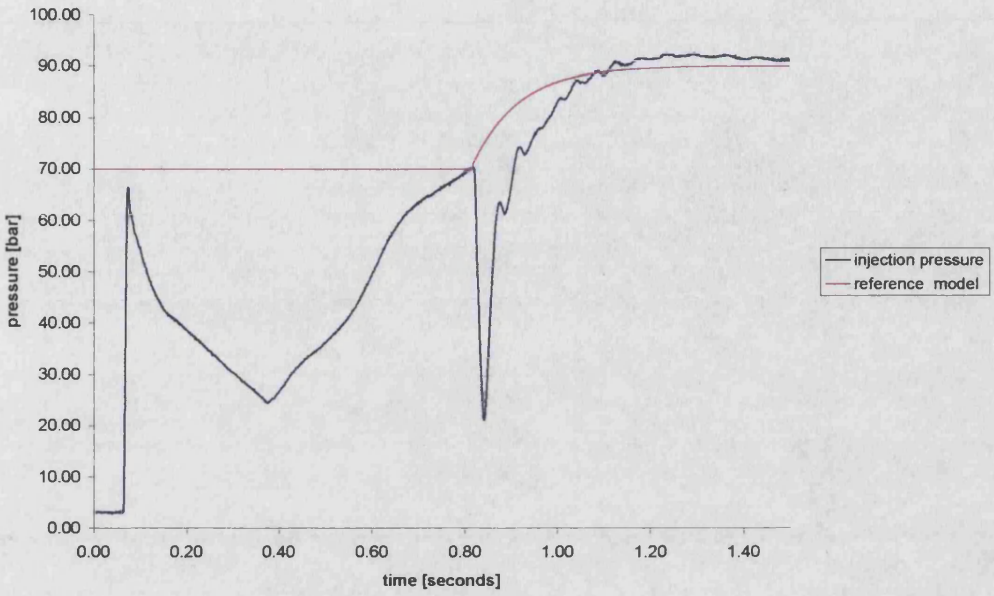

Figure 5.2 1st Order MCS Controller

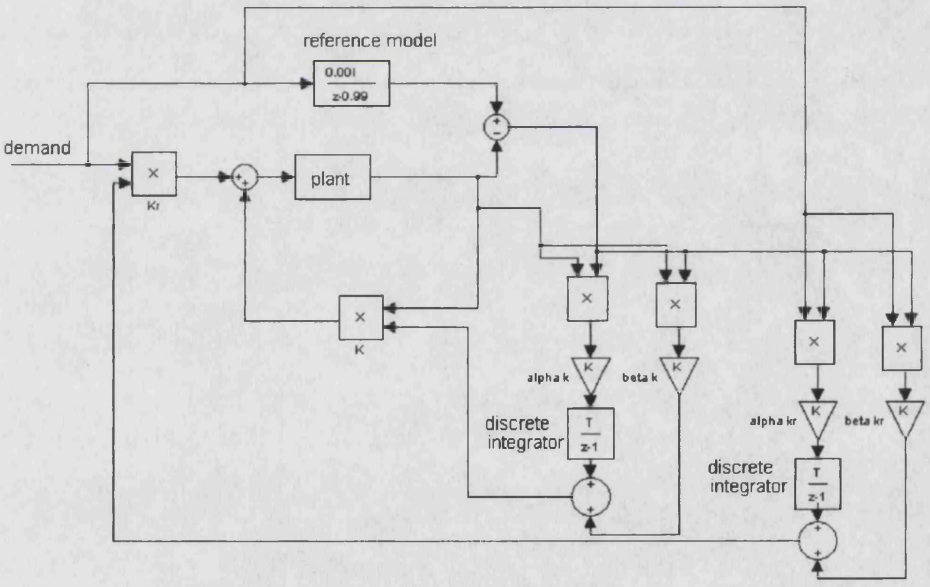

Figure 5.3 MCS Pressure Control, Integrators Initialised at Non-Zero Values

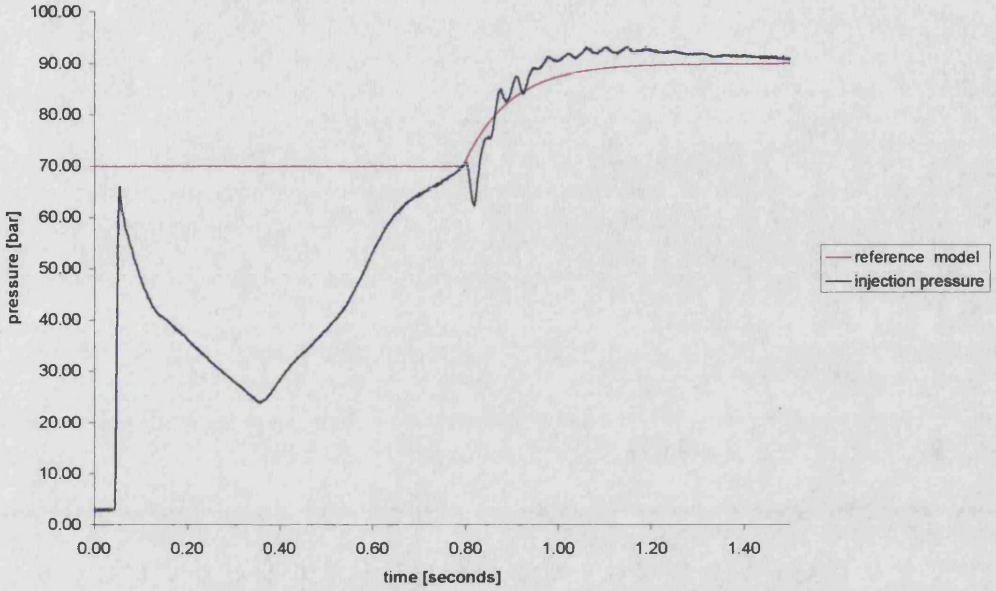

Figure 5.4 MCS Pressure Control, Integrators Initialised at Non-Zero Values, Adjusted Adaptive Gain Weight Ratio

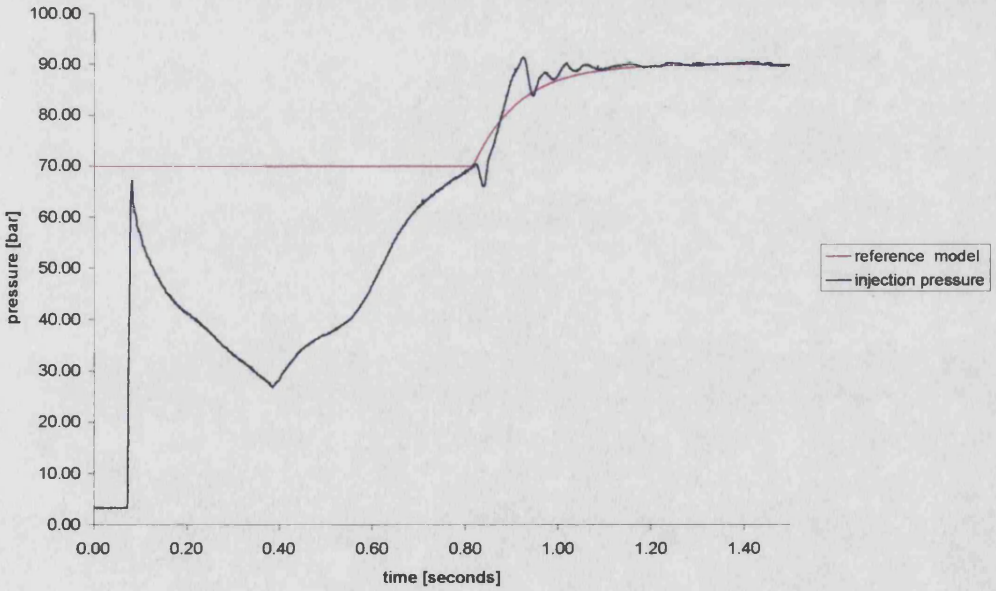

Figure 5.5 PI Controlled Packing Pressure, 0.04m/s Injection Velocity

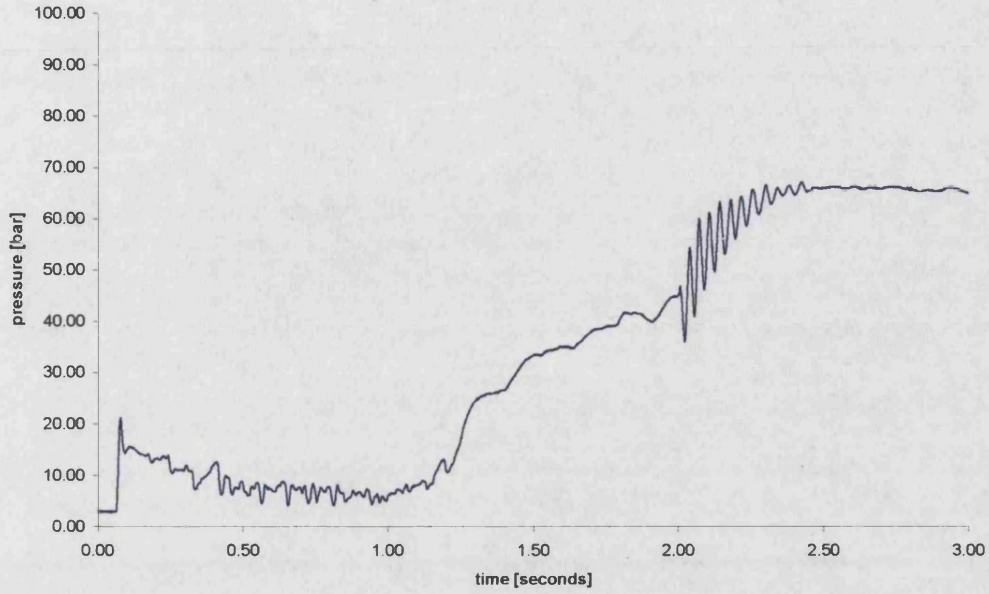

Figure 5.6 MCS Controlled Packing Pressure, 0.04m/s Injection Velocity

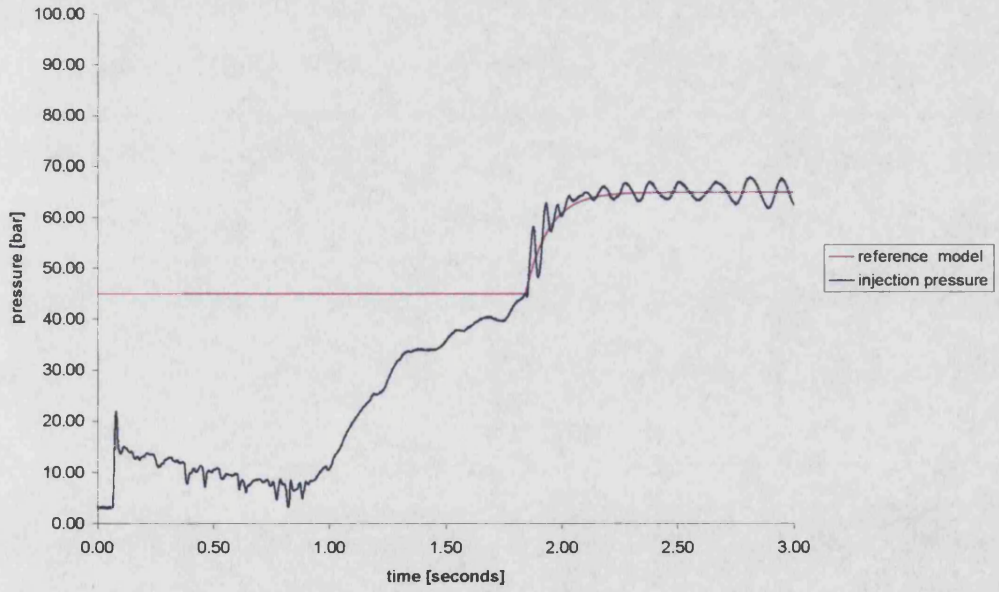

Figure 5.7 PI Controlled Packing Pressure, 0.04m/s Injection Velocity

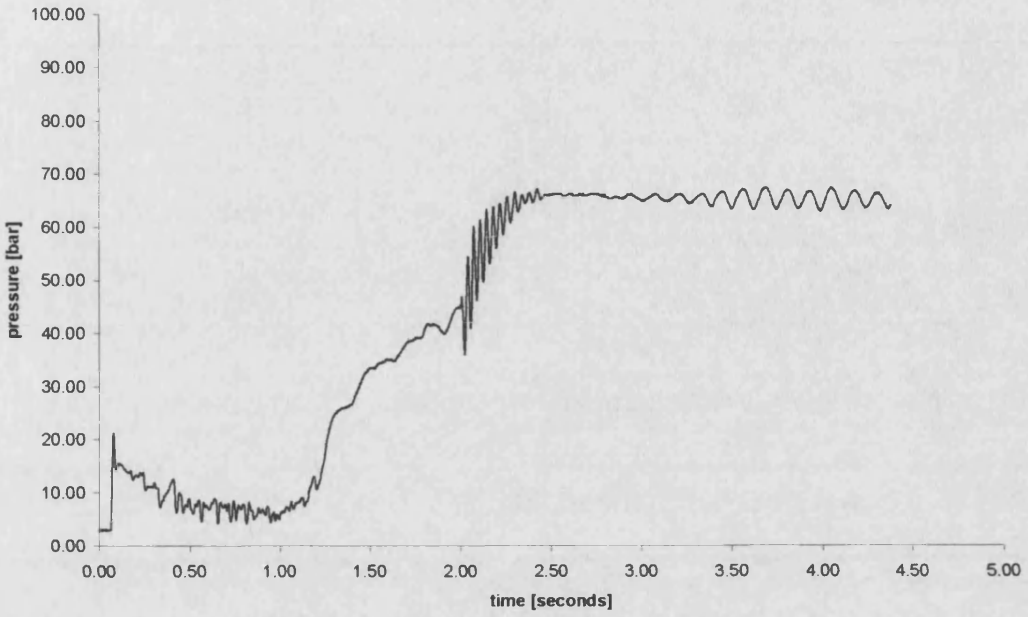

Figure 5.8 PI Controlled Packing Pressure, 0.08m/s Injection Velocity

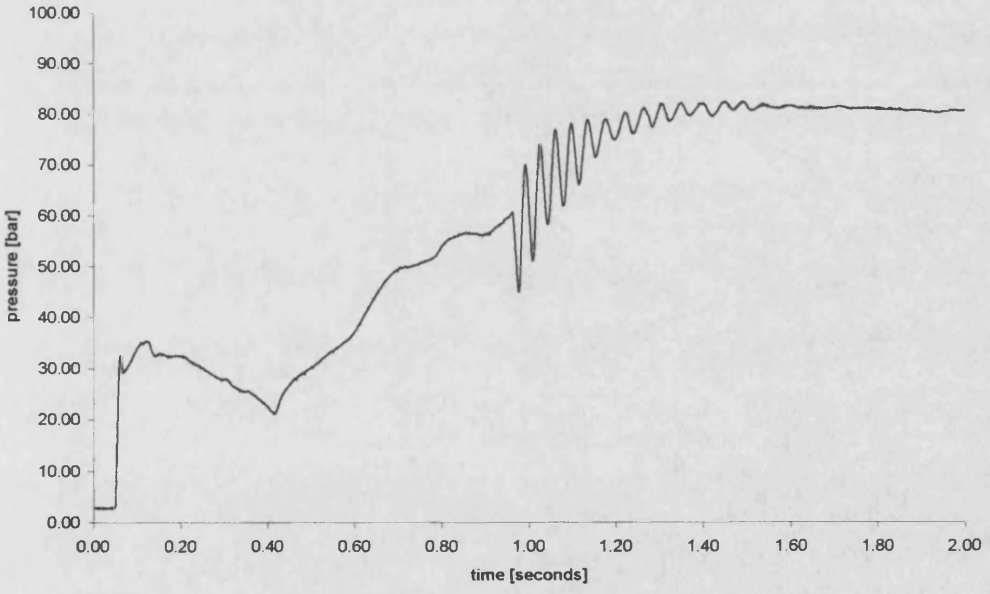

Figure 5.9 MCS Controlled Packing Pressure, 0.08m/s Injection Velocity

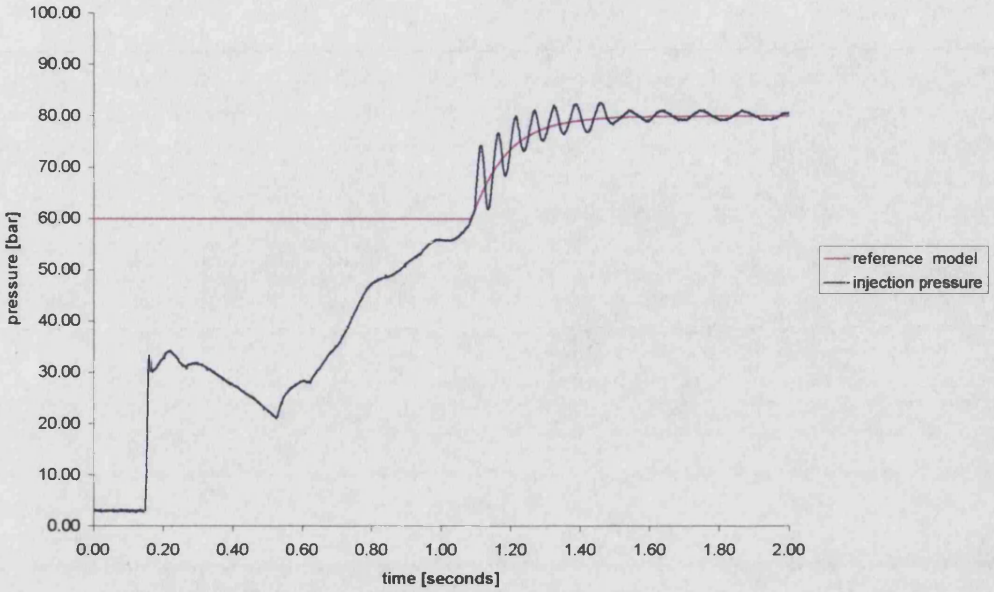

Figure 5.10 MCS Controlled Packing Pressure, 0.08m/s Injection Velocity, Reduced Adaptive Weights

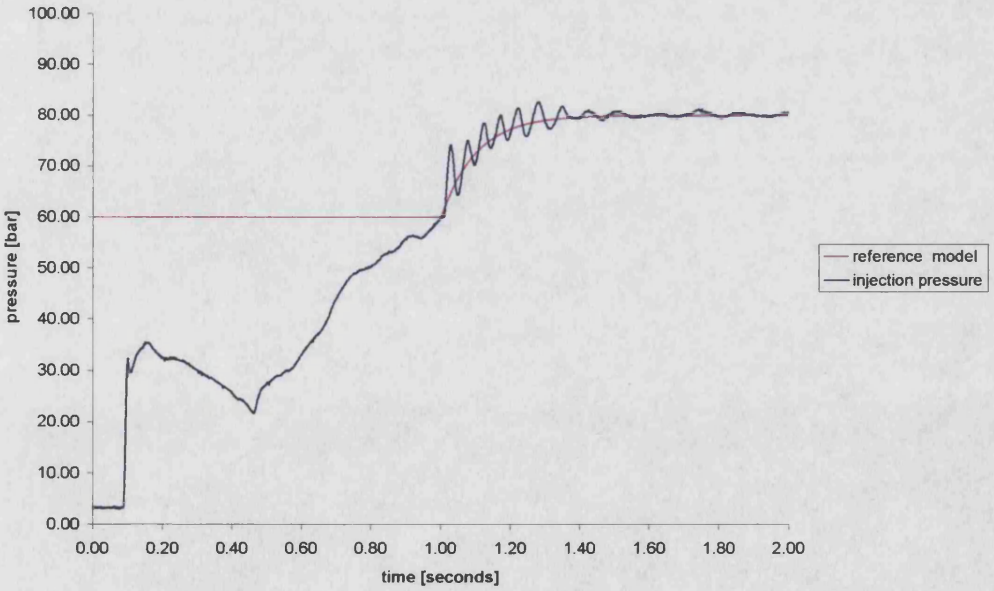

6.0 Conclusions

6.1 Injection Moulding Load Modelling

An injection moulding load model has been implemented in the Bath*fp* simulation package. For the case of a pseudoplastic material (polypropylene), injected into a 20ml mould, good agreement has been achieved between simulated and experimental results. The effects of cooling at the onset of packing even with unreasonably fast cooling were found to be small.

6.2 Load Emulation

Load emulation, using the 'hardware-in-the-loop' technique, of the *filling* and *packing* stages of injection moulding has been accomplished by metering flow out of an actuator. The test rig designed and built was a half scale model of a real injection moulding machine. Unfortunately the maximum stiffness that could be emulated was a quarter of that specified for the real load. However in light of the unmodelled barrel leakage in the real machine the load emulation is still acceptable.

6.3 Injection Moulding Controller Choice

A number of different strategies for the filling and packing stage control of injection moulding were considered. The potential controllers were split into two groups: single controllers and hybrid controllers. Single controllers were those that could control the packing phases and hybrid controllers were solutions that employed two distinct controllers one for the filling phase and one for packing phase. Of these fuzzy logic or neural network control of injection moulding filling and packing P-Q control can be discounted on the grounds that, with a controller of medium complexity, stability would be hard to prove. Hence a hybrid solution for P-Q control seems appropriate. Overall adaptive control of filling and packing with a bumpless transfer strategy connecting the pair was found to show the most promise. Of the adaptive solutions available the MRAC controller MCS showed considerable promise. From a small perturbation analysis packing pressure control is a 1^{st} order dominant 3^{rd} order system. Subsequent analysis of MCS control of different 3^{rd} order systems showed that a 1^{st} order reference model should be sufficient. A review of previous implementations of MCS control was also carried out and showed that there is

scope to match the adaptation mechanism dynamics to those of the plant by altering the adaptive gain weight ratio.

6.4 PI & MCS Packing Pressure Control

For the 20ml mould used and the duty cycle chosen, by using an adaptive weights ratio of $\alpha = 100\beta$ as opposed to the more commonly used $\alpha = 10\beta$ MCS and maintenance of the discrete integrator outputs (which form part of the adaptation mechanism) at suitable values until the controller is switched in allowed MCS packing pressure control to outperform PI pressure control of an emulated injection moulding load. For the specific case investigated the strategy was also shown to be robust to changes in operating conditions. However because of load emulation stability problems the precise level of robustness was not ascertained. By correctly selecting the MCS integrator values that were maintained until switchover an element of bumpless transfer has also been incorporated. In this respect an improved control strategy for injection moulding has been identified and shown in an emulated environment to be an improvement on the current industry standard.

6.5 Further Work

Presently commercialisation of this solution would be premature as work remains to be done. The controller has only been tested on one size of machine and for one mould. However, through the use of a small 20ml mould and a high injection velocity of 0.1m/s the test conditions were particularly demanding and sufficient promise has been demonstrated to warrant full scale testing of MCS packing pressure control as the next stage. If successful, unlike some other advanced control strategies, there should be no reason, related to guaranteeing stability, why the controller cannot be commercialised.

References

Agrawal, A.R. Pandelidis, I.O. & Pecht, M. (1987) Injection-Molding Control-A Review, *Polymer Engineering & Science*, **27**(18), pp. 1345-1357

Akpolat, Z.H. & Asher, G.M. (1999) Dynamic Emulation of Mechanical Loads Using a Vector-Controlled Induction Motor-Generator Set, *IEEE Trans. On Industrial Electronics*, **46**(2), pp. 370-379

Alleyne, A. & Liu, R. (1999) On the Limitations of Force Tracking Control for Hydraulic Servosystems, Trans. ASME Journal of Dynamic Systems, Measurement & Control, **121**, pp. 184-190

Alleyne, A. & Zheng, D. (2000) Control-Oriented Modelling of an Injection Molding Machine Including the Fill-to Pack Transition, *Proc. ASME Dynamic Systems & Controls Division IMECE*, **69**(1), pp. 345-352

Arimoto, S. Kawamura, S. & Miyazaki, F. (1984) Bettering Operation of Robots by Learning, *Journal of Robotic Systems*, **1**(2), pp. 123-140

Åström, K.J. (1983) Theory and Applications of Adaptive Control-A Survey, *Automatica*, **19**(5), pp. 471-486

Åström, K.J. & Hägglund, T. (1988) Automatic Tuning of PID Controllers, *Instrument Society of America*, ISBN 1-55617-081-5

Astrom, K.J. & Wittenmark, B. (1984) Computer Controlled Systems, *Prentice-Hall Information and System Sciences Series*, ISBN 0-13-164319-3

Aziz, K.I. & Thomson, M. (1996) Output-Driven Minimal Controller Synthesis with an Adaptive Observer, *Proc. IMechE part I Journal of Systems & Control Engineering*, **210** pp. 131-139

Beard, G.S. (1998) Adaptive Control of Energy Efficient Hydraulic Systems, *University of Bristol*, PhD thesis

Bird, R.B. Armstrong, R.C. & Hassager, O. (1987) 'Dynamics of Polymeric Liquids', *John Wiley & Sons*, 2nd edition

Bushko, W.C. & Stokes, V.K. (1995a) Solidification of Thermoviscoelastic Melts. Part 1: Effects of Processing Conditions on Shrinkage and Residual Stresses, *Polymer Engineering and Science*, **35** (4), pp. 365-383

Bushko, W.C. & Stokes, V.K. (1995b) Solidification of Thermoviscoelastic Melts. Part 2: Effects of Processing Conditions on Shrinkage and Residual Stresses, *Polymer Engineering and Science*, **35** (4), pp. 365-383

Bushko, W.C. & Stokes, V.K. (1996a) Solidification of Thermoviscoelastic Melts. Part 3: Effects of Mold Surface Temperature Differences on Warpage and Residual Stresses, *Polymer Engineering and Science*, **36** (3), pp. 322-335

Bushko, W.C. & Stokes, V.K. (1996b) Solidification of Thermoviscoelastic Melts. Part 3: Effects of Boundary Conditions on Shrinkage and Residual Stresses, *Polymer Engineering and Science*, **36** (5), pp. 658-675

Chiang, H.H., Hieber, C.A. & Wang, K.K., (1991a) 'A Unified Simulation of the Filling and Postfilling Stages in Injection Molding. Part 1: Formulation', *Polymer Engineering and Science*, **31**(2, January), pp. 117-124

Chiang, H.H, Hieber, C.A. & Wang, K.K., (1991b) 'A Unified Simulation of the Filling and Postfilling Stages in Injection Molding. Part 2: Experimental Verification', *Polymer Engineering and Science*, **31** (2, January), pp. 125-139

Chiu, C.C. Wei J.-H. & Shih, M.-C. (1991) Adaptive Model Following Control of the Mold Filling Process in an Injection Molding Machine, *Polymer Engineering & Science*, **31**(15), pp. 1123-1129

Coates, P.D. & Speight, R.G. (1995) Towards Intelligent Process Control of Injection Moulding of Polymers, *Proc. IMechE Journal of Engineering Manufacture*, **209**, pp. 357-367

D'Azzo , J.J. & Houpis, C.H. (1988) Linear Control System Analysis and Design Conventional and Modern, *McGraw-Hill International Editions*, ISBN 0-07-100191-3

Edge, K.A. (1997) The Control of Fluid Power Systems – Responding to the Challenges, *Proc. IMechE*, **211**(I), pp. 91-110

Edwards, C. & Postlethwaite, I. (1998) Anti-Windup and Bumpless-Transfer Schemes, *Automatica*, **34**(2), pp. 199-210

Gamble, J.B. (1992) Sliding Mode Control of a Proportional Solenoid Valve, PhD Thesis, *Department of Mechanical Engineering*, University of Bath

Gamble, J.B. & Vaughan, N.D. (1996) Comparison of Sliding Mode Control with State Feedback and PID Control Applied to a Proportional Solenoid Valve, *ASME Journal of Dynamic Systems, Measurement & Control*, **118**, pp. 434-438

Gao, F. Patterson, W.I. & Kamal, M.R. (1994) Self-Tuning Cavity Pressure Control of Injection Molding Filling, *Advances in Polymer Technology*, **13**(2), pp. 111-120

Gao, F. Patterson, W.I. & Kamal, M.R. (1996a) Cavity Pressure Dynamics and Self-Tuning Control for Filling and Packing Phases of Thermoplastics Injection Moulding, *Polymer Engineering & Science*, **36** (9), pp. 1272-1285

Gao, F.Patterson, W.I. & Kamal, M.R. (1996b) Cavity Pressure Control During the Cooling Stage in Thermoplastic Injection Moulding, *Polymer Engineering & Science*, **36**(19), pp. 2467-2476

Gardner, J.F. Kulakowski, B.T. Gore, S.A. & Streit, D.A. (1995) Modelling and Tuning of Hydraulic Road Simulators for Heavy Vehicle Testing, *Proc. ASME IMECE FPST Division*, volume 2, pp. 99-105

Graebe, S.F. & Ahlén, A.L.B. (1996) Dynamic Transfer Among Alternative Controllers and Its Relation to Antiwindup Controller Design, *IEEE Transactions on Control Systems Technology*, **40**(1), pp. 92-99

Hairer, E. & Wanner, G. (1991) Solving Ordinary Differential Equations, Part II, Stiff and Differential-algebraic Problems, *Springer-Verlag*, New York, ISBN 0387537759

Hanus, R. Kinnaert, M. & Henrotte, J.-L. (1987) Conditioning Technique, A General Anti-Windup and Bumpless Transfer Method, *Automatica*, **23**(6), pp. 729-739

Havlicsek, H. & Alleyne, A., (1999) Nonlinear Control of An Electrohydraulic Injection Molding Machine via Iterative Learning, *Proc. of The American Control Conference*, San Diego California, pp. 176-181

Helduser, S. (1999) Electric-Hydrostatic Drive - an Innovative Energy-Saving Power and Motion Control System, *Proc. IMechE*, **213**(I), pp. 427-437

Hodgson, S.P. & Stoten, D.P. (1998) Robustness of the Minimal Controller Synthesis Algorithm with Minimal Phase Plant Dynamics of Unknown Order but Known Relative Degree, *International Journal of Control*, **71**(1) pp. 1-17

Hu, J. & Vogel, J.H. (1994) Dynamic Modelling and Control of Packing Pressure in Injection Molding, *ASME Journal of Engineering Materials & Technology*, **116**, pp. 244-249

Huang, S.-J. & Lee, T.-H. (2000). Fuzzy Logic Controller for a Retrofitted Closed-Loop Injection Moulding Machine, *Proc. IMechE part I*, **214**, pp. 9-21

Hwang, C.L. Lan, C.H & Jieng, W.J. (1993) The Trajectory Tracking of an Electrohydraulic Servo-Mechanism via a Sliding Mode Controller, *Proc. IMechE part I: Journal of Systems & Control Engineering*, **207**, pp. 135-142

Iserman, I. Lachman, K.-H. & Matko, D. (1992) Adaptive Control Systems, *Prentice Hall International*, ISBN 0-13—005414-3

Kambour, R.P. Caraher, J.C. Schnoor, R.C. Todt, M.L. Wang, H.P. & Willey, S.J. (1996) Tensile Stresses in the Edges of Injection Moldings: Roles of Packing Pressure, Machine Compliance, and Resin Compression, *Polymer Engineering and Science*, **36** (23), pp. 2863-2874

Kazmer, D.O. & Barkan, P. (1997) Multi-Cavity Pressure Control in the Filling and Packing Stages of the Injection Moulding Process, *Polymer Engineering & Science*, **37**, pp. 1865-1879

Kazmer, D. & Hatch, D. (1999) Towards Controllability of Injection Moulding, *ASME IMECE*, pp

Kazmer, D.O. & Speight, R.O. (1997) Polymer Injection Molding Technology for the Next Millennium: A Vision to the Future, *Journal of Injection Molding Technology*, **1**(2), pp. 81-90

Kenndaten für die Verarbeitung thermoplastischer Kunststoffe herausgegeben vom VDMA Verein Deutscher Maschinenbau-Anstalten e.v., Fachgemeinschaft Gummi- und Kunststoffmaschinen, München Wien Carl Hanser, 1979-1983, ISBN 3446129308

Kim, D.I. & Kim, S. (1996) An Iterative Learning Control Method With Applications for CNC Machine Tools, *IEEE Transactions on Industry Applications*, **32** (1), pp. 66-72

Kirecci, A. & Gilmartin, M. (1998) Application of Learning to High-Speed Robotic Manipulators, *IMechE Transactions Part I*, **212**, pp. 315-323

Leith, D.J. & Leithead, W.E. (2000) Survey of Gain-Scheduling Analysis and Design, *International Journal of Control*, **73** (11), pp. 1001-1025

Lenk, R. S. (1978) 'Polymer Rheology', *Applied Science Publishers Ltd London*

Lo, J.K.W. (1995) The Use of Numerical Optimization Technique for the Selection and Sizing of Fluid Power Components, *University of Bath*, Department of Mechanical Engineering, Internal report number **035/95**

Michael, W. & Lauterbach, M. (1989) Quality Control for the Packing Pressure Phase – with pmT Control, *Advances in Polymer Technology*, 9(4), pp. 337-343

Nimegeers, C.R. Burton, R. & Schoenau, G.J. (1996) A Computer Controlled Hydraulic Loading System for Simulating Loads, *9th Bath International Fluid Power Workshop*, pp. 10-23

Ohuchi, H. & Ikai, H. (1989) Control of a Load Simulator, *Proceedings of the JHPS International Symposium on Fluid Power*, pp. 55-60

Ooi, T.H. Lau, K.T. & Lim, C.H. (1991) A Novel Emulator for VCR Servo Controller Testing, *IEEE Trans. On Consumer Electronics*, **37**(4), pp. 848-859

Pannett, R.F. Chawdhry, P.K. & Burrows C.R. (1999) Alternative Robust Control Strategies for Disturbance Rejection in Fluid Power Systems, *Proceedings of the American Control Conference*, San Diego California, pp. 739-743

Pedrycz, W. (1993) Fuzzy Control and Fuzzy Systems, Research Studies Press Ltd. *John Wiley & Sons Inc.*

Petzold, L. (1983) Automatic Selection of Methods for Solving Stiff and Non-Stiff Systems of ODEs, *SIAM Journal of Statistical Computing*, **14**, pp. 136-148

Plummer, A.R. (1997) Feedback Linearisation for Acceleration Control of Electrohydraulic Actuators, *Proc. IMechE Part I*, **211** pp. 395-406

Quinghe, L. Zongcai, P. & Shenglin, W. (1999) A Study on Producing Mechanism and Eliminating Methods of the Disturbance Torque in Electrohydraulic Load Simulator, *Fourth JHPS International Symposium*, pp. 273-278

Rafizadeh, M., Patterson, W.I. & Kamal M.R., (1996) 'Physically–Based Model of Thermoplastics Injection Moulding for Control Applications', *International Polymer Processing*, **11**, pp. 352-362

Ramden, C. Jansson, A. & Palmberg, J-O. (1997) 'Design and Analysis of a Load Simulator for Testing Hydraulic Valves', *10th Bath International Workshop*, University of Bath, pp. 260-277

Richards, C.W. & Tilley, D.G. (1997) Bath*fp* Manual Volume 2 The *Bathfp Model* Reference Guide, *Department of Mechanical Engineering*, University of Bath

Richards, C.W. Tilley, D.G. Tomlinson, S.P. & Burrows, C.R. (1990) Type-Insensitive Integration Codes for the Simulation of Fluid Power Systems, *ASME FPST Division IMECE*, **6**, pp. 1-6

Rosato, D.V. & Rosato, D.V. (1995) Injection Molding Handbook, *Chapman & Hall*, ISBN 0-412-99381-3

Saikko, V. Paavolainen, P. Kleimola, M. & Slätis, P. (1992) A Five-Station Hip Joint Simulator for Wear Rate Studies, *Proc. IMechE Part H Journal of Engineering in Medicine*, **206**, pp. 195-200

Shankar, A. & Paul, F.W. (1982) 'A Mathematical Model for the Evaluation of Injection Molding Machine Control', *Transactions of the ASME*, **104**, pp. 86-92

Stoten, D.P. (1992) Implementation of Minimal Control Synthesis on a Servo-Hydraulic Testing Machine, *Proc. IMechE part I Journal of Systems & Control Engineering*, **206** pp. 189-194

Stoten, D.P. & Benchoubane, H. (1990a) Empirical Studies of an MRAC Algorithm with Minimal Controller Synthesis, *International Journal of Control*, **51**(4), pp. 823-849

Stoten, D.P. & Benchoubane, H. (1990b) Robustnesss of a Minimal Controller Synthesis Algorithm, *International Journal of Control*, **51**(4), pp. 851-861

Stoten, D.P. & Hodgson, S.P. (1991) Comparative Implementation Studies of Five Adaptive Control Algorithms on a Class 1 Manipulator, *IMechE: Part I Journal of Systems & Control Engineering*, **205**, pp. 263-205

Stoten, D.P. (1992) Implementation of Minimal Control Synthesis on a Servo-Hydraulic Testing Machine, *Proc. IMechE part I Journal of Systems & Control Engineering*, **206** pp. 189-194

Stoten, D.P. Dye, M.G. &Webb, M. (1994) The Implementation of the Minimal Control Synthesis Algorithm on a Web Control Problem, *IMechE: Part I Journal of Systems & Control Engineering*, **208**, pp. 53-60

Stoten, D.P. & Sebusang, S.E.M. (1998). Gain Bounds in the Minimal Controller Synthesis Algorithm, *Proc. IMechE part I*, **212**, pp. 345-360

Stoten, D.P. & Webb, M.G. (1994) The Implementation of the Minimal Control Synthesis Algorithm on a Web Control Problem, *Proc. IMechE part I Journal of Systems & Control Engineering*, **208** pp. 53-60

Sugie, T. & Ono, T., (1991) An Iterative Learning Control Law for Dynamical Systems, *Automatica*, **27** (4), pp. 729-732

Suykens, A.K. Vanderwalle, J.P.L. & De Moor, B.L.R., (1996) Artificial Neural Networks for Modelling and Control of Non-Linear Systems, *Kluwer Academic Publishers*

Tilley, D.G. & Richards, C.W., (1991) 'System Analysis with Bath*fp*' *Fluid Power*, March/April, **3**, pp.50-53

Tilley, D.G & Richards, C.W. (1997) 'Bath*fp* Manual 2 Bath*fp* Model Reference Guide' *University of Bath*, Department of Mechanical Engineering

Tsoi, H.-P. & Gao, F. (1999) Control of Injection Velocity Using a Fuzzy Logic Rule-Based Controller for Thermoplastics Injection Moulding, *Polymer Engineering & Science*, **39**(1), pp. 3-17

Watton, J. (1989) Fluid Power Systems Modelling, Simulation, Analog and Microcomputer Control, *Prentice Hall International*, ISBN 0-13-323197-6

Wei, J.-H. Chang, C.-C. & Chiu, C.-C. (1994) 'A Nonlinear Dynamic Model of a Servo-Pump Controlled Injection Molding Machine', *Polymer Engineering and Science*, **34** (11, mid-June), pp. 881-887

Yanada, H. & Shimahara, M. (1997) Sliding Mode Control of an Electrohydraulic Servo Motor Using a Gain Scheduling Type Observer and Controller, *Proc. IMechE part I*, **211**, pp. 407-416

Yang, Y.T. & Chang, C.C. (1998) The Fuzzy Control of an Electrohydraulic Fatigue Testing System, *International Journal of Materials and Product Technology*, **13**(3-6), pp. 184-194

Yang, Y. & Gao, F. (1999) Cycle-to-Cycle and Within-Cycle Adaptive Control of Nozzle Pressure During Packing-Holding for Thermoplastic Injection Molding, *Polymer Engineering & Science*, 39 (10), pp. 2042-2063

Zhang, C.Y. Leonard, J. & Speight, R.G. (1996) Adaptive Controller Performance Used for Ram Velocity Control During Filling Phase, *Society of Plastics Engineers ANTEC*, pp. 593-597

Appendix A Related Publications

Paper Presented at ASME IMECE 1999

INJECTION MOULDING SIMULATION FOR HYDRAULIC VALVE-ACTUATOR SYSTEM CONTROLLER DESIGN

Paul K Guerrier and Kevin A Edge
Department of Mechanical Engineering
University of Bath, UK.
e-mail: P.K.Guerrier@bath.ac.uk

Abstract

In the development of advanced injection controllers and more effective control valves, full scale testing is often too expensive. This paper is concerned with virtual testing using simulation and experimental testing using a 'hardware-in-the-loop' technique in which a servovalve-actuator system emulates the moulding process. Simulation results for the purely simulated load and a 'hardware-in-the-loop' emulated load are compared with experimental data. Good agreement is achieved. Although the particular case of an hydraulic injection moulding machine has been considered, the model of the moulding process would be equally valid for studies of an all-electric machine.

Nomenclature

k	power law index viscosity
l	length
m	mass
n	power law index
P	pressure
Q	flow rate
R	radius
r_1	radius at the beginning of a section
r_2	radius at the end of a section
λ_T	extensional viscosity constant
μ	viscosity
η_N	zero shear Newtonian viscosity
$\dot{\gamma}$	shear rate
τ	shear stress
τ_y	yield shear stress
σ_E	extensional stress
θ	convergence angle

Introduction

For plastic and rubber part production, injection moulding is one of the most important manufacturing processes available. In hydraulically driven machines, injection actuators are typically velocity controlled until the polymer being injected has filled the mould; once the filling phase is over pressure-controlled packing begins. Many existing controllers are relatively simple but nonetheless can be difficult to commission. A particular problem is to achieve a smooth transition from the velocity control phase to the pressure control phase. With the advent of digital control, advanced flowrate and pressure filling and packing controllers are now becoming available on commercial moulding machines (Zhang et al., 1996). However high performance control is far from being an industry standard and is currently an area of research interest. This paper is concerned with the development of simulation models to aid in the process of control system design and assessment

Whilst it would be advantageous in many ways to test new control strategies on a full size injection moulding machine, this would be very costly. Simulation offers a cheap and effective way of filtering out unsuitable strategies, with only the most promising being evaluated using full scale testing. However, as a result of simplifications and assumptions some effects are not adequately modelled. For this reason a more detailed evaluation following on from simulation is required. Ideally this should be cheaper and more flexible than through full scale testing. Such a requirement can be met using a 'hardware-in-the-loop' approach (Ramden et al., 1997). In this application the moulding machine can be considered as the injection cylinder 'load' and can be emulated by a computer-controlled servo-hydraulic actuator. This will allow the evaluation of suitable control schemes over a wide range of carefully-controlled moulding situations.

Polymer Structure & Flow Characteristics

To model the injection moulding process it is essential to have an appreciation of the non-Newtonian properties of polymeric liquids.

Polymeric fluids are often called viscoelastic fluids. Such materials have elasticity and after deformation will attempt to return to the original shape but will not usually reach it because of the viscous properties. Full mathematical modelling of viscoelastic behaviour is complicated, usually

containing temperature-dependent relaxation constants which describe how the fluid body reacts to forces acting on it (Bird et al., 1987). This level of detail is unnecessary for the study reported here.

Newtonian viscosity is of little or no use for describing polymer flow. There are 5 recognised relationships for predicting shear rate of non-Newtonian fluids. These are as follows:

- Pseudoplastic (shear thinning), where n<1 and where
$$\tau = \eta_N \dot{\gamma}^n \qquad (1)$$
- Dilatant (shear thickening), which again follows equation (1) but with n>1
- Bingham, where
$$\tau - \tau_y = \eta\dot{\gamma} \qquad (2)$$
- Plastic, which is a combination of the Bingham and Pseudoplastic relationships.
- Ostwald which according to (Lenk, 1978) is yet to be fully proven as existing.

Graphical illustrations of the relationships between shear stress and shear rate for these 5 flow phenotypes together with Newtonian Behaviour are shown in Figure 1. Of these the Ostwald and Bingham types are not relevant here as they do not describe polymer flow. Pseudoplastic (shear thinning) and dilatant (shear thickening) are of greatest interest with good examples being polypropylene and a blend of polycarbonate and ABS respectively. The plastic relationship is also relevant to polymer although, in practice the yield stress needed for polymer flow to start is so low that there is no need for the inclusion of the Bingham relationship in practice.

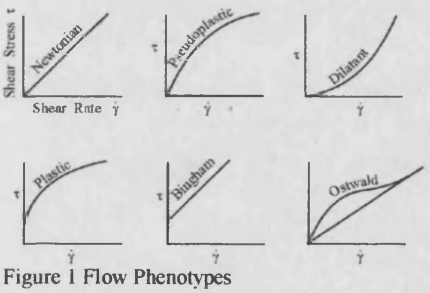

Figure 1 Flow Phenotypes

For both the pseudoplastic and dilatant relationships described by equation (1) η_N is the zero shear (Newtonian) viscosity. If n=1 then the equation (1) describes the Newtonian relationship.

Polymer Flow Governing Equations

For simulation purposes a relationship between polymer flow and injection actuator pressure is required. Incorporating the power law for viscosity into the Hagen-Poiseuille equation for flow through pipes gives equation (3) where k is both material and temperature dependent

$$\Delta P = \frac{2\left(\frac{4}{\pi}\right)^n klQ^n}{R^{3n+1}} \qquad (3)$$

(if $n=1$ then the power law index equation becomes the Hagen-Poiseuille equation)

With some manipulation, equations based on equation (2) can be derived to describe pressure requirements for diverging and converging sections. However, in such sections, a further flow elongation effect occurs that needs to be taken into account. Figure 2 shows an example of the behaviour in a converging section. The corresponding differential pressure over the converging section is described by equations (4) and (5) where λ_T is both material and temperature dependent.

$$\sigma_E = \lambda_T \frac{\dot{\gamma}}{2} \tan\theta \qquad (4)$$

$$\Delta P_E = \frac{2}{3}\sigma_E \left[1 - \left(\frac{r_2}{r_1}\right)^3\right] \qquad (5)$$

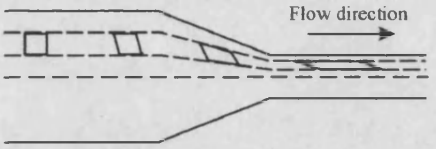

Figure 2 Flow Extension

Injection Moulding Process Modelling & Simulation

At the onset of packing the polymeric material being injected is still molten but since the mould temperature is well below the melting temperature of the polymer it soon cools and freezes. Subsequently there is a point in time called gate freeze after which material can no longer flow in or out of the mould (the gate is the opening to the mould). According to Gao et al. (1996) the only feasible way to effect the mould cavity pressure after gate freeze is by changing the temperature of the mould itself. This can be achieved by passing a cooling fluid (typically water or oil) through channels in the dies. Since the work in this paper is intended to aid the study of the control of the filling and packing phases, the cooling phase after gate freeze is not addressed here.

The Bath*fp* simulation package (Tilley & Richards, 1991) was employed for the simulation study. This package is based on a multi-step multi-order numerical integrator appropriate for the solution of fluid power systems. The mathematical model of the injection moulding process is represented in Bath*fp* as a 'load'. This can be linked to an actuator and will from this point on be referred to as the load model.

Load Model Description

The load model was developed for the case of a real mould (comprised of two materials testing specimens). An image of the part produced by this mould can be seen in Figure 3. In order to model the mould the following assumptions were made:

- Flow is one-dimensional and laminar.
- Flow is incompressible during the filling stage. This assumption is adopted in the majority of simulations detailed in previously-published work. If the flow were to be modelled as compressible during the filling phase this would complicate the model considerably and finite elements would have to be used.
- Flow is compressible as soon as the mould is full.
- Polymer flow is perfectly balanced between the 2 flow paths.
- Viscous filling forces include both the power law index and extensional viscosity.
- The process is isothermal. This is another simplification that has been used in the majority of simulations detailed in previously-published works. To include the effect of different temperatures throughout the part would add complexity and require a finite element approach. The current model can however be run at different polymer temperatures.
- The mass of the polymer being injected, about 20g for the materials testing specimen mould, is considered negligibly small in comparison to the mass of the moving parts of the machine, 60kg. The mass of the polymer is not included in any calculation.

These assumptions are generally in agreement with those adopted by previous researchers, in particular (Shankar & Paul, 1982) (Cheng-Ping Chiu et al, 1991) (Jong-Hwei Wei et al, 1994) (Rafizadeh et al, 1996) and 2 companion papers (Chiang et al 1991a) (Chiang et al 1991b)

The Bath*fp* load model has been developed such that a force is the output and injection actuator position and velocity are required as inputs. To determine the equations required to calculate the load force, the mould melt front is tracked during mould filling. The mould melt front position is calculated from the volume of material that has entered the mould, which is then compared with the total volume of the mould. This calculation is generally straightforward except in the case of converging and diverging sections when there are cubic equations to be solved. A Newton-Raphson approximation was included in the code to deal with this requirement. While this method of solution usually takes 7 iterations to converge this did not slow down computation significantly.

The Bath*fp* model treats the part shown in Figure 3 as being comprised of the following series of shapes in series; a diagram showing this representation is presented in Figure 4:
At the extreme left of the figure is a converging section, equivalent to the injection moulding machine nozzle (this has no region number as it is permanently full). This is followed by a short, constant radius, section, corresponding to the mould entry gate (region 1) and then a diverging section, corresponding to the section joining the larger diameter runner to the small cross section gate (region 2). Region 3 corresponds to a constant radius section, equivalent to the runner and region 4 compromises two constant radius sections in parallel, equivalent to the runners serving each materials testing part. The two short converging sections at the end of each runner (region 5) join the larger radius runners with the small second gates at entry to the moulded parts. This is followed by two short constant radius sections, equivalent to the gates before the moulded parts (region 6) and finally two constant area rectangular sections, equivalent to the parts to be moulded (region 7).

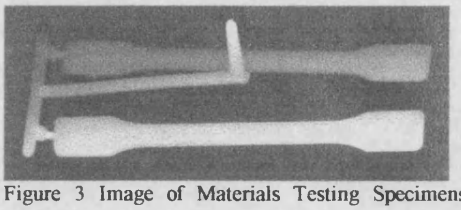

Figure 3 Image of Materials Testing Specimens Moulding

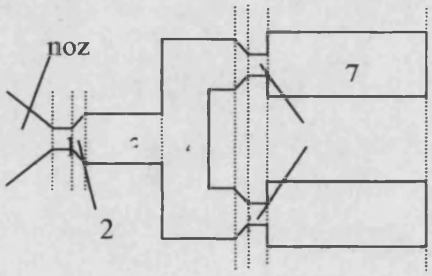

Figure 4 Simulated Mould Region Diagram

This model readily allows the simulation of other similar moulds since the dimensions of each section can be changed.

Simulation Study

The first simulation runs were done using the load model connected directly to an hydraulic actuator. The electrohydraulic circuit diagram of this is shown in Figure 5 . Except for the actuator all the hydraulic components and the signal input are standard models (Tilley & Richards, 1997). The standard actuator model was modified to have different annular areas.

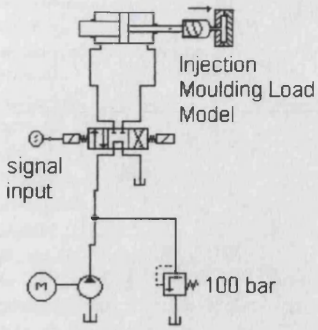

Figure 5 Hydraulic Load Simulation Circuit Diagram

Results from the simulation are shown in Figure 6. During the initial increase in pressure up to 0.18s mould regions 1-5 are filled. The subsequent short sharp rise in pressure at 0.2s occurs as regions 5 and 6 are filled. This is because flow elongation effects are significant in these regions and because region 6 is a small constriction.

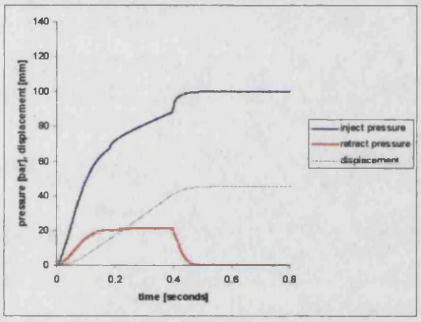

Figure 6 Load Model Simulation Results

After the initial load model simulations, a hardware-in-the-loop loading system was designed. Load emulation can be achieved hydraulically (Nimegeers et al., 1997), using a circuit consisting of a servo-valve-controlled actuator. The load emulation circuit adopted here was simulated as part of the design and evaluation process prior to implementation in the laboratory. As previously mentioned, such an arrangement would allow promising control schemes developed in simulation to be evaluated experimentally under well-controlled conditions and at a fraction of the cost of tests on a real machine. The electrohydraulic circuit diagram of this arrangement is shown in Figure 7.

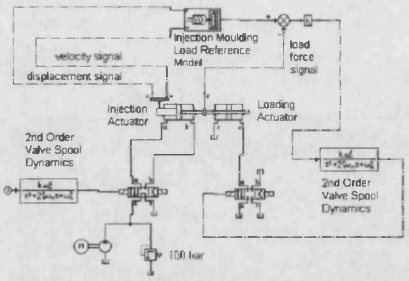

Figure 7 Hydraulic Load Emulator Circuit Diagram

The whole circuit is based around two actuators connected together with a force transducer between them and with load position and velocity transducers. The actuator on the left is the injection actuator, which is controlled by an electrohydraulic valve with a supply-to-tank central position. Second order valve spool dynamics are separate from the valve because the valve model itself was instantaneous. Position and velocity signals are fed into the injection moulding load model, which then in turn acts as a reference model, producing demanded force output. The actual force, measured by the force transducer is subtracted from the demanded force and the resultant force error is amplified and fed to the load actuator servo-valve. This forms a closed loop proportional force controller. The spool dynamics are again introduced separately. The load actuator valve meters flow out of the actuator during extension (movement to the right in Figure 7). It was found during simulation that metering out was adequate and simpler to control than having a pressure source connected via a spool valve to the load actuator.

Simulation results for the arrangement are shown in Figure 8. Again the slight sharp rise in pressure during filling, in this case just after 0.2 s, is due to the filling of mould regions 5 and 6. For the case of an injection actuator valve with a 10Hz bandwidth and a step input it was found that a 20Hz load actuator valve was sufficiently fast.

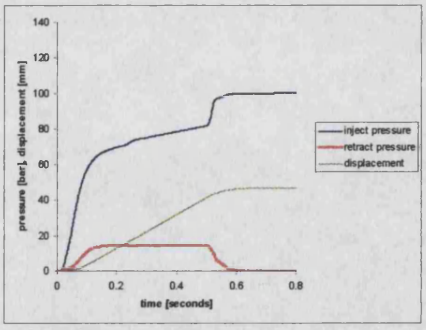

Figure 8 Load Emulator Simulation Using 20Hz Load Control Valve

Experimental Work

To achieve confidence in simulation results experimental tests were undertaken on a 25 tonne clamping force injection moulding machine using the same mould that was used in simulation. Two

injection actuators, connected in parallel and of equivalent area to the single actuator used in simulation, were instrumented with pressure transducers and a displacement transducer. The injection moulding machine was set up with just enough material in the barrel to fill the mould and the injection controller was set up to give the maximum injection velocity with no switch to pressure control. The results obtained experimentally are presented in Figure 9. The rise in pressure up to 0.2s corresponds to the mould fill up to the moulded part section. The injection pressure peak at the end of injection (0.5s) is at the point where filling is complete the material is being compressed. However, this compression only accounts for the first 5 bar of the pressure transient with the rest due to the injection actuators hitting their endstops.

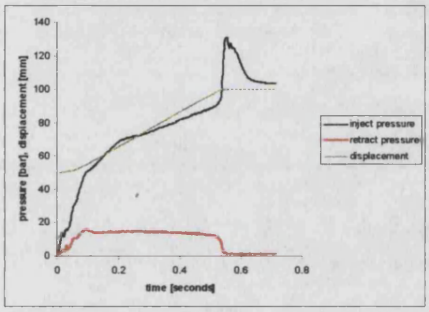

Figure 9 Experimental Results

Comparison of Experimental & Simulation Results

Experimental and load model injection pressures are compared in Figure 10. Mould fill can be seen to occur in both sets of results with the pressure increasing sharply at 0.4s in simulation and at 0.5s in the experimental results. The reason for this discrepancy is that polymer was able to leak internally in the injection barrel of the moulding machine used. This leakage was not modelled in simulation.

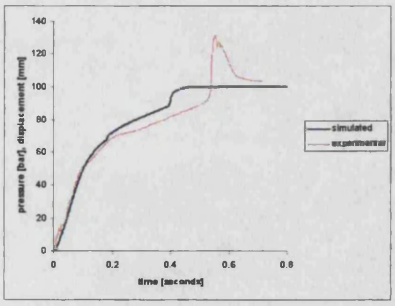

Figure 10 Experimental & load Model

A comparison of the experimental and simulated injection pressure results for the case of the load emulation circuit is shown in Figure 11. The time at which the mould is completely full is now the same in both the real and simulated results. This was achieved by slowing down the simulated injection speed to compensate for the injection barrel leakage. As with the previous simulation results the two pressure time traces are very similar.

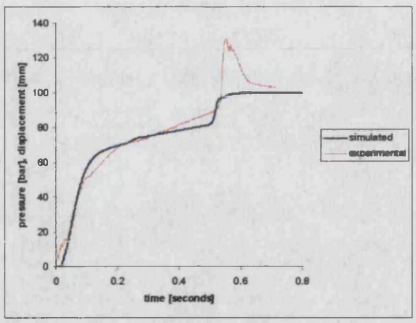

Figure 11 Experimental & Load Emulation

Conclusions

This paper has examined the feasibility of using simulation to model the injection moulding process. An injection moulding load model has been implemented in the Bath*fp* simulation package. For the case of a pseudoplastic material (polypropylene) good agreement has been achieved between simulated and experimental results. Following on from this a further simulation study was carried out to investigate the feasibility of emulating the hydraulic injection moulding process using a 'hardware-in-the-loop' approach. Again good agreement was found between simulated and experimental results. The simulated injection moulding load produced by this work will provide an effective means of evaluating both novel control schemes and new designs of control valve.

Although the particular case of an hydraulic injection moulding machine has been considered, the model of the injection moulding process produced would be equally valid for studies an all-electric machine.

Further Work

The next stage of the work will be to investigate dilatant materials and to set up a test rig incorporating an injection moulding load emulation circuit, based on the load circuit tested in simulation. New controller design and evaluation will follow.

Acknowledgements

The authors would like to thank the Engineering and Physical Science Research Council and Vickers Systems Division Aeroquip-Vickers Ltd for their financial support of this project under the CASE postgraduate studentship scheme.

References

Bird, R. B., Armstrong, R. C. & Hassager, O., 1987, 'Dynamics of Polymeric Liquids', John Wiley & Sons, 2nd edition

Chiang, H. H., Hieber, C.A. & Wang, K.K., 1991a, 'A Unified Simulation of the Filling and Postfilling Stages in Injection Molding. Part 1: Formulation', Polymer Engineering and Science, **31**(2, January), pp. 117-124

Chiang, H.H, Hieber, C. A. & Wang, K.K., 1991b, 'A Unified Simulation of the Filling and Postfilling Stages in Injection Molding. Part 2: Experimental Verification', Polymer Engineering and Science, **31** (2, January), pp. 125-139

Cheng-Ping Chiu, Jong-Hwei Wei & Ming-Chang Shih 1991, 'Adaptive Model Following Control of the Mold Filling Process in an Injection Molding Machine', Polymer Engineering and Science, **31** (15, Mid-August), pp. 1123-1129

Gao F., Patterson, W.I. & Kamal, M.R., 1996, 'Cavity Pressure Control During the Cooling Stage in Thermoplastic Injection Moulding', Polymer Engineering and Science, **36** (19, mid-October), pp. 2467-2476

Jong-Hwei Wei, Chiann-Chiunn Chang, & Cheng-Ping Chiu, 1994, 'A Nonlinear Dynamic Model of a Servo-Pump Controlled Injection Molding Machine', Polymer Engineering and Science, **34** (11, mid-June), pp. 881-887

Lenk, R. S., 1978, 'Polymer Rheology', Applied Science Publishers Ltd London

Nimegeers, C.R., Burton, R. & Schoenau (1997), 'A Computer Controlled Hydraulic Loading System for Simulating Loads', 9th Bath International Workshop, University of Bath, pp. 10-23

Rafizadeh, M., Patterson, W.I. & Kamal M.R., 1996, 'Physically–Based Model of Thermoplastics Injection Moulding for Control Applications', International Polymer Processing, **11**, pp. 352-362

Ramden, C., Jansson, A. & Palmberg, J-O., 1997, 'Design and Analysis of a Load Simulator for Testing Hydraulic Valves', 10th Bath International Workshop, University of Bath, pp. 260-277

Shankar, A. & Paul, F.W., 1982, 'A Mathematical Model for the Evaluation of Injection Molding Machine Control', Transactions of the ASME, **104**, pp. 86-92

Tilley, D.G. & Richards, C.W., 1991 'System Analysis with Bath*fp*' Fluid Power, March/April, **3**, pp.50-53

Tilley, D.G & Richards, C.W., 1997 'Bath*fp* Manual 2 Bath*fp* Model Reference Guide' University of Bath, Department of Mechanical Engineering

Zhang, C.Y, Leonard, J. & Speight, R.G., 1996, 'Adaptive Controller Performance Used For Ram Control During Filling Phase', Society of Plastics Engineers proceedings, ANTEC, pp. 593-597

Paper Presented at ASME IMECE 2000

EVALUATION OF P-Q CONTROLLERS FOR AN INJECTION MOULDING MACHINE

Paul K Guerrier and Kevin A Edge
Department of Mechanical Engineering
University of Bath, UK.
e-mail: K.A.Edge@bath.ac.uk

ABSTRACT

There are a number of problems surrounding traditional velocity and pressure controllers used on injection moulding machines. Injection moulding machines are also very expensive and full scale testing is often not appropriate at the beginning of new controller evaluation. This paper presents results for a half scale 'hardware-in-the-loop' load emulation of the filling and packing phases of injection moulding, suitable for controller evaluation. The problems linked to the current industry standard velocity and pressure controller are discussed along with alternative strategies. Schemes including single controller fuzzy logic and neural network solutions are discussed and ruled out in favour of ones containing separate velocity and pressure controllers. Results for a model reference adaptive pressure controller are presented and compared with those obtained using a closed loop PI controller experimentally and in simulation. Experimentally the model reference adaptive controller outperforms the PI controller but does suffer from gain drift.

NOMENCLATURE

k	flow coefficient
P	pressure
Q	flow rate
x	valve spool position

Introduction

The injection moulding cycle involves filling the injection barrel with polymeric material, usually pellets, which are then melted before being injected into a mould where the material cools. Once cooled the finished part is ejected from the mould and the cycle begins again. There are many problems that can occur during the process which lead to the finished part being rejected, including poor machine set-up and poor mould design.

One of the critical stages in the cycle of injection moulding is the injection of polymeric material into the mould. This can be further subdivided into 2 phases: filling and packing. Filling occurs while the mould is supplied with polymeric material and packing is the pressurisation of the material in the mould once it is full. The packing phase is required to counteract the effects of polymeric material shrinkage during cooling.

In valve-controlled hydraulic machines filling is generally controlled by metering the flow to the injection actuator (which controls its velocity) and packing is generally pressure controlled. These two requirements are met by a combined pressure and flow controller (P-Q controller). This paper examines the performance characteristics of the current industry standard P-Q controller and then considers alternative schemes.

Injection Moulding Modelling & Simulation

Injection moulding machines are expensive and during the preliminary stages of controller design and evaluation it is desirable to carry out investigations in simulation. A mathematical model of the process suitable for controller evaluation was presented in Guerrier & Edge, 1999. The model requires information on injection actuator velocity and displacement from which it calculates resistive force. While simulation is very useful it is an approximation because of unmodelled high order dynamics and (usually) the absence of signal noise.

An intermediate step between pure simulation and full scale testing is the 'hardware-in-the-loop' technique. In this approach, selected subsystems are represented by software emulations, which through appropriate physical interfaces, interact with the remainder of the system.

In this application the force acting on the actuator during injection can be recreated in software and used to control a loading actuator. In Guerrier & Edge, 1999 an injection moulding load emulation circuit was proposed and tested. It was shown that the load could be reproduced using an hydraulic valve-actuator circuit. Since the load was purely resistive during filling and then spring-like during packing it was possible to recreate the principal characteristics by metering flow out of a loading actuator. A circuit diagram showing this arrangement is shown in Figure 1.

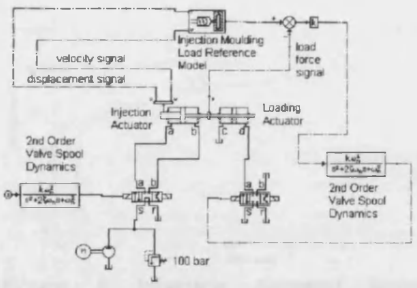

Figure 1 Hydraulic Load Emulator Circuit Diagram

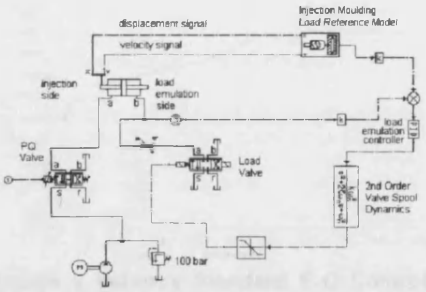

Figure 2 Hydraulic Load Emulator Circuit Diagram

While the circuit in Figure 1 was shown to work effectively in simulation it may be difficult to reproduce safely in the laboratory. This is because the forces produced by the actuators in a full size representation of an injection moulding machine would be very large. As a consequence a substantial structure would have to be constructed to contain the forces without deflection. The actuators would then be connected together. However to accommodate possible misalignment a flexible coupling would be required. Unfortunately a flexible coupling would add unwanted dynamics to the system, most likely during packing emulation. Also if the actuators deflected even slightly, actuator friction levels would change during the test. One way to circumvent these problems would be to use scaled down cylinders. However this would require smaller injection and load valves which would not be representative of a real machine.

These difficulties motivated the consideration of an alternative circuit layout, which relied upon a particular feature of injection control valves. The injection valve used in the simulation study (detailed in Guerrier & Edge, 1999) had a symmetric straight cut spool. However, injection moulding P-Q valves used in industry generally have asymmetric notched spools. Using such a valve in a simulation study showed that it is essentially a meter-in device. This means that the b port of the injection valve in Figure 1 can be blanked off and the b port of the injection actuator connected to tank without significantly effecting results during emulation of the injection process. The fact that the middle 2 ports (b and c) of the actuators were, in essence, not in use means that the two actuators in Figure 1 can be replaced with a single actuator fulfilling the roles of both injection actuator and load emulator. To achieve this simplification it is necessary to assume that cross-piston leakage is negligible. Whilst a close approximation to this can be achieved in practice, the approach does not permit experimental investigations into the effects of different levels of leakage. The circuit in Figure 2 was tested in simulation and was found to be sufficiently promising to justify experimental investigations.

Rig Load Emulation Results

It was decided that a half scale representation of the original injection moulding machine would capture all the key features and simulations confirmed this to be the case. On the strength of this outcome, the rig was built as an identical copy of the circuit diagram in Figure 2. In order to control the test rig and evaluate new P-Q controllers, MATLAB was used in conjunction with the Real Time Workshop and Real Time Windows Target toolboxes. To implement the load model previously developed and tested in the Bath*fp* environment (see Tilley & Richards, 1991), the code simply had to be changed from Fortran to C and incorporated in a MATLAB S-function.

The main difference between simulation and experimental studies is that all control activities on the rig are done in discrete time with a 1ms sample time while simulations are in continuous time.

The mould shape selected for investigation is the same as that described by Guerrier & Edge, 1999. Initial investigations were performed to verify the accuracy of the emulation. This was done by subjecting both the simulated and emulated systems to a step change in PQ valve demand signal from zero to maximum. This results in the actuator responding as swiftly as possible. No pressure control was implemented so that at the onset of packing the pump discharges through the relief valve. Simulated injection pressure for the circuit shown in Figure 1 is presented in Figure 3. This can be compared with Figure 4 which shows the measured performance obtained from the circuit shown in Figure 2. There is a small amount of noise superimposed on the measured injection pressure (none of the signals are filtered). The shapes of the curves are very similar with both pressures rising sharply as the load is accelerated from rest. The pressure then rises at a slower rate until the onset of packing when the pressure rises sharply until the system relief valve opens. This then leads to a slight pressure instability in the experimental results which is not present in simulation. Also an initial pressure oscillation is evident in the experimental results which is not found in the simulation results. Both these discrepancies are because of differences between the actual relief valve dynamics and those used in simulation as well as differences between simulated and actual load valve dynamics.

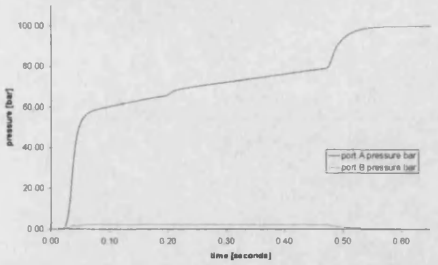

Figure 3 Injection Actuator Pressure Simulation Results

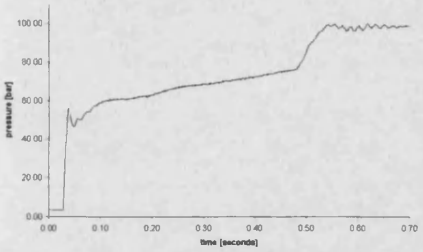

Figure 4 Rig Load Emulation Results

Traditional P-Q Control

The industry standard P-Q controller considered here is a fixed gain closed loop (or open loop) velocity controller which is linked by a P-Q switch to a closed loop proportional plus integral (PI) pressure controller. Switching between flow and pressure control is initiated on either actuator position, pressure (injection pressure) or time. The switch from flow to pressure control is irreversible during a cycle and the output of the pressure controller integrator is held at zero until the controller is activated.

Industry Standard Controller Simulation Results

The electrohydraulic circuit in Figure 1 was set up in simulation using an industry standard P-Q valve and an industry standard P-Q controller. All circuit components were sized so that the emulation was a 1:1 model of the original injection moulding machine used in Guerrier & Edge, 1999. An industry standard controller was set up with an open loop velocity controller; with this arrangement the velocity profile is dictated solely by the nature of the demand signal. The switch to pressure control was set to occur at an injection pressure of 80bar, with a final target of 90bar. During the packing phase it is the throttling action of the P-Q valve which dictates the injection pressure; once again the excess pump pressure is discharged through the relief valve. The goal was to achieve the smoothest pressure response without overshoot. This was done by setting the integral gain 13 times higher than the proportional gain. The injection pressure results are shown in Figure 5.

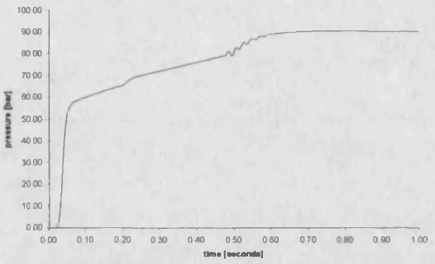

Figure 5 Industry Standard P-Q Controller Simulation Results

There is slight undesirable pressure oscillation after switchover from flow to pressure control but overall performance is probably acceptable.

Industry Standard Controller Rig Results

The same test was carried on the test rig in the laboratory and the injection pressure results are shown in Figure 6. Again the integral gain of the PI pressure controller was set approximately 13 times higher than the proportional gain.

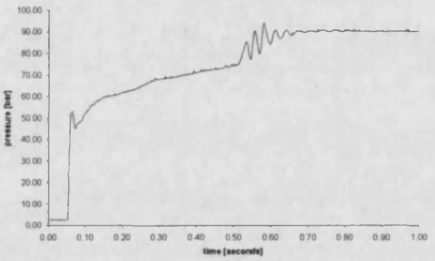

Figure 6 Industry Standard P-Q Controller Rig Results

There is greater pressure oscillation after switchover compared to simulated behaviour which would most likely impair part quality. Differences between the simulated load valve and actual load valve dynamics as well as differences between the volume of oil between the load valve and load actuator account for the initial pressure peak in results from the rig.

Problems

The main problems with traditional P-Q controllers controlling injection moulding machines are:

- The selection of the control gains relies on significant knowledge and skill of the commissioning engineer.
- The switch from flow to pressure control may lead to a short oscillatory pressure transient. Ideally a smooth critically damped or overdamped increase in pressure up to the packing pressure is required at the onset of packing.
- If short pipes are used between the P-Q valve and the actuator, the PI pressure controller tends to be particularly difficult to tune.

These problems arise essentially for the same reasons. The velocity controlled filling phase is a low gain system and the pressure controlled packing phase is a high gain system.

Currently a commissioning engineer has to tune and test each closed loop PI pressure controller separately. Great cost savings could be made if a more advanced self-commissioning P-Q controller could be implemented.

Alternative Control Strategies

Alternative control strategies can be conveniently sub-divided into 2 main groups. These are single controller solutions and hybrid controller solutions. Single controller solutions cover both velocity and pressure control embodied within a single structure with both velocity and pressure demand inputs and a single output. Hybrid controller solutions are those with separate controllers for velocity and pressure control and some form of transfer mechanism between the two. The industry standard P-Q controller detailed earlier in this paper is a hybrid controller.

Firstly, single controller solutions will be considered. Two candidates are considered here: neural networks and fuzzy logic. Hybrid solutions are then considered, with discussions of adaptive controllers, linearised valve velocity control, sliding mode pressure control, bumpless transfer and learning control.

Neural Network Pressure & Flow Control

The potential benefits of using artificial neural networks for the control of non-linear systems are identified by Suykens et al,. 1996. Stability issues aside, one possible method of control using a neural network is the inverse model method. A neural network is set up and trained to be an accurate model of the system to be controlled. The model is then inverted and the required system outputs fed into the model. The neural network model returns the system input necessary, which is then fed into the real system to be controlled. This might be a good method of controlling a complex highly non-linear system but would only work if the system parameters were fixed or did not change significantly. While it is very possible that a neural network could be devised and trained for a *particular* injection moulding machine, the system characteristics can change quite significantly. For example if a mould or material is changed this would certainly require retraining and might even require a different neural network structure.

Even if a neural network solution were employed satisfactorily it may be practically impossible to guarantee stability at all operating conditions. This stems from the fact that the non-linear equations describing a neural network of any significant complexity are very difficult to obtain. As such it is difficult to construct an analytical proof of stability. The legal implications of this may be such that a neural network controller would be unmarketable. Of course an analytical proof of stability for a simple neural network should be possible.

A further reason why a neural network solution is inappropriate is that they can only be trained from data that exists. To retain the same level of performance each new mould, material, or control valve encountered would very likely require a new controller. This would then constitute a new controller, which would require testing before it could be guaranteed to perform correctly. It would be a very time consuming exercise to test as many moulds and materials as possible to be able to supply a family of trained controllers. Also since new mould designs and to a lesser extend new materials are continually being developed there would be a continuing requirement to test and retrain new controllers.

As a single controller a neural network solution is therefore eliminated on the grounds that it is inappropriate for controlling a system with an unknown range of parameter variations.

Fuzzy Logic Pressure and Flow Control

As explained in Pedrycz, 1993 fuzzy logic is typically very useful for constructing controllers from human experience of controlling a system manually. Mathematical models are not required. This is because fuzzy logic is used to create a controller from a set of rules. Consequently fuzzy logic controllers are often found in process control applications where they replace human operators. In such cases fuzzy logic is a suitable solution because little information is required about the system plant. All that is required is a set of rules describing how the system input signal should be regulated to give the correct system output.

The work by Yang & Chang, 1998 details the implementation and testing of a fuzzy logic controller on an electrohydraulic materials testing machine. The main conclusion arrived at is that a fixed rule base fuzzy logic controller is not sufficiently robust for fatigue testing over a wide range of frequencies. Instead the authors argue that a self-organising fuzzy logic approach needs to be used to give sufficient robustness. While this appears to work adequately, a stability proof for such a controller would be extremely difficult to carry out. Again the legal implications of this may be such as to make the controller unmarketable. It is also worth noting that although the controller detailed in the work by Yang & Chang, 1998 was successful this is not always the case with self organising fuzzy logic controllers. The work by Pannett et al., 1999 on self-organising fuzzy control states that 'performance and robustness are not predictable'. Work by Tsoi & Gao, 1999 on an injection moulding *speed* controller showed that a fixed rule base fuzzy logic gave good performance and was more robust than a fixed gain PID controller. Three different moulds were tested with 2 different materials and 2 different barrel

temperature settings (12 different configurations in all). However there was no mention of the implications of either making the controller commercially available or linking it to a pressure controller.

While it may be possible to construct a fuzzy logic P-Q controller it is likely that it would be complex and necessary to have a self-organising element to take account of plant (mould or polymeric material) changes. Analysis to guarantee stability would be difficult. For this reason a fuzzy logic P-Q controller has been discounted.

Linearised Valve Velocity Control

One of the fundamental non-linearities of hydraulic systems is the relationship between valve position and the flow rate through the valve, equation (1) below. This arises from the relationship between valve position and the pressure drop across the valve.

$$Q = kx\sqrt{\Delta P} \qquad (1)$$

If the force required to inject molten polymeric material into a mould was constant and independent of position and velocity then the flow through the valve would be proportional to valve position. However, it has previously been established in Guerrier & Edge, 1999 that the force required to inject molten polymeric material into a mould increases non-linearly with injection actuator position. Therefore in injection moulding the function relating valve position to flow rate will be non-linear and dependent on actuator position.

Since a pressure transducer in the inject side of the injection actuator will be necessary for closed loop pressure control it seems attractive to use the pressure information during velocity control to linearise the valve characteristic. One application where this has been used successfully is in the acceleration control of hydraulic actuators for flight simulators. A good paper on the subject is by Plummer, 1997. However, system simulations have shown that the supply pressure from the pump is not constant during the injection moulding cycle. During filling the total pump flow is used and the pump supply pressure depends on the injection actuator velocity and the position of the melt front in the mould. Hence if the valve characteristics were to be linearised a second pressure transducer would be required, upstream of the injection control valve, to measure pump supply pressure. This would increase the cost and complexity of the P-Q controller but not so much as to rule this method out.

Adaptive Velocity Control

Because the relationship relating injection moulding force to position and velocity is non-linear it would seem sensible to adjust the controller gain during injection to reflect the melt front position. One possible way to do this is by using an adaptive controller. Various strategies are available. A good introduction to three of the main types (gain scheduling, self-tuning regulation, model reference adaptive control) is found in Åström, 1983. It is envisaged that any advanced P-Q control strategy will require displacement, velocity and pressure measurement, at the very least. Hence the common problem of a gain scheduling solution requiring one or more measurable parameters with which to vary the regulator does not arise. It is very likely that gain would be scheduled against at least injection pressure and actuator position and possibly actuator velocity as well. The construction of a gain scheduling map is not a trivial task and the design of such a map would be feasible for an injection moulding machine that was only ever going to be used with one particular mould, one material and the same temperature set point. Such a map would be at the very least be mould and material specific and require redesign for new moulds and/or materials. In light of this gain scheduling is not appropriate.

Self-tuning regulation is another possible candidate as an adaptive controller. The biggest problem likely to be encountered is that of obtaining an accurate system model and then performing a parameter identification. Another problem commonly encountered is when to stop tuning. If tuning is stopped too soon then the regulator will not be optimised but more importantly if tuning is not stopped when the process has reached a steady state regulator gains can drift. The same problem can be encountered in model reference adaptive control (MRAC) and is explained in more detail below.

The key components of an MRAC controller are the reference model and the regulator adaptive gain or gains. The reference model is usually defined to give an achievable output for the plant output to track, with dynamic characteristics similar to those of the plant. The scheme then works by trying to minimise the error between the plant output and the reference model output by varying the regulator adaptive gain. While the concept of MRAC itself may not seem to have many advantages over gain scheduling or self-tuning control, certain types do. This is because an accurate reference model is not always needed. An adaptive *velocity* controller for injection moulding has already been designed and tested with some success, as described by Zhang et al., 1996. Unfortunately only scant detail is given

One problem that can be encountered with adaptive control is gain drift. If no safeguards are put in place, adaptive gains can change until they saturate. At this point the system output would deviate from the demand until sufficient information is available to re-tune the adaptive gains. The cycle would then start again forming a type of limit cycle. If an MRAC controller were to be implemented this issue would have to be addressed.

Bumpless Transfer

Considering the alternatives, a hybrid strategy appears to be the most promising. With this approach a bumpless transfer strategy will be required to avoid the problem of a high pressure transient when switching from flow to pressure control. A good overview of anti-windup and bumpless transfer schemes is given by Edwards & Postlethwaite, 1998. A general anti-windup and bumpless transfer method is presented by Hanus et al., 1987. However by far the most useful work for this application is that by Graebe & Ahlén, 1996. Their scheme acts to make the output of the latent (offline) controller track the output of the active controller. This means that on transfer the system input will have the correct initial conditions. The bumpless transfer strategy was devised to change between 2 controllers controlling the same plant output. This is not the same as bumpless transfer of flow to pressure control but the principle of forcing the latent controller to track the output of the active one can still be applied. In the case of flow and pressure control the flow controller would be the active controller and the pressure controller the latent one.

Learning Control

Since injection moulding is a repetitive process it is attractive to try to harness this fact and implement a scheme which takes account of past controller performance. This type of controller is generally referred to as a *learning controller* or an *iterative controller*.

One of the earlier publications to use the term *learning control* is that by Arimoto et al., 1984. In this work a *betterment process* for the control of a mechanical robot is presented. While this work is important in that it defines and explains the concept and some of the practicalities of learning control, one major disadvantage is that the conclusions are entirely based on theory and simulation rather than experimental work. Another major problem is that the method is only applied to a linear system and proof of convergence for the controller has only been derived for the linear case. Possible problems identified by the authors include the need for clean and continuous transducer signals and the choice of a suitable function for determining the changes that are made to the system input, based on the error between demanded and actual system output. It was also concluded that the rate of convergence varies as this function is altered.

Sugie & Ono, 1991 prove in theory that certain types of non-linear system can be controlled by a controller with an iterative structure, without knowledge of the system being controlled. Even so the point that the derivative of the controlled variable error is important for stability is again raised as it was for the linear plant case considered by Arimoto et al., 1984. In the case of P-Q control this means the use of the derivative of velocity and the derivative of pressure. While the derivative of velocity could be obtained without too much difficulty it is notoriously difficult to obtain a useful derivative of pressure. This is because the measured pressure signal usually contains a pump pressure ripple and filtering the signal introduces an unacceptable phase lag.

The paper by Kirecci & Gilmartin, 1998 reveals some practical problems. The system being controlled was a robot with 2 degrees of freedom; the learning controller used positional error and was set up to give good position tracking performance. The main problem reported was a high frequency ripple on the command signal from the controller. This occurred during high speed robot movement after a few iterations of the controller's learning cycle. The solution used by Kirecci & Gilmartin, 1998 was to add a digital filter to the learning controller algorithm. Such controller instability, occurring after good performance has been achieved, can be considered analogous to gain drift in adaptive control.

The work presented in the paper by Kim & Kim, 1996 is also based on experimental results. In this case a PID controller with the addition of a learning gain-changing element was implemented. The aim was to improve CNC machine tool position demand tracking and was carried out without full knowledge of plant parameters and with the knowledge that there were non-linear external disturbances. In this study the disturbances were repeatable which is one reason why the controller was successful. Since tool was following a circular trajectory cutting through the same depth of material the controller gains did not vary during each cycle. However fixing gains for an entire cycle may not be appropriate for injection moulding filling control. Overall the controller developed was successful in halving the tracking error within 5 cycles, although this is not so instructive since there is no mention of initial gain estimation.

Results for separate learning velocity and learning pressure controllers have been published by Havlicsek & Alleyne 1999. However the initial estimate of the controller output had to be quite good for convergence and at the time of writing this paper (from the results presented later on) the authors have more confidence in adaptive schemes. This is not to say that an learning element could not be incorporated into an adaptive scheme, which would have certain advantages. Velocity and pressure control aside, in a fully automatic P-Q injection moulding controller there is still a requirement to switch from velocity to flow control at the correct point in the cycle. This task is perhaps best suited to iterative control. One possible way of doing this is to monitor the derivative of pressure, which should indicate the onset of packing as the pressure rises rapidly. However as mentioned previously, a useful derivative of pressure is difficult to obtain.

Sliding Mode Pressure Control

One promising pressure control strategy is sliding mode control. This is a robust control strategy and there is no doubt that in the case of hydraulic spool valve position control, it is superior to PID control as demonstrated by Gamble & Vaughan, 1996. As explained by Gamble, 1992 the design of a sliding plane is not a trivial task. Hence for pressure control, it is possible that a sliding mode controller would need an observer to instigate a hyperplane change for different mould volumes. The work by Hwang et al., 1993 showed that a fixed gain sliding mode controller was suitable for the position control of a valve actuator system but the parameter changes the system had to cope with were relatively small. In contrast, in injection moulding, while the plant structure will remain the same, parameters will change significantly with new moulds or materials. One way of coping with this would be to use a gain-scheduling observer sliding mode controller much like the one for electrohydraulic motor speed control detailed in Yanada & Shimahara, 1997. This would be more robust than a fixed gain method.

While the strategy cannot be ruled out, a sufficiently short sample time cannot be achieved in this test facility, so it is not the authors' intention to take this further.

Model Reference Adaptive Pressure Control

Pressure-controlled packing can be approximated to the control of pressure in an actuator compressing a stiff spring. It is not surprising therefore that constructing an accurate plant model is relatively easy. For this reason MRAC is particularly appropriate for pressure controlled packing. To demonstrate this an MRAC controller has been implemented on the rig.

Results from the rig using an MRAC pressure controller are shown in Figure 7 below. The velocity controller was, once again, open loop and the switch to pressure control was as for the PI scheme previously described. While the pressure transient that was evident with the industry standard P-Q controller in Figure 6 is still in part present it is important to note that it is much reduced. Moreover, the adaptive controller has self tuned. The pressure oscillation between 0.8s and 0.9s is due to adaptive gain drift.

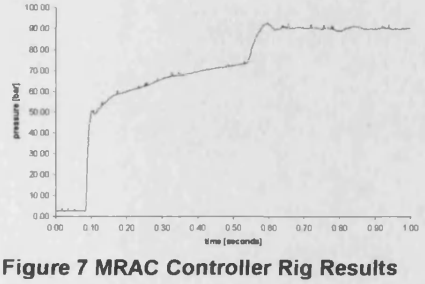

Figure 7 MRAC Controller Rig Results

Conclusions

This paper has shown that it is possible to emulate the load produced during the filling and packing phases of injection moulding using an appropriate hydraulic cylinder and valve. The problems that occur with the current industry standard P-Q controller used for injection moulding were then reproduced both in simulation and on the rig. Alternative P-Q controller strategies were then considered. Since the plant depends on mould shape and material injected both neural network and fuzzy logic single controller solutions were ruled out. Hybrid controliers considered include linearised valve velocity control, adaptive velocity control, MRAC pressure control and sliding mode control. None of these strategies can be entirely ruled out but it was felt that by the authors of this paper that MRAC pressure control was particularly appropriate. An MRAC pressure controller was implemented using an emulated load and results showed better performance compared to a closed loop PI pressure controller.

Further Work

The next stage of the work will be to investigate an adaptive velocity controller for filling and a bumpless transfer scheme.

Acknowledgements

The authors would like to thank the Engineering and Physical Science Research Council and Vickers Systems Division Aeroquip-Vickers Ltd for their financial support of this project under the CASE postgraduate studentship scheme.

References

Arimoto, S., Kawamura, S. & Miyazaki, F., (1984). Bettering Operation of Robots by Learning, Journal of Robotic Systems, **1**(2), pp. 123-140

Åström, K. J., (1983). Theory and Applications of Adaptive Control-A Survey, Automatica, **19**(5), pp. 471-486

Edwards, C. & Postlethwaite, I., (1998). Anti-Windup and Bumpless-Transfer Schemes, Automatica, **34**(2), pp. 199-210

Gamble, J. B., (1992). Sliding Mode Control of a Proportional Solenoid Valve, PhD Thesis, Department of Mechanical Engineering, University of Bath

Gamble, J. B. & Vaughan, N. D., (1996). Comparison of Sliding Mode Control with State Feedback and PID Control Applied to a Proportional Solenoid Valve, ASME Journal of Dynamic Systems, Measurement & Control, **118**, pp. 434-438

Guerrier P. K., Edge, K. A., 1999, 'Injection Moulding Simulation For Hydraulic Valve-Actuator System Controller Design', ASME, **36** (19, mid-October), pp. 2467-2476

Graebe, S. F. & Ahlén, A. L. B., (1996). Dynamic Transfer Among Alternative Controllers and Its Relation to Antiwindup Controller Design, IEEE Transactions on Control Systems Technology, **40**(1), pp. 92-99

Hanus, R., Kinnaert, M. & Henrotte, J-L., (1987). Conditioning Technique, A General Anti-

Windup and Bumpless Transfer Method, Automatica, **23**(6), pp. 729-739

Havlicsek, H. & Alleyne, A., (1999). Nonlinear Control of An Electrohydraulic Injection Molding Machine via Iterative Learning, Proc. of The American Control Conference, San Diego California, pp. 176-181

Hwang, C. L., Lan, C. H & Jieng, W. J., (1993). The Trajectory Tracking of an Electrohydraulic Servo-Mechanism via a Sliding Mode Controller, Proc. IMechE part I: Journal of Systems & Control Engineering, **207**, pp. 135-142

Kim, D., I. & Kim, S., (1996). An Iterative Learning Control Method With Applications for CNC Machine Tools, IEEE Transactions on Industry Applications, **32** (1), pp. 66-72

Kirecci, A. & Gilmartin, M., (1998). Application of Learning to High-Speed Robotic Manipulators, IMechE Transactions Part I, **212**, pp. 315-323

Pannett, R. F., Chawdhry, P. K. & Burrows C. R., (1999) Alternative Robust Control Strategies for Disturbance Rejection in Fluid Power Systems, Proceedings of the American Control Conference, San Diego California, pp. 739-743

Pedrycz, W., (1993). Fuzzy Control and Fuzzy Systems, Research Studies Press Ltd. John Wiley & Sons Inc.

Plummer, A. R., (1997). Feedback Linearisation for Acceleration Control of Electrohydraulic Actuators, Proc. IMechE Part I, **211** pp. 395-406

Sugie, T. & Ono, T., (1991). An Iterative Learning Control Law for Dynamical Systems, Automatica, **27** (4), pp. 729-732

Suykens, A. K., Vanderwalle, J. P. L. & De Moor, B. L. R., (1996). Artificial Neural Networks for Modelling and Control of Non-Linear Systems, Kluwer Academic Publishers

Tilley, D. G. & Richards, C. W., (1991) 'System Analysis with Bath*fp*' Fluid Power, March/April, **3**, pp.50-53

Tsoi, H.-P. & Gao, F., (1999). Control of Injection Velocity Using a Fuzzy Logic Rule-Based Controller for Thermoplastics Injection Moulding, Polymer Engineering & Science, **39**(1), pp. 3-17

Yanada, H. & Shimahara, M., (1997). Sliding Mode Control of an Electrohydraulic Servo Motor Using a Gain Scheduling Type Observer and Controller, Proc. IMechE part I, **211**, pp. 407-416

Yang, Y. T. & Chang, C. C., (1998). The Fuzzy Control of an Electrohydraulic Fatigue Testing System, International Journal of Materials and Product Technology, **13**(3-6), pp. 184-194

Zhang, C. Y, Leonard, J. & Speight, R. G., (1996). Adaptive Controller Performance Used For Ram Control During Filling Phase, Society of Plastics Engineers proceedings, ANTEC, pp. 593-597